Synthesis and characterization of novel *N*,*N*-di(ethyl)-*N*'-benzoylthiourea complexes of Pd(II), Pt(II), Cu(II) and Zn(II) bearing phenanthroline ancillary ligand $[M^{II}(diimine)(L\text{-}\kappa O,S)]^{+}$ as potentially anticancer agents.

A dissertation submitted to the Faculty of Science, Witwatersrand University, Johannesburg, In fulfilment of requirement for the degree of Master of Science (MSc) in Chemistry

By

Lindela Matiti

Student number:

2215966

Supervised by:

Dr I A Kotze

Molecular Sciences Institute, School of Chemistry

University of the Witwatersrand

Private Bag 3, Wits, 2050

South Africa

Declaration

I, hereby declare that this dissertation is my own. It is being submitted in the faculty of science at the University of the Witwatersrand for the degree of Master of science in chemistry and has not been previously submitted to any University.

……..

Lindela Matiti

On this …27th…day of…October…2021

Abstract

A series of acylthioureato complexes of Pd(II), Pt(II), Cu(II), and Zn(II) bearing phenanthroline-based ancillary ligands were investigated in this study. The target complexes were prepared by the reaction between a phenanthroline-substituted precursor complex and the *N,N*-di(ethyl)-*N'*-benzoylthiourea in the presence of a deprotonating agent. The target complexes were isolated as atmospherically stable solids with a yield ranging from 45 – 60%. Complete characterization of these acylthioureato complexes includes 1D and 2D nuclear magnetic resonance spectroscopy, infrared spectroscopy, mass spectrometry, elemental analysis, and single-crystal X-ray diffraction (where applicable).

These complexes were screened against A549 lung carcinoma and HEK-293 embryotic kidney cancer cell lines. For the complex cytotoxicity effect, two concentrations were used (100 µM and 10 µM). MTT assay together with an organic solvent (DMSO: EtOH) was used to solubilize the cells. Evaluation of these complexes was done by exposing them to the cell for 24 hours and the absorbance was recorded. Most of the complexes were highly active against the HEK-293 cancer cell line at 100 µM with 90-100 cell-death. However, the [Zn(phen)(L-κ*O,S*)Cl] variation complex was the least active at 100 µM with cell viability of 40%. [Cu(phen)(L-*S,O*)]Cl was the most active compound against the A549 lung carcinoma cancer cell-line with less than 1% cell viability at 100 µM and less than 20% cell viability at 10 µM and which can be assumed for the copper influence. There was a significant improved cytotoxicity effect for complexes bearing methyl in 5 and 6 positions of the 1,10-phenanthroline than those with unsubstituted 1.10-phenanthroline. When comparing square-planar complexes from the PGM group (Pd and Pt), we found that Pt(II) displayed the highest activity. Three zinc complexes were compared to each other for their cytotoxicity effect, substituted phen was observed to be the most active followed by the acetate coordinated complex, and chloride variation been the least active. [Cu(phen)(L-*S,O*)]Cl compound was found to be the most active compound and its Cu(II) complexes bearing mixed ligand diimine and acylthioureato are not yet mentioned as an anti-cancer drug, which makes the novel interesting to start acylthiourea and diimine ligand variation and test IC_{50} for the structural relationship with DNA interaction.

Acknowledgement

Writing an MSc dissertation is not an easy task, and this thesis is the product of a team's work. I want to extend my sincere gratitude to my supervisor Dr I A Kotze for his support, motivation, encouragement and guidance. I would like to thank Dr JV Van Wyk for her support and encouragement. I would also like to extent my sincere gratitude to Dr L Harmse for the work she had done in this project. Dr E Kangara, thanks you for assisting with the thesis, support, and knowledge. I would also like to thank Ms. T Peega for her assistance with the screening and valuable discussions in the biological section. The National Research Foundation and the University of the Witwatersrand (school of chemistry) for funding. Thanks to the coordination chemistry group (Lab 122) for the support and encouragement. I would like to extend a special thanks to My aunt Feziwe Mbulali for her support and encouraging me to come to the University of the Witwatersrand.

Table of Contents

List of Figures

List schemes

List of Tables

List of Abbreviations

CDK	Cyclin-dependent kinases
$CDCl_3$	Deuterated chloroform
COSY	Correlated spectroscopy
DCM	dichloromethane
dppz	dipyrido[3,2a:2',3'-c] phenazine
dmp	5,6-dimethyl-1.10-phenanthroline
DMSO	dimethylsulfoxide
DNA	Deoxyribose Nucleic Acid
ESI(+)	positive electron spray ionization
EtOH	ethanol
FDA	Federal Drug Administration
FT-IR	fourier transform infrared
HET	Hydroxythanethiolate
H_2O	water
IARC	International Agency of Research on Cancer
IC_{50}	half maximal inhibitory concentration
KTS	3-ethoxy-2-oxobutyraldehyde bis(thiosemicarbazone)
L1210	mouse lymphocytic leukemia cell line
MDR	Multiple Drug Resistance
MeOH	methanol
MS	mass spectroscopy
MTT	3-(4-5-dimethylthioazol-2-yl-)-2,5-diphenyl-tetrazolium bromide
mp	melting point
NaCl	sodium chloride
NMR	Nuclear magnetic resonance
NOE	nuclear overhauser effect
pH	Potential of hydrogen
Phen	Phenanthroline
ppm	parts per million
RNA	Ribose Nucleic Acid

ROS	Reactive Oxygen Species
S,S-dach	1S,2S-diaminocyclohexane
USA	United State of America
terpy	2,2',2''-terpyridine
WHO	World Health Organization

CHAPTER 1

Literature review on anticancer activity of metal complexes

1.1 The prevalence of cancer

Cancer is the first leading health concerns around the globe.[1] The World Health Organization (WHO) reported that in 2018, 18.1 million people were diagnosed with cancer, and 9.5 million were reported to have died due to complications associated with cancer globally.[2] In 2012, WHO estimated that the number of cancer diagnosis cases would've doubled by the year 2040.[3] The International Agency of Research in Cancer (IARC) estimated that 1.7 million new cases were reported in 2018 within the United States of America.[4] Cancer is more prevalent in the United States of America (USA) compared in any other country in the world. Breast cancer was reported as the major problem compared to other cancer types.[5] According to the reports given by the IARC,[6] statistics show that more death cases occur amongst men than women.

Cancer is described as a genetic disease developed by the changes in genes responsible for the way cells function and how they grow and divide (*Figure 1.1*).[7] The mutations involve changes in the arrangement of the bases that make up a gene. These mutations are caused by different things, which includes, aging, exposure to chemicals, radiation, factors in the body or hormones and environment. These mutations are a result of these different cancer types which are carcinoma, leukemia, sarcoma, lymphoma, multiple myeloma, melanoma, brain, and spinal cord tumors.

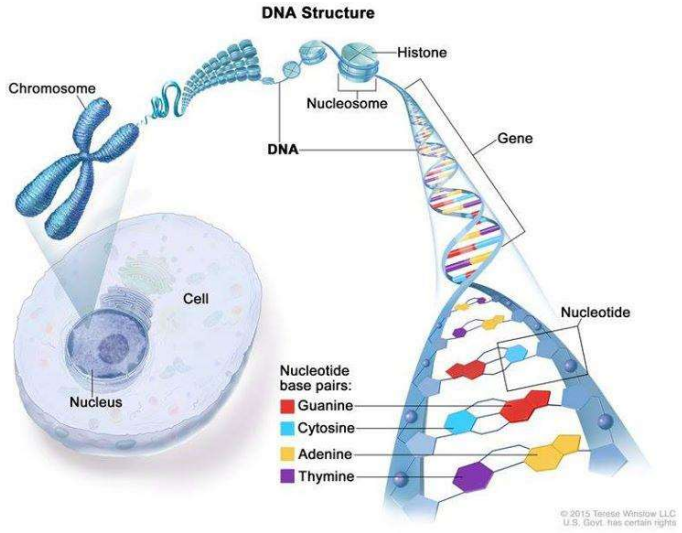

***Figure 1.1**: Illustration of cell division into the DNA strand.*[7]

1.2 Treatment for Cancer

Several types of treatments have been developed, which includes radiotherapy, surgery, and chemotherapy. In the radiotherapy method, X-rays are shined directly onto the affected cells to kill those cells so that they do not duplicate and migrate to other parts of the body. The surgical, involves the complete removal of the damaged cells by operation. The use of chemotherapy method involves the use of drugs to kill cancerous cells systematically.[8] The first scientist to use the word chemotherapy was the immunologist Paul Ehrlich. The word chemotherapy simple refers to the treatment of diseases using chemicals.[9–11] There have been many research studies conducted for the cancer chemotherapy. These research proceedings were done since the beginning of the 20th century (*Figure 1.2*).[10]

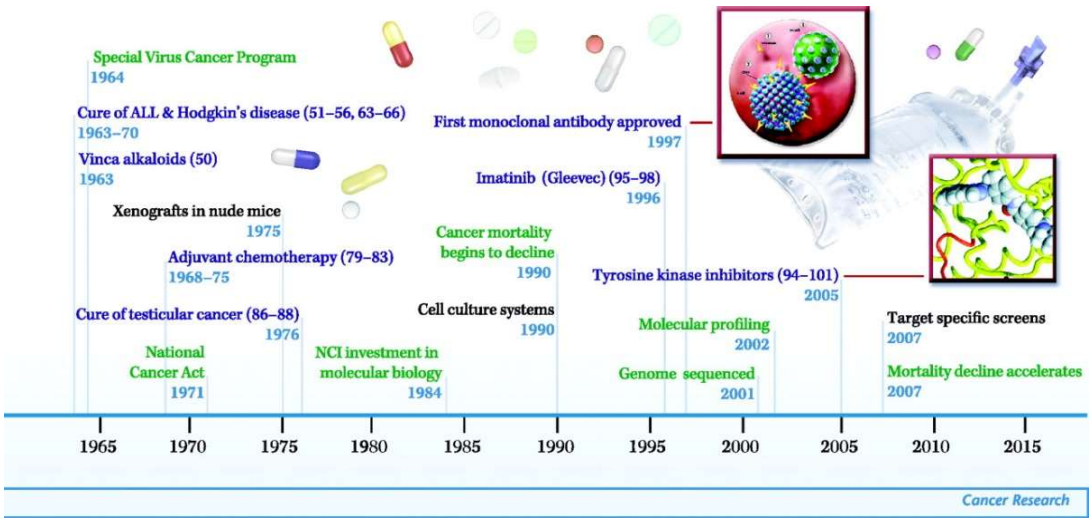

***Figure 1.2**: Key facilitate in the cancer chemotherapy drug over the years.[10]*

A series of antimetabolite drugs were synthesized, which includes antifolates, thiopurines and methotrexate.[11] These drugs are a purine analogue, and their mechanism of action is at the level of DNA. Thus it is believed that they incorporate into replicating DNA and thus block the pathway of purine synthesis, inhibiting cellular proliferation.[12] For example, mercaptopurine, a type of purine antagonists, was used to treat acute leukaemia.[13] The second group of chemotherapeutic drugs that found their use in colorectal cancer and pancreatic cancer are pyrimidine analogues and methotrexate, of which their mechanism of action involves inhibiting thymidylates synthase.[14] The biggest problem encountered by these drugs is their capacity of safety because of non-selective bio-distribution throughout the body, thus leading to toxicity of these drugs.[14]

An additional constructive way to transport a drug is targeted therapy. This kind of therapy aims to deliver the drug to the affected cancer cells without the major disturbance of the unaffected cells.[15] The monitoring of the chemotherapy is important so that it can improve its activity.[16] Furthermore, the administration of the chemotherapy drugs serve a distinctive characteristics of the tumour, such as hypoxia, selective enzyme expression, and minimal extra-cellular acidic and/ base content.[17] Major challenges or problems encountered by chemotherapy is drug resistance. For instance, cells are found to grow a cross-resistance based on the structure of a drug, this process is known as multi-drug resistance (MDR) (*Figure 1.3*).[15,18] Drug modification and inactivation are mechanisms caused by multi-drug resistance.[19]

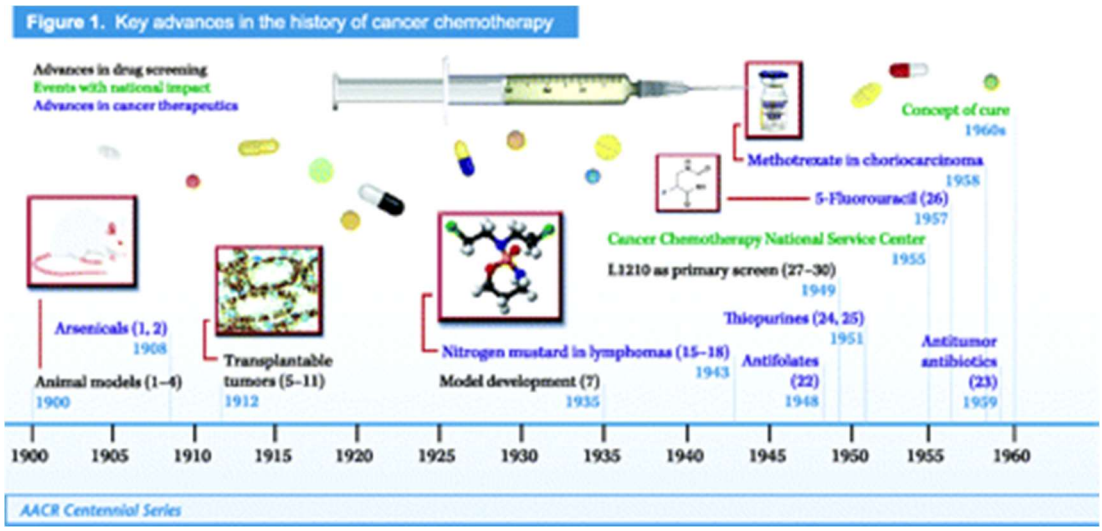

***Figure 1.3**: Illustration of key adavances in cancer chemotherapy drugs in years.*[19]

In 1965, the platinum complex cis-diamminedichloridoplatinum (II) was discovered by Barnett Rosenberg, this discovery of this compound led to a stoppage the cell multiplication of the bacteria Escherichia coli.[20] The finding of cisplatin allowed an intensive interest into the search of anticancer agents based on other metal complexes.[21] Apart from platinum, researchers are also trying to look at the other metals as potential anticancer agents such as copper, palladium, gold, ruthenium, cobalt, zinc, etc.[21] This discovery has given rise to the field of metal-based anticancer agents, a discipline that has quickly increased and spark the drive for the researchers to consider more metal-based complexes as chemotherapy agents.

1.3 Metal ion complexes as anticancer agents

Inorganic chemicals utilization as cancer drugs was relatively uncommon before the discovery of cisplatin.[22] The main concern was that they were poisonous, and researchers did not anticipate that they could be potentially useful as anticancer drugs.[23] The arsenotherapy was the earliest inorganic complexes given dive as the chemotherapy drug and this method was called the Fowler's solution.[24] Work with metal complexes concerning their structure-efficacy-relationships initiated in the year 1931 by Collier and Krause. They used the logic for the activity of metal complexes that states: "the effect of heavy metals on experimental murine cancer is not only due to the metal alone but also to the compound's structure and type".[25]
Metal complexes they were involved more in the development of the chemotherapy due to their chemical reactivity.[26] Furthermore, the possibility of numerous coordination geometries which allows the synthesis of the metal complexes with stereochemistry that is quite distinctive and not found in the group of none inorganic complexes.[26] The most important factors in the geometry of metal complexes are the nature of ligands and the oxidation of the metal, which influence the cytotoxicity of the metal-based drug. In often time, oxidation states of the metal influences the coordination geometry.[27]

A gradual use of the metal complexes as chemotherapy drug has been expanded in the last few years.[28] It has been documented that metal and metal complexes have played the most crucial role in developing pharmacy and modern chemotherapy.

1.3.1 Platinum complexes with anti-tumour activity

The lifetime of metal-based complexes as chemotherapeutic agents started with the fluke finding of the Pt(II) based chemotherapeutic discoverd by Bannert Rosenberg, as mentioned earlier.[29] A search of platinum complexes already approved as anticancer drugs yielded three drugs: cisplatin, carboplatin, and oxaliplatin (*Figure 1.3.1.1*). The compounds display a wide range of the anticancer.[30]

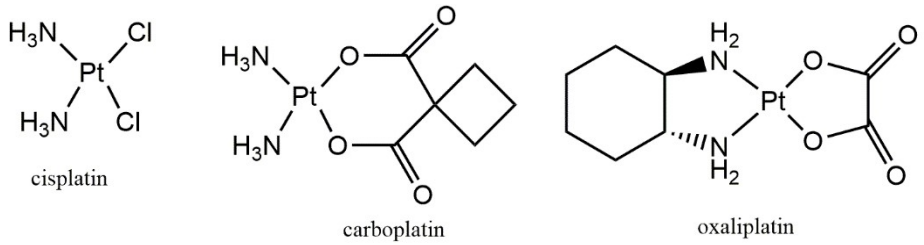

Figure 1. 3.1.1*: Platinum complexes which are used in the chemotherapeutic* [30]

The cisplatin showed limitations in the use of the chemotherapy which was a drug resistance.[31] This setback was found to occur within the carriers of the drug (cisplatin) via the cutback in the vacuole.[32] After this problem (cutback) was observed, an establishment of the new metallodrugs containing the different ligands were the solution.[31] Jennet *et al.*[33] discovered the intercalation to the double-stranded DNA by the [Pt(2,2',2''-terpyridine)S($(CH_2)_2OH$)]$^+$ and [Pt(2,2',2''-terpyridine)(HET)]$^+$ complexes, using viscosity studies. Ligands such as 1.10-phenanthroline and 2,2'-bipyridine showed intercalation to the biding sites of the DNA.[34,35] Studies showed that when these ligands intercalate DNA in a non-square planar complex, the intercalation becomes weak, this is caused by the size of the complex.[36] However, the square planar complexes showed several ways to bind with the DNA, which include binding through a major groove or minor groove or even partial intercalation.[31] Wong *et al.*[17] discovered that the [Pt(terpy)(HET)]$^+$ complex binds with the DNA strand via the major groove. In another study discovered, it was found that the platinum metallodrugs containing phenanthroline and phenanthraquinone ligands bind the short sequence of nucleotide through the minor groove.[36,37]

Inorganic metals attracted more attention since they showed activity against the cancer cells at a much lower concentration compared to the alkylating agent cisplatin.[38] The newly discovered metal complexes showed to overcome the drug resistance suffered by the cisplatin drug.[37] Aldrich-Wright and Co-workers investigated the relationships between the structure [Pt(dmp)(SS-dach)]$^{2+}$ complexes and the anticancer activity.[36] Their studies showed that this complex was exhibited 12 times the cytotoxic activity compared to cisplatin.

Brodie investigated platinum complexes (*Figure 1.3.1.2*) bearing 5,6-dimethyl-1.10-phenanthroline derivatives against the L1210 mouse leukaemia cell line showed significant activity.[37] The dmp in particular was shown to exhibit higher activity compared to cisplatin. This ligand type when coordinated to the metal also showed a significant activity on several different cancer cell lines which were found to be barrier to the platinum based (*Figure* 1.3.1.2).[38]

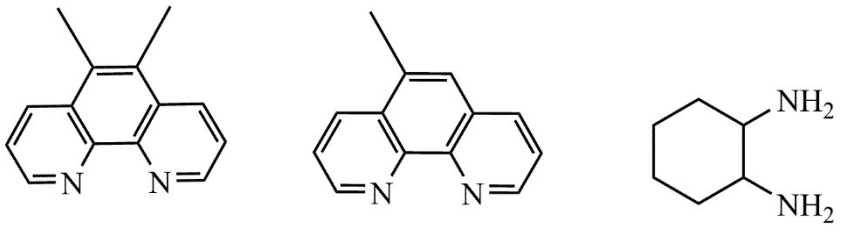

Figure 1.3.1.2*: Shows 1.10-phenanthroline derivatives and chiral diimine ligand tested for cancer against L1210 mouse leukaemia*[38]

Although platinum bearing diimine ligands showed high activity against cancer, the solubility of such Pt(II) complexes is minimal Kotze *et al.*[39] Acylthiourea has a vital role in the design of metal complexes as it improves the solubility and have some potential chemotherapy activity.[40]

1.3.2 Palladium (II) complexes tested for cancer activity

There are many similarities between Pd (II) and Pt (II), such that there is a sizable interest in investigating Pd (II) complexes for potential cancer drugs.[41] It had been reported in the literature that the aquation and ligand exchange rate of Pd(II) compounds are about 10^5 times faster compares to those of Pt analogues and shows improved lipophilicity than Pt complexes.[41,42] Consequently, much attention has been focused on investigating new palladium metallodrugs with upgraded pharmacological properties.[43] Because of this faster exchange of the ligand, the palladium complexes tend to lose their structural identity in the biological fluids sufficiently to get to the pharmacological target.[44] Therefore, finding a suitable ligand that would stabilized the structural lose of the complex is important.[45] It has also been reported that numerous palladium complexes with aromatic N – and N, N-containing ligands, N, O- containing ligands, and ligands chelating with *N, S* donor atoms have very encouraging anti-tumour characteristics.[46] Palladium complexes containing *N, N*-diethyl-*N'*-4-nitro benzoyl thiourea and *N,N*-di(ethyl)-*N'*-4-nitrobenzoylselenourea and 1.10-phenanthroline or its derivatives have been shown to intercalate with DNA, consequently displaying significant in vitro anti-tumour activity.[47] Both complexes were reported to show square-planar coordination (*Figure 1.3.2.*1) with chalcogenoureato and 1.10-phenanthroline ligands coordinated in a bidentate fashion.[47]

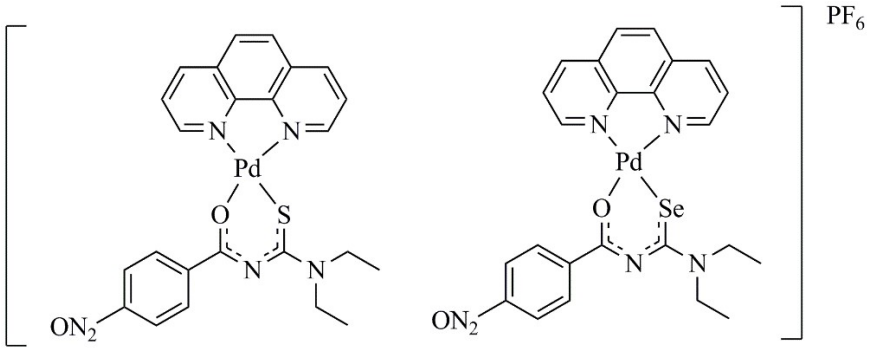

Figure 1.3.2.1*: Structures of some Pd(II) complexes tested for a potential anti-cancer*[47]

A series of glyco-conjugated Pd(II) complexes (*Figure 1.3.2.2*) were reported to have been synthesized by Tanaka *et al*.[48] [$PdCl_2$(2-deoxy-2-(2-pyridinylmethylene)amino]-α-D-glucopyranose was analyzed for its cytotoxicity, ability to induce apoptosis, and further ability to induce DNA double-strand breaks in cis-platin sensitive and cis-platin resistant gastric cancer cell lines in *vitro* and in *vivo.*[49] It was reported that this glyco-conjugated Pd(II) complex show a notable cancer activity.[50]

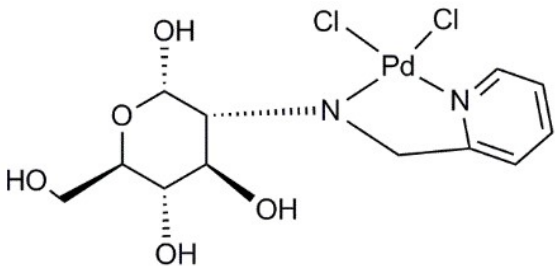

Figure 1.3.2.2*: glyco-conjugated Pd(II) complex chemical structure*[50]

Some of the palladium complexes bearing various types of nitrogen ligands, such as 1.10-phenanthroline, have been utilized in coordination chemistry in research to design anticancer drugs.[51][52] Due to its planarity, therefore, it could be spatulated that the palladium complexes would have similar DNA intercalator.[46] Complexes bearing 1.10-phenanthroline (*Figure 1.3.2.3*) and those containing bipyridine were evaluated and found to be active.

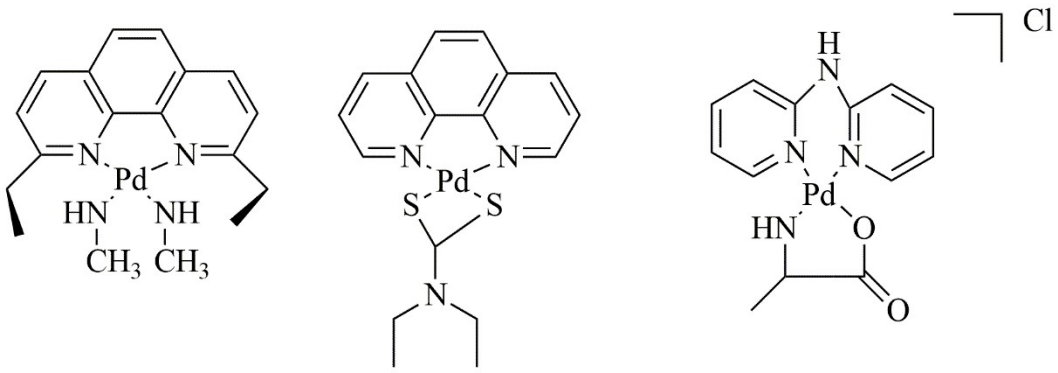

Figure 1.3.2.3*: Palladium(II) complexes bearing various types of nitrogen ligands*[46]

1.3.3 Copper complexes with anticancer activity

Cu(II) salt was reported to exhibit cytotoxicity effect when tested against none-human cancer cells.[53] Interestingly, a further study discovered that copper compounds exhibited higher cancer activity.[54] The first compounds found to be active against the cancer cells were the thiosemicarbazones. Mono-thiosemicarbazone and bis-thiosemicarbazone copper compounds were developed to investigate their potential as anti-cancer agents (*Figure 1.3.3.1*).[55]

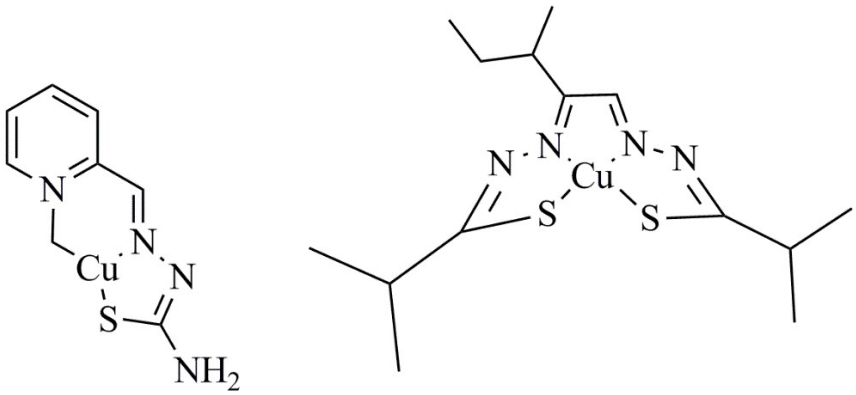

Figure 1.3.3.1*: Illustration of structures for copper(II) minithiosemicarbazone and bisthiosemicarbazone* [55]

Another copper (II) thiosemicarbazone was synthesized and tested for in *vivo* anti-tumour activity (*Figure 1.3.3.2*).[56] The oxidation and reduction happening in copper metals could somehow be the important factor for its cytotoxicity effect.[57]

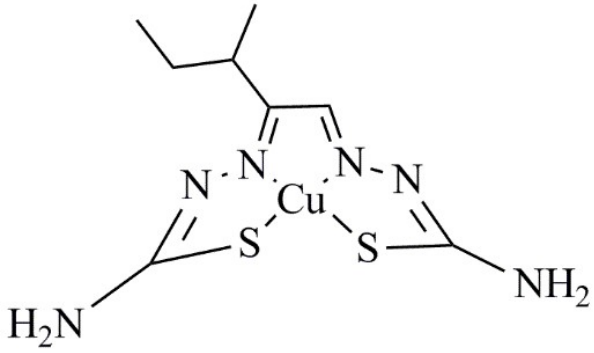

Figure 1.3.3.2*: Cu(II) KTS-One of the first compounds for copper complexes to be screened against cancer cells* [57]

A macrocyclic copper chelate was also synthesized, and interestingly, this compound was found to have some form of activity against against P388 leukaemia a (*Figure 1.3.3.3*).[58]

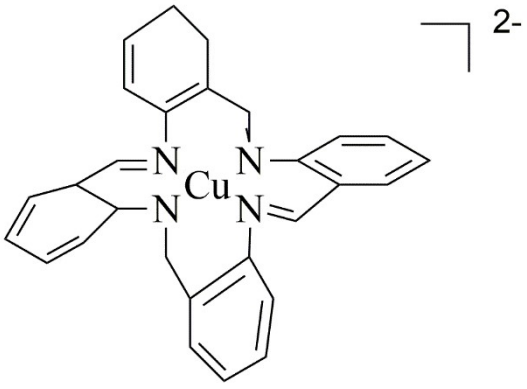

Figure 1.3.3.3*: square planar chelate of the macrocyclic ligand with cancer activity*[58]

Linus Pauling reported that the Cu(II) complex of the glycyl histidine linked with vitamin C showed a complete regressions of the osteosarcoma cancer cells.[59] A Cassiopeia copper complexes was tested against the cancer cells and it was discovered to have shown activity (*Figure 1.3.3.4*).[60] The mechanism of action for this complex was believed to include imbalance between free radicals and antioxidants. Another study about the Casiopeina IIgly indicated that the excess sensitive response of the oxygen led to the powerhouse disruption as well as killing of cells.[61] The complex was also tested against brain tumour stem cells in *vitro* as well as in *vivo* Still.[62]

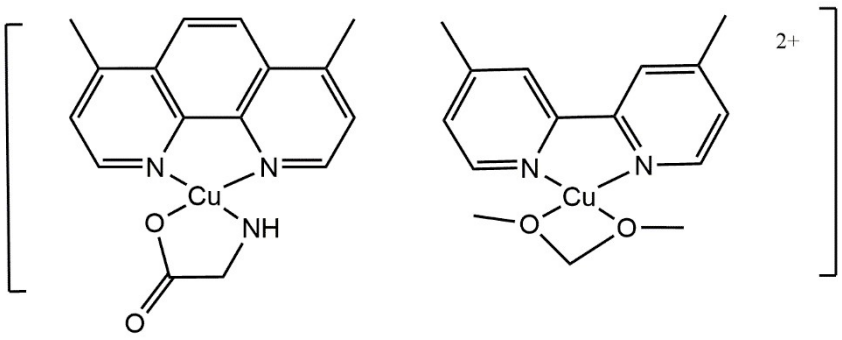

Figure 1.3.3.3.4*: The structure of casiopeina IIgly and casiopeina IIIi*[60]

1.3.4 Zinc Complexes with Antitumor Activity

Semi carbazones complexes have shown some activity against cancer cells.[63] Reports have suggested that semi carbazones have strong antiproliferative properties, which are even more potent than cisplatin.[63] The carbazones complexes were discovered to be active against the tumour vacuole.[64] Zinc complexes with a group of p-isopropyl benzaldehyde thiosemicarbazones showed specific cytotoxic activity against Pam-ras cancer.

Additionally, the N-glycosyl saccharide synthesized from the 4-phenylthiosemicarbazide were screened against the cancer cells.[65] Zn(II) complexes exhibited IC_{50} lower than cisplatin in the Ehrlich Ascites Carcinoma model.[66] Such complexes were then regarded as future safer drugs. Selenosemicarbazone was another example of a complex that was derived from semi carbazones and showed activity.[67] These selenosemicarbazone were discovered to have coordinated differently to the transitional metals.[67]

The Zn(II) complexes bearing the cyclin-dependent kinases (CDK_s) were discovered and this type of the complex showed better cytotoxicity activity compared to the selenosemicarbazones complex.[68] Another interesting part was that three of four zinc complexes of the 3,6,9-

trisubstituted purine derivatives showed a significant increase in activity over their corresponding free ligands.[69] The Zn(II) complexes were obtained with derivatives of the isoflavones, 4'-methoxy-5,7-dihydroxy-isoflavone ligands (*Figure 1.3.4.1*). these zinc complexes exhibited moderate anti-tumour activity in *vivo*. However, the complex showed more activity than free ligand and metal ion.[70] In comparison with the cisplatin, the complex was less active.

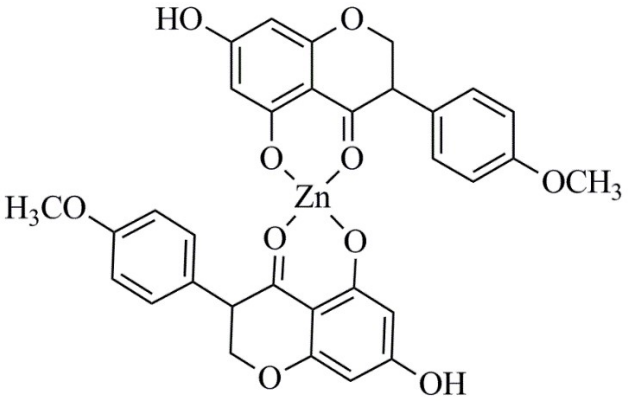

***Figure 1.3.4.1**: Zinc(II) complex of bis-4'-methoxy-5,7-dihydroxy-isoflavone* [70]

In literature, it was reported that the mechanism of potential anticancer activity of Zn^{2+} complexes was presumed to relate to (i) rapid inter-conversion between coodination states (4, 5, and 6) and (ii) variable coordination geometries that it can form with diverse donor site of the appropriate nucleophile.[71,72] A couple of planar aromatic ligands have been employed to synthesize monomeric and binuclear complexes (*Figure 1.3.4.2*).[73] These complexes were tested against several cancer cells, and they showed cancer activity and selectivity. Penta-coordinated complexes were found to be more active than hexacoordinated complexes.

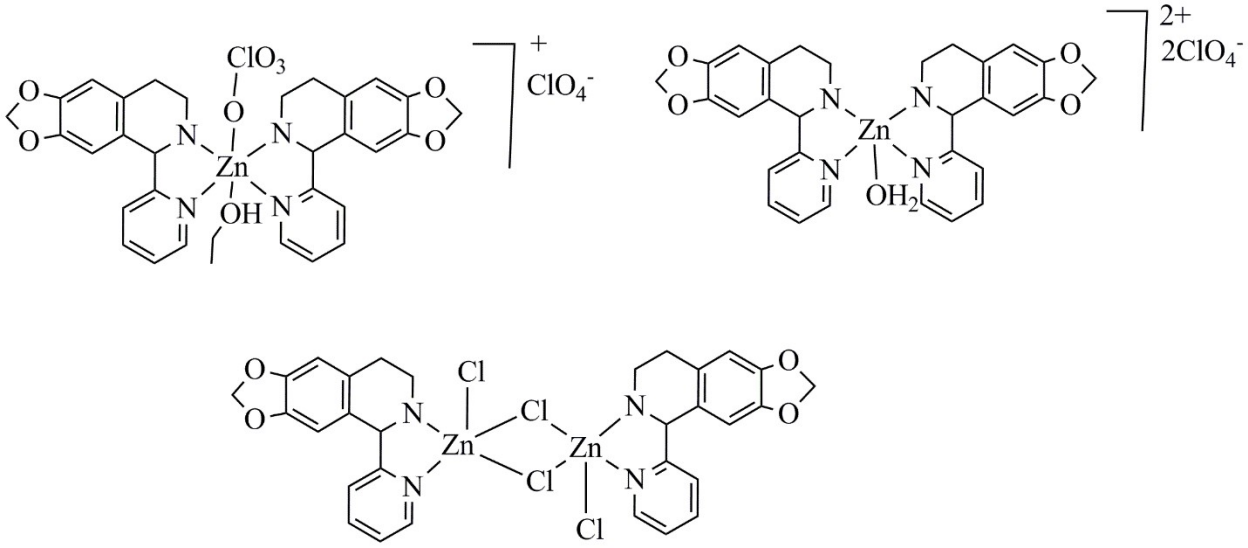

***Figure 1.3.4.2**: penta-coordinated and hexacoordinated Zn(II) complexes*[7

1.4 Coordination of metals to *N, N*-diethyl-*N*-benzoyl thiourea

N, N-di(ethyl)-*N*'-benzoylthiourea (*Figure 1.4.1*) was first synthesized by K. Nuecki in 1873.[74] Since then, many ligands have been synthesized following the same route of varying the alkyl or aryl group, and some of these ligands have shown some very significant properties.

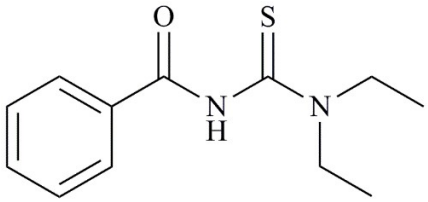

Figure 1.4.1*: showing a general structure of N,N-di(ethyl)-N'-benzoylthiourea ligand*

These ligands coordinate with a metal centre via the oxygen and sulphur atoms, and this happens after the deprotonation from the central nitrogen atom. Hoyer and Beyer studied the acid and the stability constant of some of the acylthiourea such as *N, N*-di(2-hydroxyethyl) *N*-benzoylthioureato with the first plus second row transitional metals.[75] Koch *et al.* showed that these ligands coordinated the central metals like palladium and platinum via the sulphur and oxygen atoms forming a stable cis-[M(L^n-*S, O*)$_2$] (M=Pd(II), Pt(II) complexes. *N,N*-di(ethyl)-*N'*-benzoylthiourea was also found to coordinate with the metals such as Pd(II), Cu(II), Ni(II) via sulphur and oxygen atoms.[76] Such complexes produced from such coordination have useful applications in medicine.[76] Coordination of the *N, N*-di(ethyl)-*N'*-acyl (aryl)thiourea to Pt(II) is expected to depend on the acidity of the reaction medium. The effect of acid on the ease of such complex formation with the *N, N*-(dialkyl)-*N*-benzoylthioureto ligands have previously been studied by Schuster and co-workers under various the pH conditions.[77] The study of pH-dependent complex formation was useful for solvent–solvent extraction, pre-concentration of the metals from acid solutions, and separating the solutions.

It was discovered that the present of the strong donors (O/N) and soft donor (S) in the complexes may results in different coordination to the metal.[78] One of the coordination modes includes the bidentate coordination mode (L-κ*O,S*) that occurs after deprotonation of the N-H.[79] The second type of coordination would be monodentate, which occurs through the sulphur atom which is a softer donor (L-κ*S*) (*Figure 1.4.2*).[79]

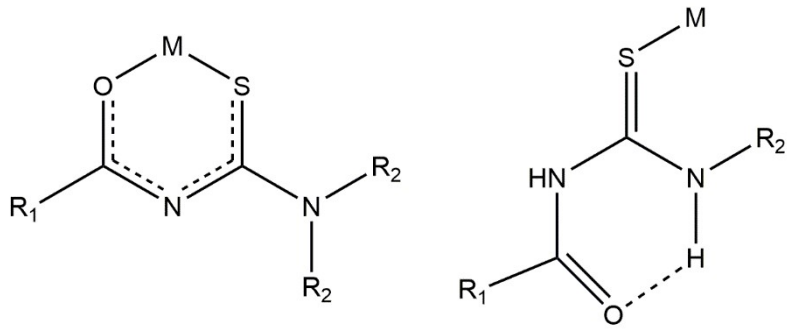

Figure 1.4.2*: The structure of acylthiourea ligand showing different coordination modes*

Another group of ligands like the *N, N*-(dialkyl)-*N*-acyl(aryl)thiourea are the mono-saturated analogues generally known as n-alkyl-N-acyl(aryl)thioureas.[80] Coordination of this set of ligands to transition metals is also possible but occurs only through the sulphur atom of the ligands.[81] Complexes of Cu (II), Ni (II), Pt (II), Pd (II), Co (II) with *N*-phenyl-*N*-(2-phenolyl) thiourea formed after such coordination have been previously obtained, and their biological activity on some category of bacteria also tested.

In the *N*-alkyl-*N*-acyl(aryl)thioureas, an intramolecular hydrogen bond linking the carbonyl and thiourea NH moieties is possible.[81] This leads to structural and conformational differences between the ligands compared to the *N, N*-dialkyl-*N*-acyl(aryl)thioureas. The intramolecular hydrogen bond locks the C(O)NHC(S)NHR group in a six-membered ring conformation; whereas, a twisted conformation is formed for the *N, N*-dialkyl-*N*-acyl(aryl)thiourea in which hydrogen bonding is absent.[82]

The difference in the structural conformation when the two sets of acylthiourea ligands has been used in the reaction mixture for the complex formation results in the distribution of cis/trans isomerism.[82] The formation of a cis-[Pt(H_2*L*-*S*)$_2$$Cl_2$] complexes formed could undergo a solvent dependent isomerization.[83]

1.5 Reversible Binding modes into DNA-Strand

There are various modes in which a drug interact with DNA, namely, covalent binding or/ cross-linking, non-covalent binding, intercalation, DNA cleavage, or nucleoside-analogue incorporation.[84]

Groove binding is customarily based on polyamines that are protonated under functional states that firmly interact with the deoxyribonucleic acid.[85] These molecules usually have the shape that allows them to bind into the major or minor groove of the DNA.[85] The minor groove can only be observed when the part in the DNA backbones are nearer to one another in the double helix (*Figure 1.5.1*).

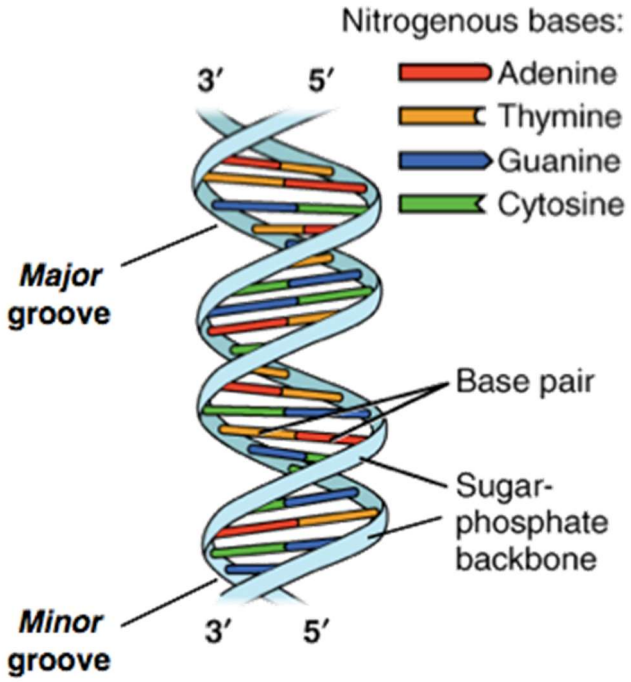

Figure 1.5.1*: Arrangement of the minor and major groove in DNA double helix*[85]

Within the DNA strands, there are intermolecular interactions that serve to stabilize the groove binding.[86] This type of binding does not give a significant amount of configuration changes in the DNA because it acts as the isolator.[86]

Whereas the electrostatic interaction merely involves metal cations like Mg^{+}/Na^{+}, the strength of the DNA conformation requires ion-pairing with the metal through the method called the counter ion conjecture.[87] The interaction of the organic cationic molecules with the DNA counterbalances phosphate charges, resulting to the release of condensed counter ions.[88]The aromatic molecules groove binders can intercalator the DNA site through the positive charge of the binder (*Figure 1.5.2*).[89]

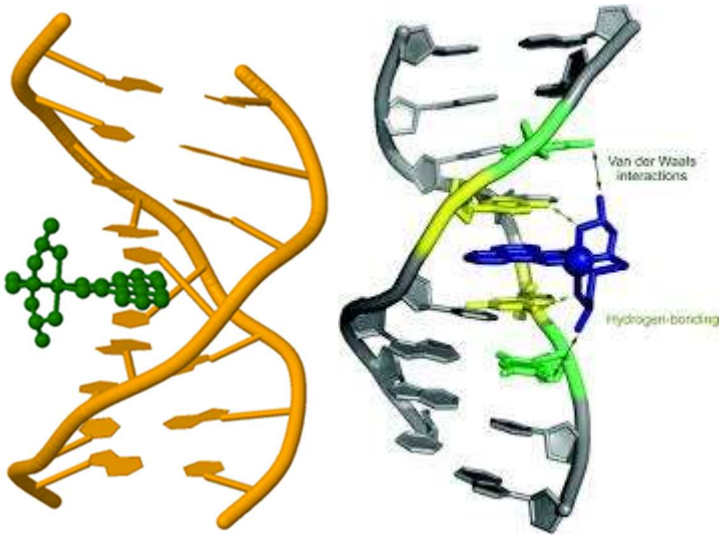

***Figure 1.5.2**: Illustration of metallo-intercalator and groove binding showing Van der Waals interactions* [89]

According to Mcghee and Hippel, intercalations can occur even without destruction of hydrogen bonding within the base pairs.[90] In order for this process to occur, the base pairs within the DNA must move apart to at least 3.4 Å apart to allow the coming planar complex to widen the DNA site and attach freely . The B-form DNA can rotate at an acute angle for the accommodation of the ligand by the DNA strand.[91] This intercalation is understood to occur due to hydrophobic interaction with the ligand.

1.6 Aims and Objectives of this study

From the review of *N,N*-di(alkyl)-*N'*-acylthiourea and 1,10-phenanthroline ligands and their various metal complexes, it is clear that these ligands lead to stable complexes that can be isolated as useful complexes. Due to the interest in developing new metal complexes as anticancer agents, the primary aim was to prepare Pd(II), Pt(II), Cu(II), and Zn(II) bearing phenanthroline derivatives, and *N,N*-di(ethyl)-*N'*-benzoylthiourea as an ancillary ligand. The choice of complexes emanates from earlier studies that showed that [Pt(diimine)(L-κ*O*,*S*)]Cl complexes have anticancer activity. The secondary aim was to screen the synthesized complexes as potential anticancer agents. To achieve the primary and secondary aims of this project, objectives are as follows; (i) synthesis and characterization of *N,N*-di(ethyl)-*N'*-benzoylthiourea, (ii) synthesis and characterization of [MCl_2(diimine)] metal precursors (where M = Pd^{2+}, Pt^{2+}, Cu^{2+} and Zn^{2+}), (iii) synthesis and characterization of [M(diimine)(L-κ*S, O*)]X complexes where L = *N,N*-di(ethyl)-*N'*-benzoylthioureato ligand and X =

counterion), and (iv) evaluation of the synthesized complexes for anticancer activity against A549 lung carcinoma as well as HEK-293 human Embryonic kidney cancer cell lines.

1.7 REFERENCES

[1] X. Ma, H. Yu, *Yale J. Biol. Med.* **2006**, *79*, 85–94.

[2] V. Hanf, R. Kreienberg, *Corpus Uteri*, **2003**,197-279

[3] R. L. Siegel, K. D. Miller, A. Jemal, *CA. Cancer J. Clin.* **2019**, *69*, 7–34.

[4] V. Ruiz-Torres, J. A. Encinar, M. Herranz-López, A. Pérez-Sánchez, V. Galiano, E. Barrajón-Catalán, V. Micol, *Molecules* **2017**, *22*, DOI 10.3390/molecules22071037.

[5] G. Dranitsaris, M. Johnston, S. Poirier, T. Schueller, D. Milliken, E. Green, B. Zanke, *J. Oncol. Pharm. Pract.* **2005**, *11*, 69–78.

[6] H. Sung, J. Ferlay, R. L. Siegel, M. Laversanne, I. Soerjomataram, A. Jemal, F. Bray, *CA. Cancer J. Clin.* **2021**, *71*, 209–249.

[7] T. A. Shapiro, P. T. Englund, *Annu. Rev. Microbiol.* **1995**, *49*, 117–143.

[8] K. A. Higgins, K. O'Connell, Y. Liu, T. W. Gillespie, M. W. McDonald, R. N. Pillai, K. R. Patel, P. R. Patel, C. G. Robinson, C. B. Simone, T. K. Owonikoko, C. P. Belani, F. R. Khuri, W. J. Curran, S. S. Ramalingam, M. Behera, *Int. J. Radiat. Oncol. Biol. Phys.* **2017**, *97*, 128–137.

[9] S. Schwarzbich, C. Horstmann Née Gruschka, J. Simon, L. Siebe, A. Moreth, C. Wiegand, A. Lavrentieva, T. Scheper, A. Stammler, H. Bögge, G. Fischer Von Mollard, T. Glaser, *Inorg. Chem.* **2020**, *59*, 14464–14477.

[10] T. Glaser, J. Simon, A. Stammler, J. Oldengott, H. Bögge, *Inorg. Chem.* **2020**, *59*, 14615–14619.

[11] S. H. E. Kaufmann, *Nat. Rev. Drug Discov.* **2008**, *7*, 373.

[12] R. Martinez, L. Chacon-Garcia, *Curr. Med. Chem.* **2012**, *12*, 127–151.

[13] R. Palchaudhuri, P. J. Hergenrother, *Curr. Opin. Biotechnol.* **2007**, *18*, 497–503.

[14] R. Siegel, C. DeSantis, K. Virgo, K. Stein, A. Mariotto, T. Smith, D. Cooper, T. Gansler, C. Lerro, S. Fedewa, C. Lin, C. Leach, R. S. Cannady, H. Cho, S. Scoppa, M. Hachey, R. Kirch, A. Jemal, E. Ward, *CA. Cancer J. Clin.* **2012**, *62*, 220–241.

[15] T. Ozben, *FEBS Lett.* **2006**, *580*, 2903–2909.

[16] A. Z. Ayob, T. S. Ramasamy, *J. Biomed. Sci.* **2018**, *25*, 1–18.

[17] H. L. Wong, R. Bendayan, A. M. Rauth, Y. Li, X. Y. Wu, *Adv. Drug Deliv. Rev.* **2007**,

59, 491–504.

[18] V. S. Donnenberg, A. D. Donnenberg, *J. Clin. Pharmacol.* **2005**, *45*, 872–877.

[19] L. Kelland, *Nat. Rev. Cancer* **2007**, *7*, 573–584.

[20] J. A. Ferreira, A. Peixoto, M. Neves, C. Gaiteiro, C. A. Reis, Y. G. Assaraf, L. L. Santos, *Drug Resist. Updat.* **2016**, *24*, 34–54.

[21] E. C. Sutton, C. E. McDevitt, M. V. Yglesias, R. M. Cunningham, V. J. DeRose, *Inorganica Chim. Acta* **2019**, *498*, 118984.

[22] A. F. A. Peacock, P. J. Sadler, *Chem. - An Asian J.* **2008**, *3*, 1890–1899.

[23] A. D. Richards, A. Rodger, *Chem. Soc. Rev.* **2007**, *36*, 471–483.

[24] J. E. House, *Inorg. Chem.* **2019**, *4*, 1–978.

[25] S. Basu, S. Pacelli, Y. Feng, Q. Lu, J. Wang, A. Paul, *ACS Nano* **2018**, DOI 10.1021/acsnano.8b02434.

[26] M. Fuertes, J. Castilla, C. Alonso, J. Pérez, *Curr. Med. Chem.* **2012**, *10*, 257–266.

[27] P. L. Privalov, C. Crane-Robinson, *Prog. Biophys. Mol. Biol.* **2018**, *135*, 30–48.

[28] S. N. Georgiades, N. H. Abd Karim, K. Suntharalingam, R. Vilar, *Angew. Chemie - Int. Ed.* **2010**, *49*, 4020–4034.

[29] S. Gómez-Ruiz, D. Maksimović-Ivanić, S. Mijatović, G. N. Kaluderović, *Bioinorg. Chem. Appl.* **2012**, *2012*, 15–17.

[30] B. Desoize, C. Madoulet, *Crit. Rev. Oncol. Hematol.* **2002**, *42*, 317–325.

[31] I. Eryazici, C. N. Moorefield, G. R. Newkome, *Chem. Rev.* **2008**, *108*, 1834–1895.

[32] F. K. Keter, J. Darkwa, *BioMetals* **2012**, *25*, 9–21.

[33] L. Strekowski, B. Wilson, Biometal **2007**, *623*, 3–13.

[34] G. Yahioglu, S. Studies, Chemical society **1972**,23(5),327-334

[35] S. Roy, K. D. Hagen, P. U. Maheswari, M. Lutz, A. L. Spek, J. Reedijk, G. P. Van Wezel, *ChemMedChem* **2008**, *3*, 1427–1434.

[36] C. R. Brodie, J. G. Collins, J. R. Aldrich-Wright, *J. Chem. Soc. Dalt. Trans.* **2004**, *4*, 1145–1152.

[37] J. Moretto, B. Chauffert, F. Bouyer, *Metallointercalators* **2011**, DOI 10.1007/978-3-211-99079-7.

[38] A. M. Krause-Heuer, R. Grunert, S. Kuhne, M. Buczkowska, N. J. Wheate, D. D. Le Pevelen, L. R. Boag, D. M. Fisher, J. Kasparkova, J. Malina, P. J. Bednarski, V. Brabec, J. R. Aldrich-Wright, *J. Med. Chem.* **2009**, *52*, 5474–5484.

[39] Izak Aldert Kotzé Thesis Presented for the Degree of Masters in Chemistry, **2009**.Stellenbosch University.

[40] K. R. Koch, J. Toit, M. R. Caira, C. Sacht, **1994**, *88*, 785–786.

[41] E. Z. Jahromi, A. Divsalar, A. A. Saboury, S. Khaleghizadeh, H. Mansouri-Torshizi, I. Kostova, *J. Iran. Chem. Soc.* **2016**, *13*, 967–989.

[42] A. G. Quiroga, C. N. Ranninger, *Coord. Chem. Rev.* **2004**, *248*, 119–133.

[43] G. Marverti, G. Gozzi, A. Lauriola, G. Ponterini, *International of molecular sciences* **n.d.**, 1–19.

[44] L. Giovagnini, C. Marzano, F. Bettio, D. Fregona, *J. Inorg. Biochem.* **2005**, *99*, 2139–2150.

[45] D. Karakas, B. Cevatemre, N. Aztopal, F. Ari, V. T. Yilmaz, E. Ulukaya, *Bioorganic Med. Chem.* **2015**, *23*, 5580–5586.

[46] A. Abu-Surrah, H. Al-Sa'doni, M. Abdalla, *Cancer Ther.* **2008**, *6*, 1–10.

[47] A. Molter, S. Kathrein, B. Kircher, F. Mohr, *Dalt. Trans.* **2018**, *47*, 5055–5064.

[48] P. Banerjee, P. Majumder, S. Halder, M. G. B. Drew, S. Bhattacharya, S. Mazumder, *Free Radic. Res.* **2015**, *49*, 253–268.

[49] I. P. Ferreira, G. M. De Lima, E. B. Paniago, J. A. Takahashi, C. B. Pinheiro, *Inorg Chim. Act* **2014**, *423*, 443–449.

[50] A. Jahanian-Najafabadi, M. Mirian, F. Rohani, K. Karami, M. H. Kharat, H. Sadeghi-Aliabadi, *Iran. J. Pharm. Res.* **2019**, *18*, 1323–1331.

[51] A. Savić, T. Marzo, F. Scaletti, L. Massai, G. Bartoli, R. Hoogenboom, L. Messori, R. Van Deun, K. Van Hecke, *BioMetals* **2019**, *32*, 33–47.

[52] L. Tabrizi, H. Chiniforoshan, *Invest. New Drugs* **2016**, *34*, 723–732.

[53] D. S. Sigman, A. Mazumder, D. M. Perrin, *Chem. Rev.* **1993**, *93*, 2295–2316.

[54] J. Easmon, G. Pürstinger, G. Heinisch, T. Roth, H. H. Fiebig, W. Holzer, W. Jäger, M. Jenny, J. Hofmann, *J. Med. Chem.* **2001**, *44*, 2164–2171.

[55] D. Palanimuthu, S. V. Shinde, K. Somasundaram, A. G. Samuelson, *J. Med. Chem.* **2013**, *56*, 722–734.

[56] R. Anjum, D. Palanimuthu, D. S. Kalinowski, W. Lewis, K. C. Park, Z. Kovacevic, I. U. Khan, D. R. Richardson, *Inorg. Chem.* **2019**, *58*, 13709–13723.

[57] B. Imaging, *Ann. Nucl. Med.* **2001**, *15*, 499–504.

[58] C. Santini, M. Pellei, V. Gandin, M. Porchia, F. Tisato, C. Marzano, *Chem. Rev.* **2014**, *114*, 815–862.

[59] R. M. Whittal, H. L. Ball, F. E. Cohen, A. L. Burlingame, S. B. Prusiner, M. A. Baldwin, *Protein Sci.* **2008**, *9*, 332–343.

[60] V. Pinto, R. Bergantim, H. R. Caires, H. Seca, J. E. Guimarães, M. H. Vasconcelos,

Cancers (Basel). **2020**, *12*, 1–32.

[61] A. Rivero-Müller, A. De Vizcaya-Ruiz, N. Plant, L. Ruiz, M. Dobrota, *Chem. Biol. Interact.* **2007**, *165*, 189–199.

[62] G. Vértiz, L. E. García-Ortuño, J. P. Bernal, M. E. Bravo-Gómez, E. Lounejeva, A. Huerta, L. Ruiz-Azuara, *Fundam. Clin. Pharmacol.* **2014**, *28*, 78–87.

[63] S. Bjelogrlic, T. Todorovic, A. Bacchi, M. Zec, D. Sladic, T. Srdic-Rajic, D. Radanovic, S. Radulovic, G. Pelizzi, K. Andelkovic, *J. Inorg. Biochem.* **2010**, *104*, 673–682.

[64] A. Garufi, V. Ubertini, F. Mancini, V. D'Orazi, S. Baldari, F. Moretti, G. Bossi, G. D'Orazi, *J. Exp. Clin. Cancer Res.* **2015**, *34*, 1–10.

[65] M. K. Buczkowska, Synthesis, Characterization, Antitumor and Antimicrobial Activities of Heterocyclic Transition Metal Complexes, **2011**,(1)29

[66] N. Raman, R. Jeyamurugan, R. Senthilkumar, B. Rajkapoor, S. G. Franzblau, *Eur. J. Med. Chem.* **2010**, *45*, 5438–5451.

[67] N. Gligorijević, T. Todorović, S. Radulović, D. Sladić, N. Filipović, D. Godevac, D. Jeremić, K. Andelković, *Eur. J. Med. Chem.* **2009**, *44*, 1623–1629.

[68] C. Y. Gao, X. Qiao, Z. Y. Ma, Z. G. Wang, J. Lu, J. L. Tian, J. Y. Xu, S. P. Yan, *Dalt. Trans.* **2012**, *41*, 12220–12232.

[69] C. Republic, C. Republic.*Veterinary parasitology.* **2006**, *100*, 214–225.

[70] X. Chen, L. Tang, Y. Sun, P. Qiu, G. Liang, *J. Inorg. Biochem.* **2010**, *104*, 379–384.

[71] A. Tarushi, G. Psomas, C. P. Raptopoulou, D. P. Kessissoglou, *J. Inorg. Biochem.* **2009**, *103*, 898–905.

[72] R. R. Roe, Y.-P. Pang, *J. Mol. Model.* **1999**, *5*, 134–140.

[73] M. Porchia, M. Pellei, F. Del Bello. *Med.chem* **2020**.

[74] H. A. Nkabyo, K. R. Koch, *J. Mol. Struct.* **2019**, *1190*, 47–53.

[75] N. Selvakumaran, S. W. Ng, E. R. T. Tiekink, R. Karvembu, *Inorg .Chim. Act* **2011**, *376*, 278–284.

[76] K. R. Koch, C. Sacht, S. Bourne.*Inorg,chim, Act* **1995**, *232*.

[77] K. R. Koch. Inorg. chim. Act **1993**, *206*, 193–199.

[78] I. L. Mawnai, S. Adhikari, W. Kaminsky, M. Rao, *J. Organomet. Chem.* **2018**, *869*, 26–36.

[79] C. Sacht, M. S. Datt. *Polyhed.* **2000**, *19*, 1347–1354.

[80] A. M. Cop. *Mat chem and physc*.**2002**, 231–234.

[81] A. M. Plutín, A. Alvarez, R. Mocelo, R. Ramos, E. E. Castellano, M. Monize, L.

Colina-vegas, F. R. Pavan, A. A. Batista, *INOCHE* **2016**, *63*, 74–80.

[82] S. Yaseen, M. Khawar, S. Zaib, A. Badshah, M. Nawaz, M. Irshad, M. Shahid, J. Iqbal, *Inorg Chim. Act* **2016**, *443*, 69–77.

[83] O. Diphenylthioureato-, S. N. Ii, H. Pérez, R. S. Corrêa, B. O. Reilly, A. M. Plutín. *J str chem.* **2012**, *53*, 921–926.

[84] H. Song, J. T. Kaiser, J. K. Barton. *Nat chem*. **2012**, *4*, 615-620

[85] S. Dna, B. S. P. Reddy, S. M. Sondhi, J. W. Lown.*Pharm and therap.* **1999**, *84*, 1–111.

[86] S. Zachariah, A. Nowroozi, K. Sadrjavadi, S. Moradi, K. Mansouri, L. Hosseinzadeh, M. Shahlaei, *Int. J. Biol. Macromol.* **2018**, *114*, 40–53.

[87] S. B. Howerton, A. Nagpal, L. D. Williams, *Biopolymers* **2003**, *69*, 87–99.

[88] J. Cheng, T. J. Deming, *Synthesis of Polypeptides by ROP of NCAs*.*Chem com*. **2011**,139-155.

[89] D. T. Odom, C. S. Parker, J. K. Barton, *Biochemistry* **1999**, *38*, 5155–5163.

[90] J. D. McGhee, P. H. von Hippel, *Biochemistry* **1977**, *16*, 3276–3293.

[91] F. A. Tanious, W. D. Wilson, S. F. Yen, *Biochemistry* **1991**, *30*, 1813–1819.

CHAPTER 2

Synthesis and characterization of N,N-di(ethyl)-N'-benzoylthiourea and mixed ligand Cu(II), Pd(II), Zn(II), Pt(II) diimine complexes

2.1 Introduction

This chapter discusses the syntheses of different mixed ligand metal complexes bearing *N,N*-di(ethyl)-*N*'-benzoylthiourea (**HL**), and 1,10-phenanthroline (phen) or 5,6-dimethyl-1,10-phenanthroline (dmp). Lately, there has been significant interests in other transition metal complexes as potentially anticancer agents which are less toxic and have improved cytotoxicity compared to cisplatin. Palladium(II)-acylthiourea complexes have been reported to have anticancer activity against the MCF-7 breast cancer line and also exhibits anti-*Mycobacterium tuberculosis* and anti-*Trypanosoma cruzi* activity.[1,2] Copper(I) and copper(II)-acylthiourea complexes were shown to have potent antibacterial and antitumor activity;[3,4] while platinum(II)-acylthiourea complexes have been found to have anticancer activities.[5,6] The biological activity of metal complexes reported in these studies inspired us to explore the antitumor activities of the $[M^{II}(phen)(L\text{-}\kappa O,S)]^+$ and $M^{II}(dmp)(L\text{-}\kappa O,S)]^+$ complexes (where M^{II} = Pd(II), Zn(II), Cu(II) and Pt(II) and L = *N,N*-di(ethyl)-*N*'-benzoylthioureato ligand). In a study by Magwaza *et al*., Pt(II) complexes bearing the dmp ligand displayed higher cytotoxicity compared to complexes containing the phen ligand against the A549 cancer cell line. Ligand design is key in discovering transition metal complexes with improved solubility. The ligand design may involve tailoring the ligand's orientation, electronic properties, steric properties, and ligand-exchange chemistry.[7] The metal centre properties (such as redox chemistry, geometry and reactivity) may also significantly influence the potential biological activity of the metal complexes.

N,N-di(ethyl)-*N*'-benzoylthiourea (**HL**) belongs to the disubstituted acylthiourea group, a valuable group of organo-sulfur compounds with interesting potential applications,[8] which are produced *via* a facile synthesis as reported by Douglass and Dains.[9] There are numerous ways to synthesize disubstituted acylthiourea ligand that include (i) reaction of aminothiocarbonylimidoyl chlorides with potassium thiocyanate followed by hydrolysis;[10] (ii) acylation of *N,N*-disubstituted thioureas;[11] (iii) reaction of *N*-acyl aminoimidoyl chlorides[12] or (iv) *N*-acylisothioureas[13] with hydrogen sulfide, reactions of amines with (v) methyl *N*-acylcarbamodithioates[13] and (vi) acyl isothiocyanates;[14] (vii) reactions of iminophosphorane derivatives of thioureas with carboxylic acids,[15] and (viii) hydrolysis of *N*-aminothiocarbonylcarbodiimides with mineral acids.[16] After deprotonation at the central nitrogen, acylthiourea ligands coordinate the metal centre mainly through the sulfur and oxygen donor atoms. The mechanism below (*Scheme 2.1*)illustrates possible electron movements

distribution between the sulfur and oxygen atom after deprotonation resulting in three possible resonance structure.

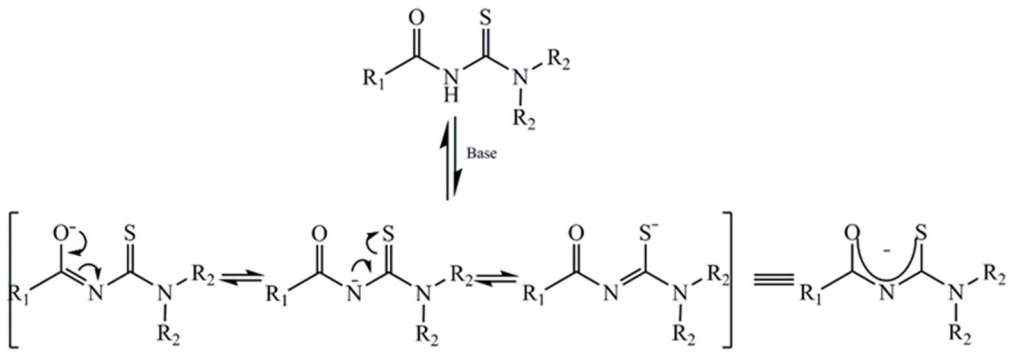

Scheme 2.1: *A summary of the main contributing resonance structure that can occur following the deprotonation of the N,N-di(ethyl)-N'-benzoylthiourea ligand.*

The synthesis of metal complexes of acylthioureas generally involves two common steps, either *in-situ* or stepwise. These include the abstraction of the amidic proton of the acylthiourea ligand with a mild base and substitution of the chloro ligands of the metal precursor with the acylthioureato ligand. In this study, the preparation of several complexes of the form $[M^{II}(phen)(L\text{-}\kappa O,S)]X$ and $[M^{II}(dmp)(L\text{-}\kappa O,S)]X$ were (*Figure 2.2*).

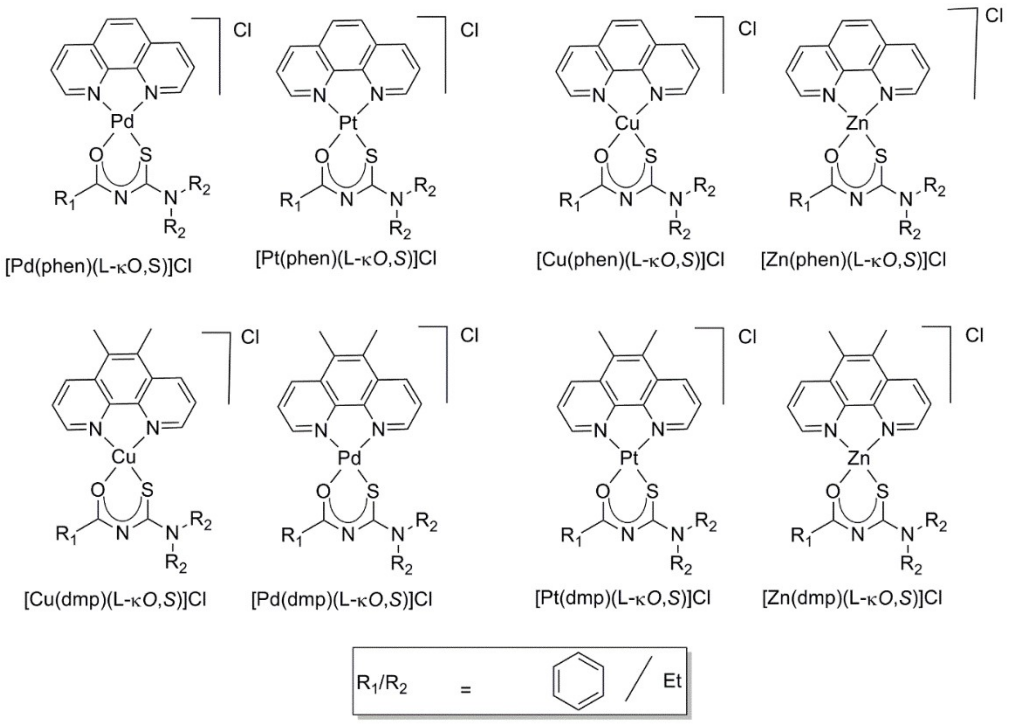

Figure 2.2: *Schematic representation of $[M^{II}(diimine)(L\text{-}\kappa O,S)]X$ complexes of interest in this study.*

2.2 Results and discussion

2.2.1 Synthesis and characterization of *N*, *N*-di(ethyl)-*N*'-benzoylthiourea (HL)

N,*N*-di(ethyl)-*N*'-benzoylthiourea (**HL**) was synthesized according to a slightly modified Douglass and Dains[17] one-pot method (*Scheme 2.3*). This method firstly involved adding benzoyl chloride to a solution of anhydrous potassium thiocyanate in anhydrous acetone under inert conditions and refluxing the mixture for 30 minutes. In this step, the nucleophilic attack can either occur from the two thiocyanate and isothiocyanate mesomeric forms (through the nitrogen of the thiocyanate anion or sulfur of the isothiocyanate anion in acetone).[18] Theoretically, two products are possible depending on the isomer involved; however, in practice, only the acyl isothiocyanate reacts. The acyl-isothiocyanate react with diethylamine in anhydrous acetone under reflux for 30 minutes before the reaction mixture was cooled to room temperature. The *N*,*N*-di(ethyl)-*N*'-benzoylthiourea (**HL**) was obtained as colourless crystals in excellent yield of 87%. The ligand was characterized using NMR spectroscopy, FT-IR spectroscopy, and elemental analysis.

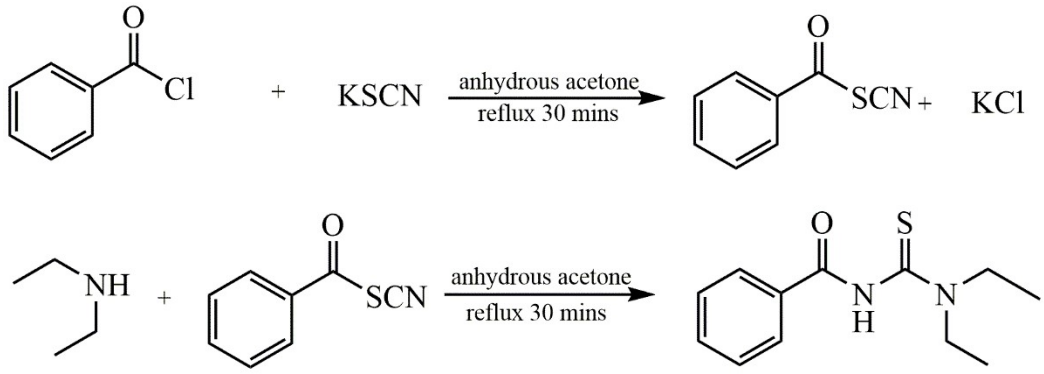

***Scheme 2.3**: Synthesis of N,N-di(ethyl)-N'-benzoylthiourea (**HL**).*

2D-NMR techniques; COSY, HSQC and HMBC was used to unambiguously assign the ^{1}H and ^{13}C spectrum of the **HL**. The ^{1}H NMR spectrum of **HL** (*Figure 2.1*) exhibited peaks due to the amide, phenyl ring and the ethyl substituents. A broad singlet at 8.37 ppm was assigned to the amidic proton (N-H). The aromatic signals $H^{2'+6''}$, $H^{3'+5'}$ and $H^{4'}$ were assigned with the aid of COSY NMR spectroscopy, with the most deshielded signal being $H^{2'+6'}$ due to the electron-withdrawing carbonyl group.

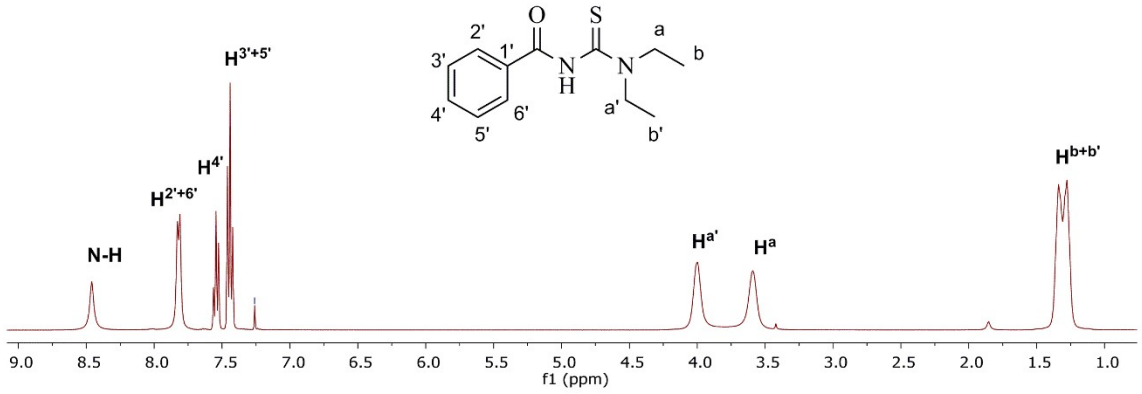

***Figure 2.1**: [1]H NMR spectrum of N,N-di(ethyl)-N'-benzoylthiourea (**HL**) in $CDCl_3$ at 300K assigned as per the numbering scheme indicated.*

The most shielded aromatic proton resonance is observed at 7.47 ppm and assigned to $H^{3'+5'}$ as it shows three bond coupling with two different protons. The proton resonance at 7.57 ppm was assigned to $H^{4'}$ because it only shows strong three bond coupling to one proton.[19]

Integration of the ^{1}H-NMR peaks indicates an agreement in the ratio of protons within the different chemical environments of the ligand. Further characterization was done using ^{13}C NMR spectroscopy. The most deshielded signals at 178 ppm and 164 ppm in the ^{13}C NMR spectrum (*Figure 2.2*) were assigned to the carbonyl and thiocarbonyl carbons. The carbonyl carbon showed three bonds coupling with the phenyl protons $H^{2'+6'}$ in the HMBC NMR spectrum.

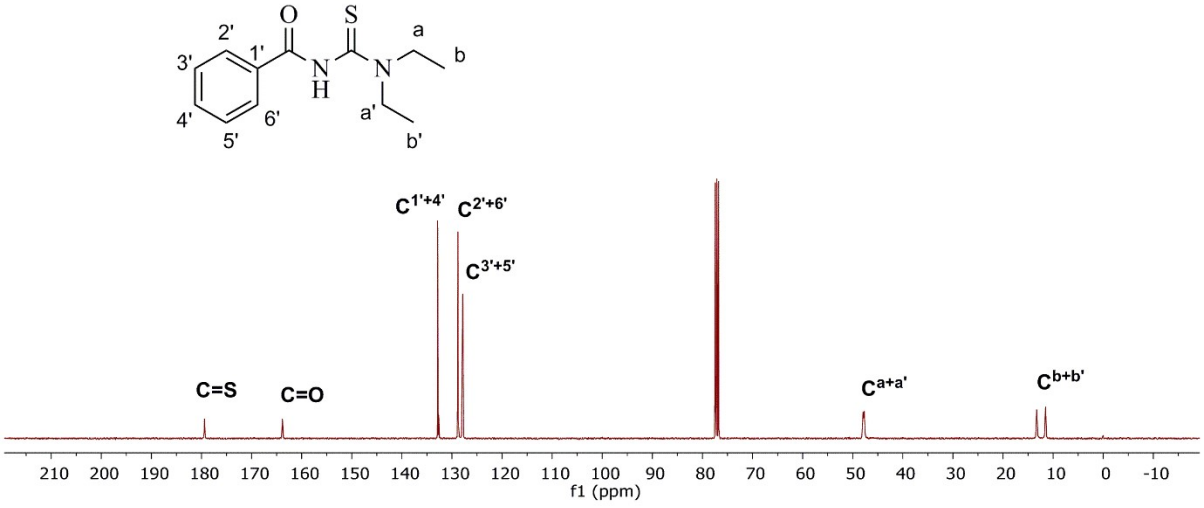

***Figure 2.2:** [13]C NMR spectrum for N,N-di(ethyl)-N'-benzoylthiourea in $CDCl_3$ at 300K.*

The other ^{13}C NMR signals were assigned accordingly using 2D-NMR HSQC spectroscopy. The FT-IR spectrum of *N*,*N*-di(ethyl)-*N*'-benzoylthiourea (**HL**) confirmed the presence of the N-H group with a stretching vibration of a secondary amine at 3206 cm^{-1}. The aromatic and aliphatic C-H, carbonyl C=O, and imine C-N stretching vibrations were observed at 2970 cm^{-1}, 1678 cm^{-1}, 1650cm^{-1}, and 1220 $cm^{-1,}$ respectively. These are a typical stretching frequency for a free ligand (*Figure 2.3*).

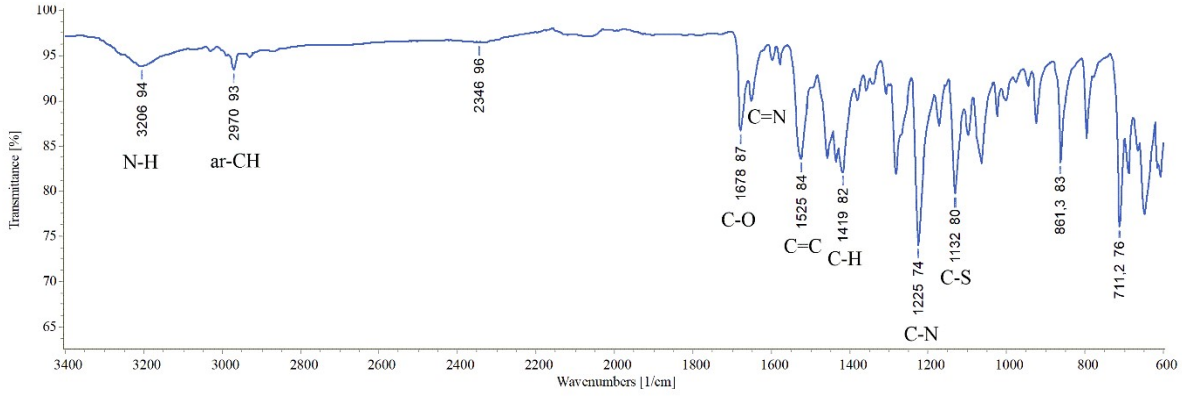

***Figure 2.3**: Infrared spectrum of N,N-di(ethyl)-N'-benzoylthiourea ligand.*

2.2.3 Synthesis and characterization of the [Pd(diimine)(L-κ*O*,*S*)]Cl and its precursors

The palladium precursors [$PdCl_2$(phen)] and [$PdCl_2$(dmp)] were synthesized according to the method described by Morgan and Bustall.[17] The method involved adding 1.10-phenanthroline derivatives (phen or dmp) ligand to an acidic water solution containing either sodium or potassium tetrachloropalladate and refluxing this reaction mixture for 3 hours (*Scheme 2.4*). After a few minutes, a yellow precipitate was formed. The mixture was cool to room temperature and the precipitate was isolated and washed several times with water and acetone to remove traces of unreacted species.

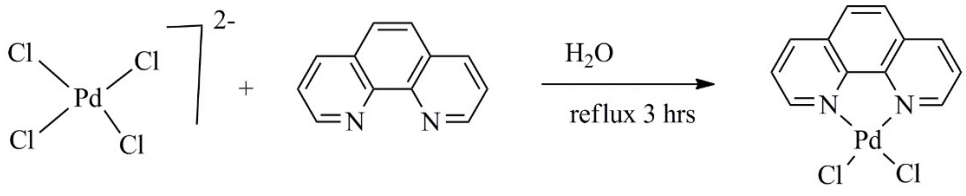

***Scheme 2.4**: Synthesis of [$PdCl_2$(phen)] precursor.*

The metal complex isolated was characterized using NMR spectroscopy, FT-IR spectroscopy and elemental analysis. Due to the C_2 symmetry in [$PdCl_2$(phen)] and [$PdCl_2$(dmp)], only four sets of proton signals were observed in the ^{1}H-NMR spectrum of [$PdCl_2$(phen)] (*Figure 2.4*) and only four sets of proton signals in the ^{1}H-NMR spectrum of [$PdCl_2$(dmp)] (*appendix Figure 1*).

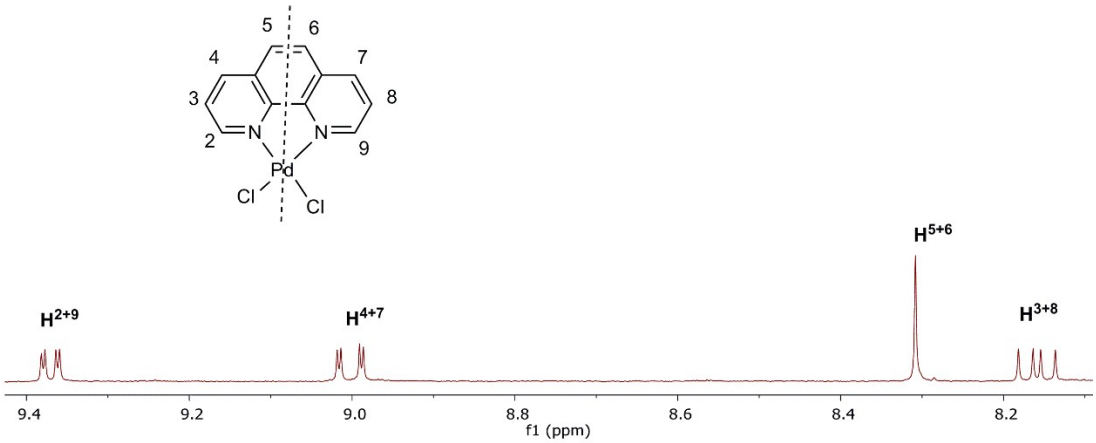

***Figure 2.4**: ^{1}H NMR spectrum for [$PdCl_2$(phen)] in DMSO-d_6 at 300K.*

The ^{1}H proton NMR of the complex [$PdCl_2$(phen)] is broadly discussed. The most downfield doublet of doublets centred at 9.38 ppm ($J_H{}^{2+9}$-$_H{}^{3+8}$ = 1.85 Hz and $J_H{}^{2+9}$-$_H{}^{4+7}$ = 3.68 Hz) was assigned to H^{2+9} due to the electron-withdrawing effects of the nitrogen. The second most deshielded doublet of doublets at 9.0 ppm was assigned to H^{4+7} as short-range coupling with H^{3+8} ($J_H{}^{4+7}$-$_H{}^{3+8}$) = 2.18 Hz) is observed influenced by the electronegative nitrogen and long-range coupling observed with H^{2+9} ($J_H{}^{3+8}$-$_H{}^{2+9}$ = 4.33 Hz). The singlet at 8.3 ppm was assigned to H^{5+6} because there is no coupling present. The doublet of doublets centred at 8.15 ppm was assigned to H^{3+8} due to the short-range coupling observed with both H^{2+9} and H^{4+7} ($J_H{}^{3+8}$-$_H{}^{2+9}$ = $J_H{}^{3+8}$-$_H{}^{4+7}$ = 3.87 Hz). All the ^{1}H-NMR signals integrated for 2 protons each.

The synthesis of [Pd(phen)(L-κ*O*,*S*)]Cl and [Pd(dmp)(L-κ*O*,*S*)]Cl were initially attempted using the method described by Kotze *et al.*[39] A solution of *N,N*-di(ethyl)-*N'*-benzoylthiourea dissolved in dichloromethane was added drop-wise to a suspension of [$PdCl_2$(phen)] or [$PdCl_2$(dmp)] and sodium acetate in the water at room temperature. *N,N*-di(ethyl)-*N'*-benzoylthiourea and [$PdCl_2$(diimine)] were reacted in a 1:1 mole ratio (*Scheme 2.5*) to avoid producing mixture of complexes.

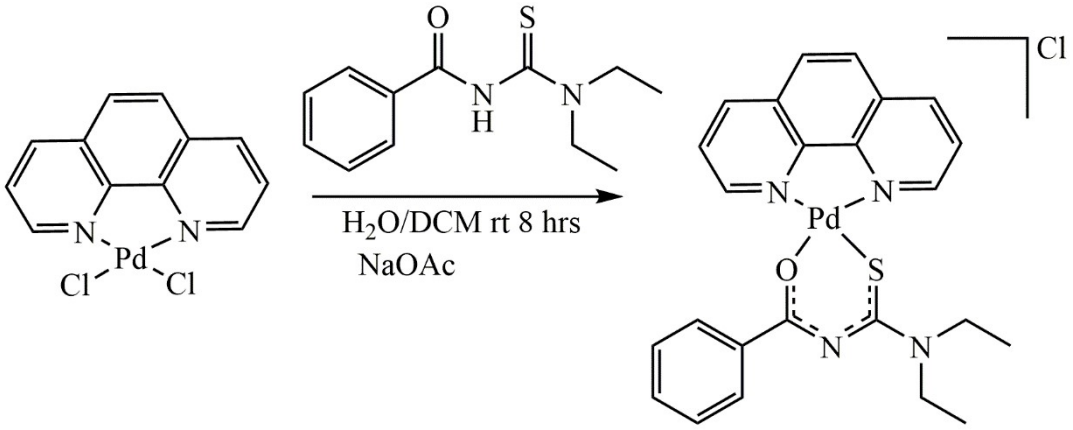

***Scheme 2.5**: General synthesis of the [Pd(phen)(L-κO,S)]Cl at room temperature where a weak base deprotonate a ligand.*

The complex [Pd(phen)(L-κO,S)]Cl was initially characterized using ^{1}H-NMR spectroscopy, and the ^{1}H NMR spectrum (*Figure 2.5*) revealed that this method most likely yielded a [Pd(phen)(L-κ*S*)$_2$] complex with the acylthioureato ligand coordinated in a monodentate fashion. Tentative assignments of the proton signals suggested a symmetric complex with only four sets of proton signals due to the phen ligand. The most shielded aromatic proton signals, which were tentatively assigned to the benzoyl moiety, also suggested monodentate coordination as was observed for complexes reported by Kotzé *et al*.[22] It was thus necessary to optimize this method get the desired complex as proposed in the schematic diagram.

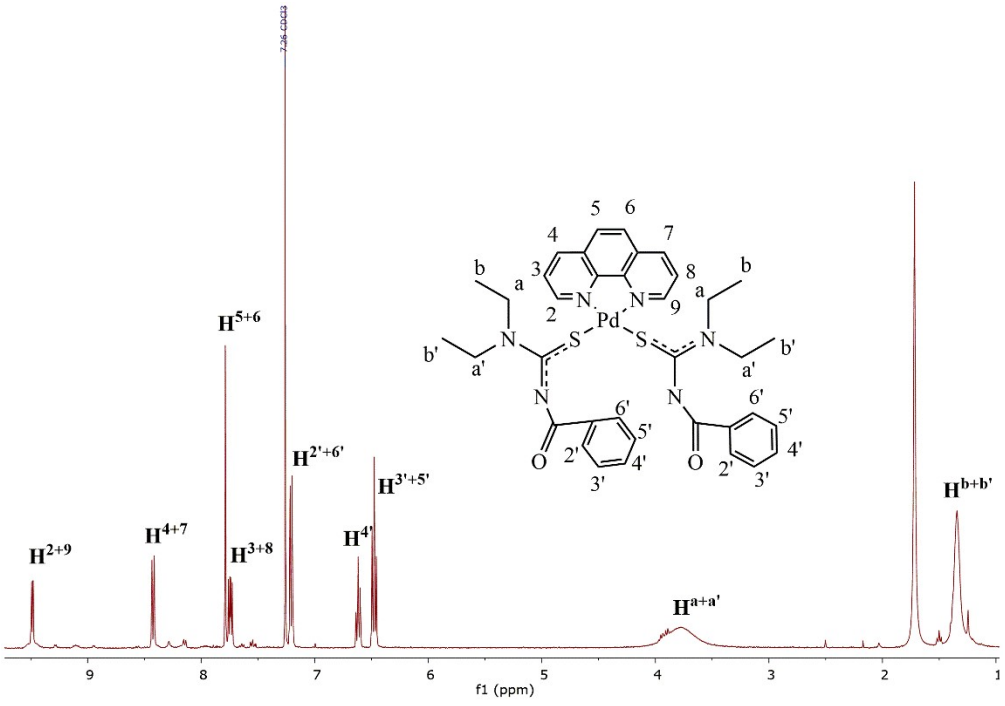

***Figure 2.5**: ^{1}H NMR spectra for themonodentate [Pd(phen)(L-κS)$_2$]Cl in CDCl3 at 300K.*

The method was further modified by performing the reaction in an ice bath. After a few drops of the ligand solution were added, a yellow colour started to appear in the aqueous phase of the two immiscible solvents. The reaction was stirred for a further 3 hours after the last drop of the ligand solution was added (*Scheme 2.6*). After the reaction was complete, the aqueous phase was collected, and the water was removed under vacuum. The solid residue was then dissolved in cold methanol and filtered off to remove sodium acetate and sodium chloride. The methanol was removed under vacuum, and the solid produced was collected as a yellow powder.

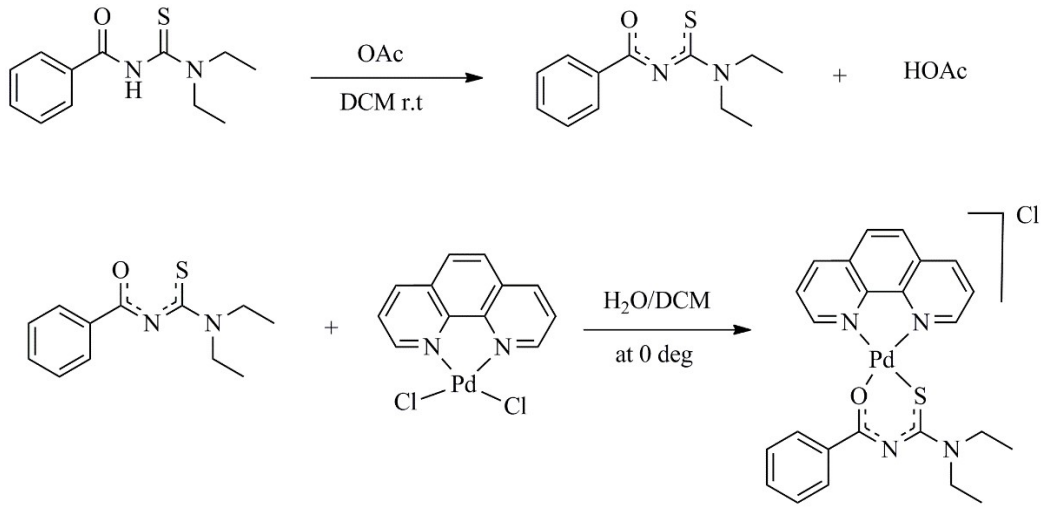

Scheme 2.6*: Synthesis of the [Pd(phen)(L-κO,S)]Cl complex showing a deprotonated* ***HL****.*

The yellow powder was characterized using ^{1}H and ^{13}C NMR spectroscopy, FT-IR spectroscopy, mass spectrometry and elemental analysis. The ^{1}H NMR spectrum (*Figure 2.6*) of the product now showed an increased number of proton signals which suggested a non-symmetrical [Pd(phen)(L-κ*O,S*)]Cl complex. The initial attempt to assign the signals was made based on the NOE experiment carried out for the Pt complexes of this kind,[22] which showed through space coupling between the most deshielded proton and nitrogen of the phen moiety. Thus the most deshielded proton was assigned as H^{2}.[19]

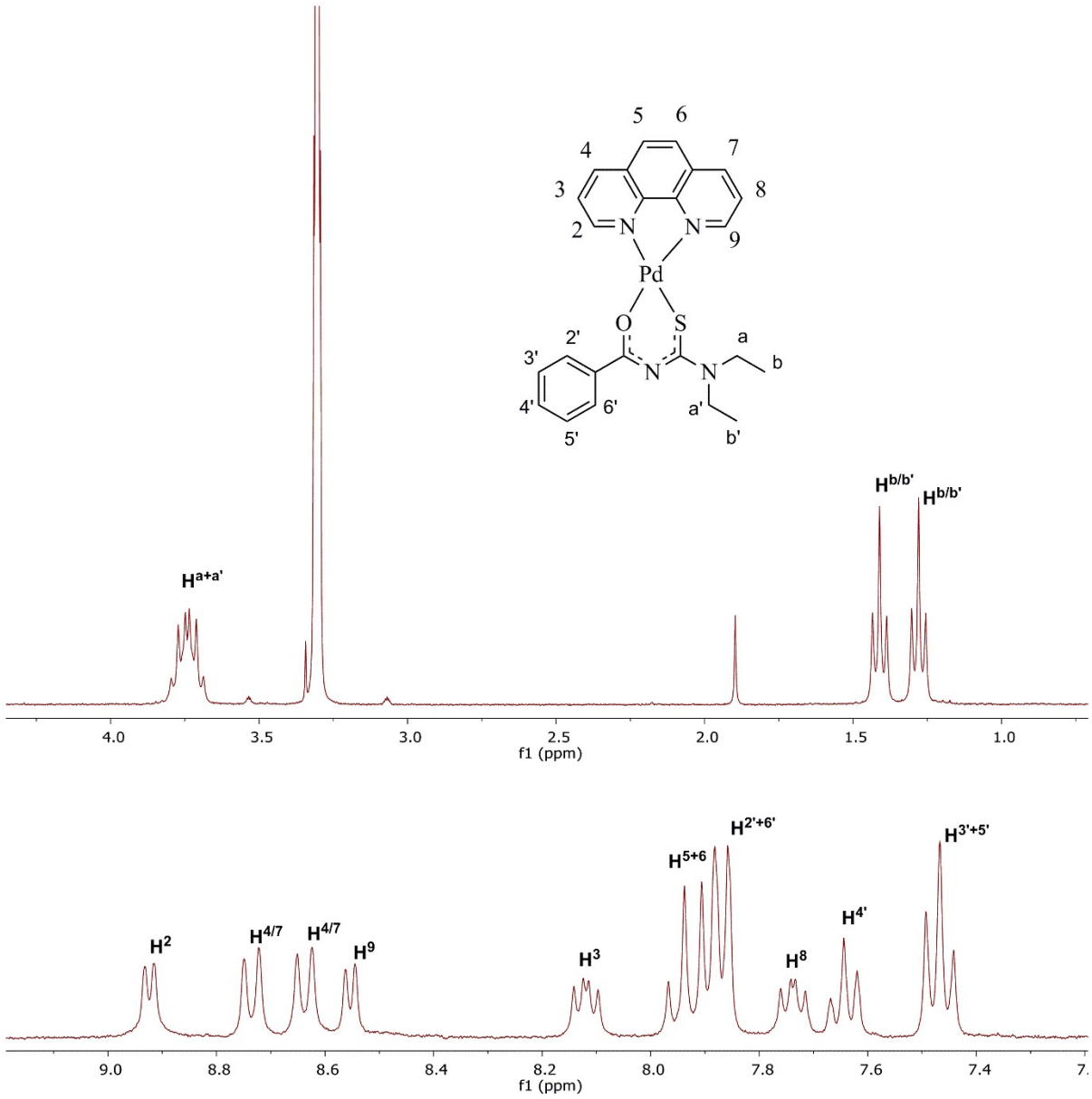

***Figure 2.6**: [1]H NMR spectra of [Pd(phen)(L-κO,S)]Cl in methanol-d4 at 300K showing aliphatic region on top, and aromatic region at the bottom.*

The [1]H-NMR spectrum of [Pd(phen)(L-*κO,S*)]Cl was complicated because the signals from 1,10-phenanthroline were not separated and overlapped with phenyl ring proton signals of the *N, N*-di(ethyl)-*N'*-benzoylthiourea ligand. One main observation from the [1]H-NMR spectrum was the disappearance of the N-H signal, indicating the deprotonation of the acylthiourea ligand. Eleven different aromatic proton environments were observed, of which eight were due to the 1.10-phenanthroline ligand and three from *N,N*-di(ethyl)-*N*'-benzoylthiourea. 2-D NMR experiments were conducted to aid with the signal assignments (*Figure 2.7*). The most

deshielded proton signal was assigned as H^2 using criteria used in assigning the same protons in a similar Pt(II) complex.[19]

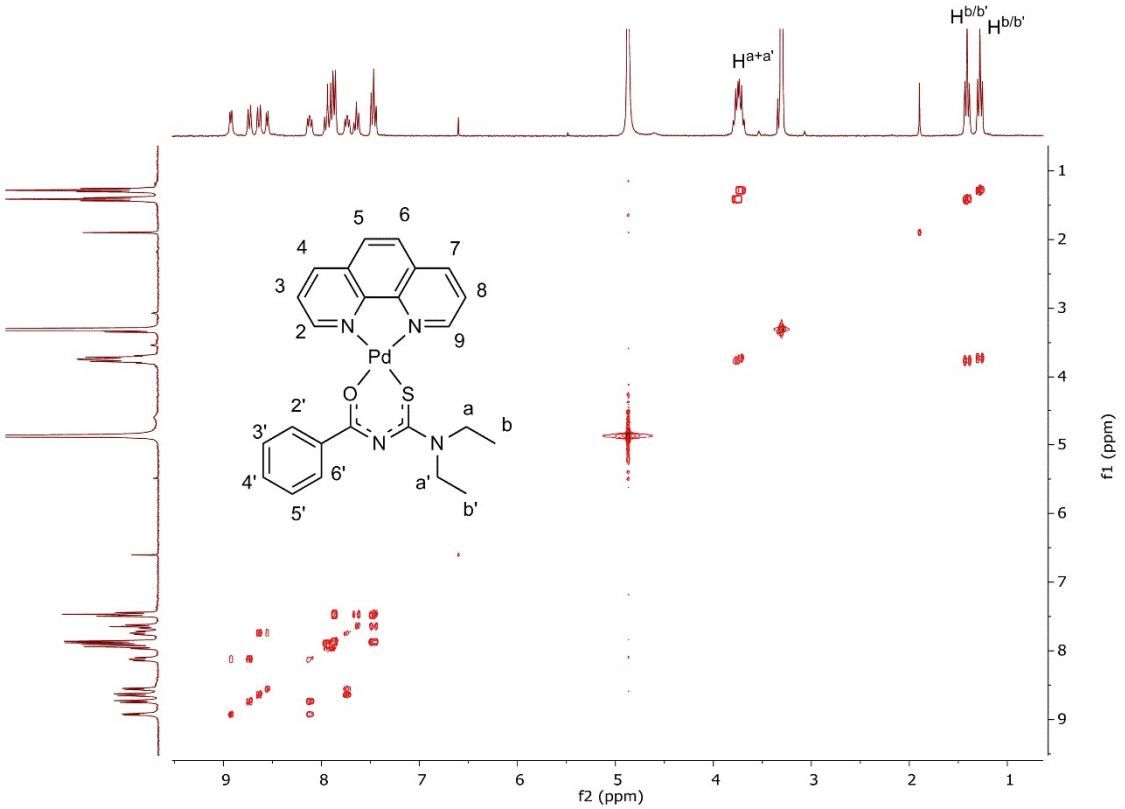

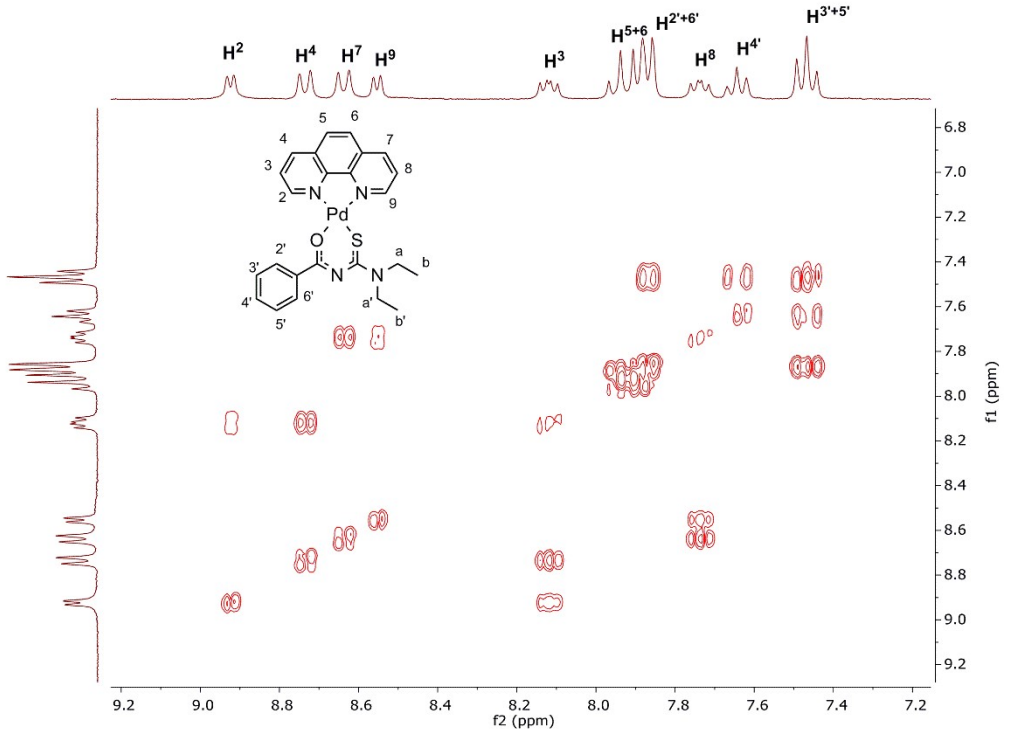

Figure 2.7*: COSY spectrum of the [Pd(phen)(L-κO,S)]Cl, top spectrum showing the full view for the aliphatic and aromatic region while the bottom spectrum is the zoom in aromatic region in methanol-d4 at 300K.*

Referring to the NOE data of the Pt(II) complex,[22] which showed H^2 proton to be the most deshielded over H^9, COSY was used to assign all the protons of the phen ligand. H^4 was assigned as the second deshielded proton signal because of its coupling with H^2. The peak at 8.10 ppm was assigned to H^3, as it showed three bonds coupling to both H^2 and H^4. The signal at 7.95 ppm showed no cross-peaks, and it was assigned to protons H^{5+6} (since they do not couple to other protons over three bonds). H^9 was assigned to the proton signal at 8.70 ppm because of the electronegative nitrogen; and its coupling with one of the remaining phenanthroline protons assigned as H^8. The signal at 8.60 was assigned to H^7 due to three bonds coupling to H^8. The remaining signals were discussed above for **HL**. [Pd(phen)(L-κ*O*,*S*)]Cl was then further characterized using ^{13}C NMR (*Figure 2.8*) supported by HSQC for full assignment (*Figure 2.9*).

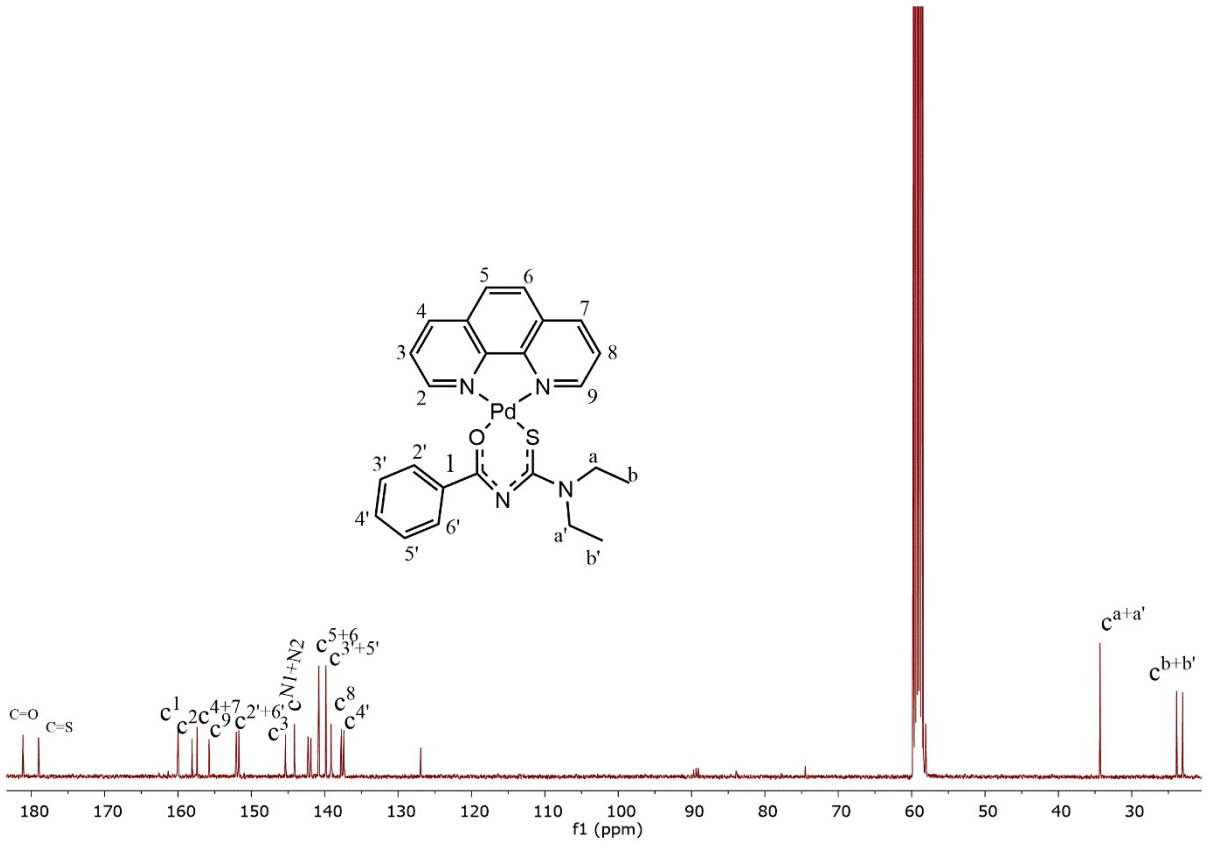

***Figure 2.8**: [13]C NMR spectrum of [Pd(phen)(L-κO,S)]Cl complex with a full view in methanol-d_4 at 300K.*

Carbonyl and thiocarbonyl carbons were assigned as the most deshielded carbon signals at 181.6 and 179 ppm, respectively. Compared to the free ligand, these two carbons were observed close to each other, separated only by 15 ppm (with the carbonyl carbon being the most deshielded signal). Proton H^2 correlates to C^2 at 149.5 ppm, while H^4 correlates to the C^4 at 148 ppm. The rest of the ^{13}C NMR signals were assigned following the correlation pattern of the HSQC spectrum (*Figure 2.9*). There were unidentified signals which are labelled with stars.

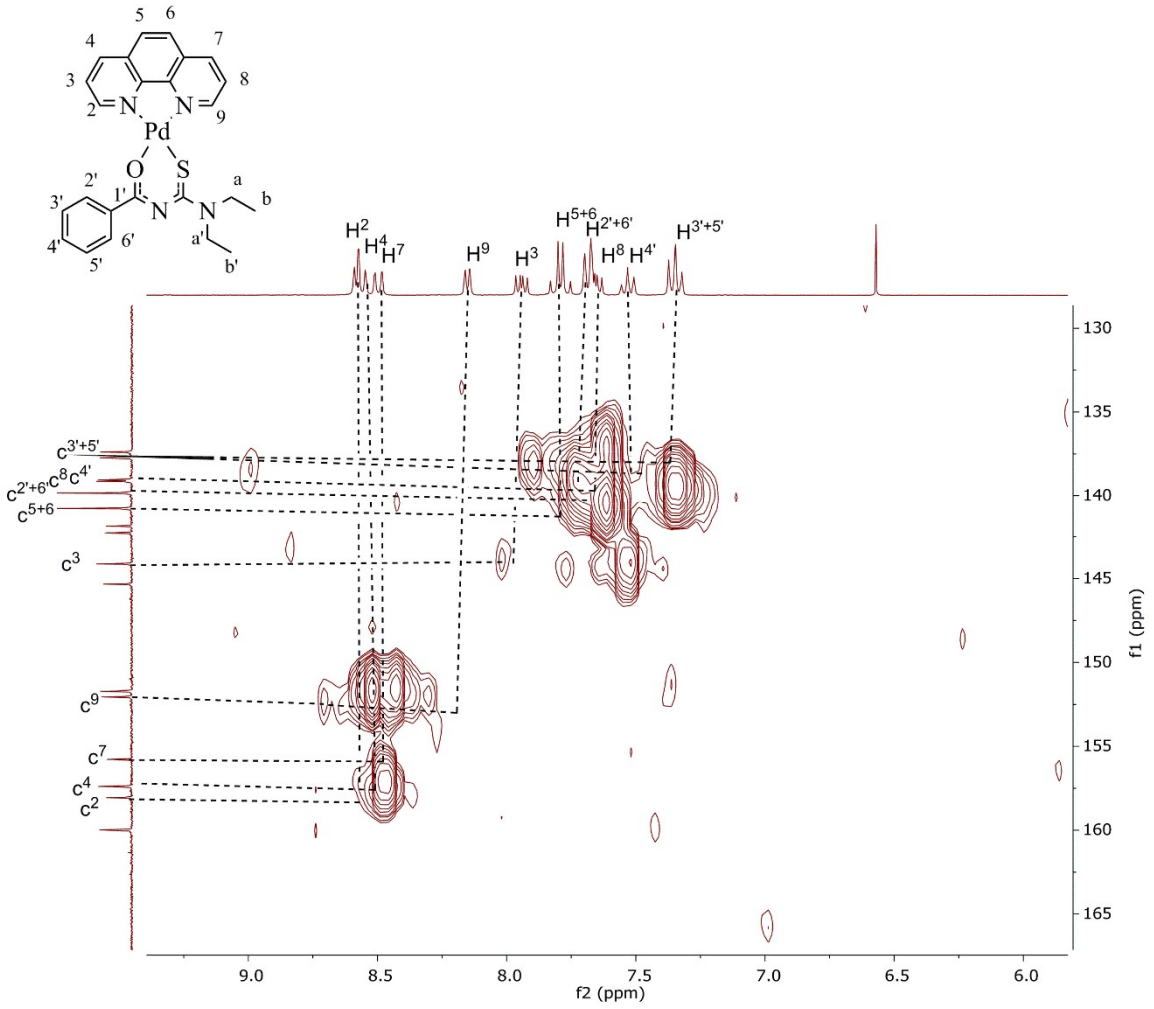

***Figure 2.9**: HSQC NMR spectra and assignments ofthe [Pd(phen)(L-κO,S)]Cl in methanol-d_4 at 300K.*

The complex was further characterized using FT-IR spectroscopy (*Appendix-c Figure 2*), broad signal observed in this spectrum due to N-H stretch frequency indicating that the ligand was deprotonated. The stretching frequency of the carbonyl shifted from 1650 cm^{-1} in the free ligand to 1548 cm^{-1} for the complex. Characterization of [Pd(phen)(L-κ*O,S*)]Cl using mass spectrometry (+ESI-MS) in the positive mode showed a molecular ion peak at 521.0639 m/z for the $[Pd(phen)(L\text{-}\kappa O,S)]^+$ complex species. The observed isotopologue pattern was in good agreement with the predicted theoretical pattern.

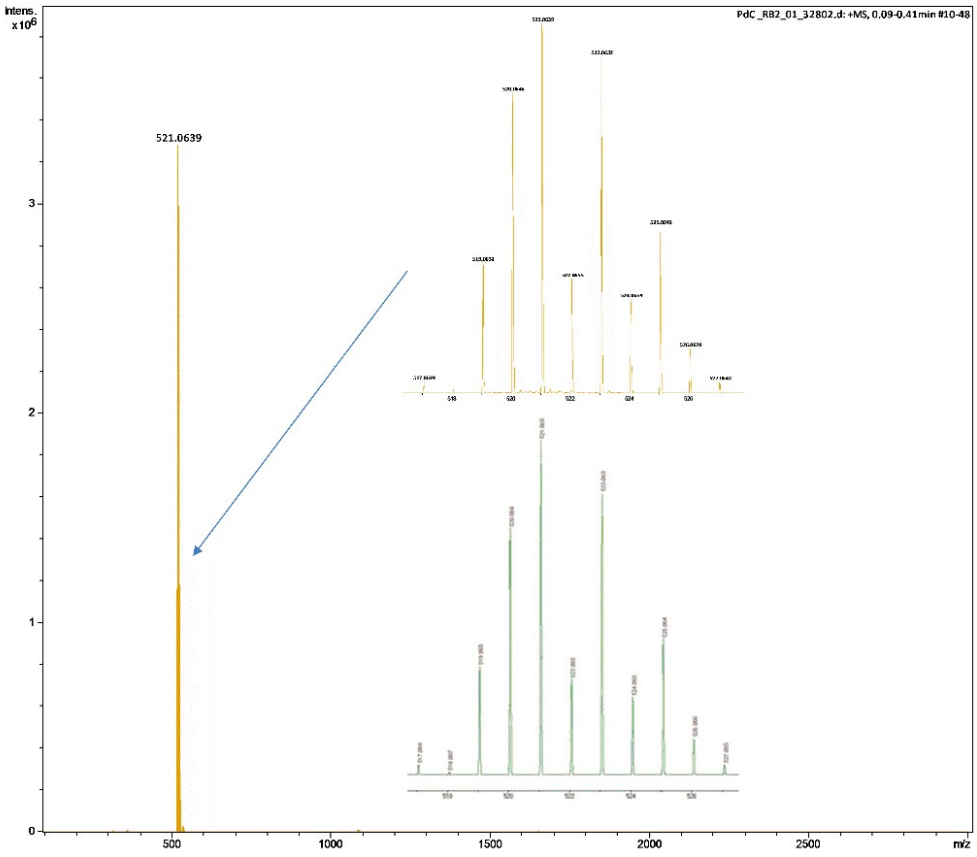

***Figure 2.10**: ESI+ mass spectrum of [Pd(phen)(L-κO,S)]Cl in methanol.*

Brown needle-like crystals of [Pd(phen)(L-*κO,S*)]NO_3 (*Figure 2.11*) were obtained from slow evaporation of the solvent. The nitrate as the counterion was observed in the molecular structure instead of the expected chloride, this can be speculated that the nitrate come from the nitric acid during the synthesis of the [$PdCl_2$(phen)] precursor batch, where HNO_3 was used instead of the HCl. This would be investigated for the future; however, this was beyond the scope of this research as it would require enough time for its characterization. [Pd(phen)(L-*κO,S*)]NO_3 crystallized as a solvate in a monoclinic system with $P2_1/c$ space group. The molecular structure exhibited a slightly distorted square planar geometry with the *N, N*-di(ethyl)-*N'*-benzoylthiourea ligand coordinated in a bidentate fashion through the oxygen and sulfur donor atoms.

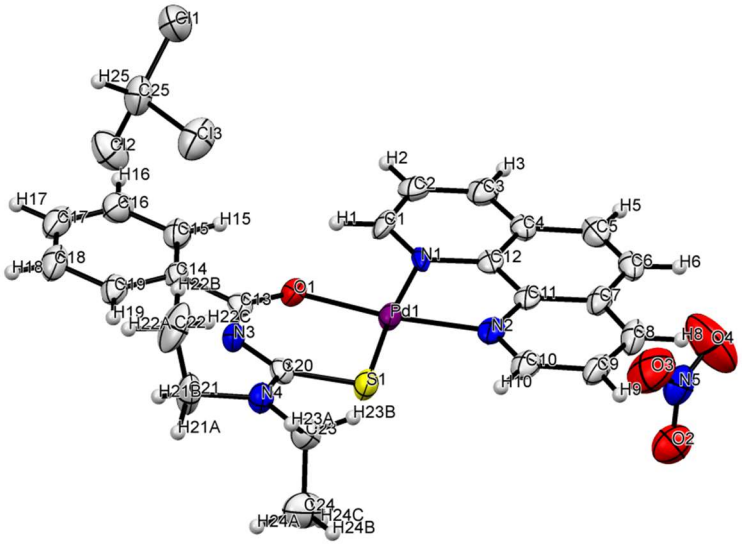

***Figure 2.11**: Molecular structure of [Pd(phen)(L-κO,S)]NO_3 showing bidentate coordination for N,N-di(ethyl)-N'-benzoylthiourea ligand to the metal.*

A comparison of the C=S bond length of the free ligand (**HL**) to the complex ([Pd(phen)(L-*κO,S*)]NO_3) showed an increase from 1.66 Å to 1.73 Å, implying a reduction in bond order. The C=O bond length also increased from 1.22 Å in the free ligand (**HL**) to 1.29 Å after complexation, these observation of the bond lengths were in disagreement with the bond lengths reported in literature.[51] Due to geometric constraints imposed by the **HL**, the N2-Pd-N1 bond angle deviated from [80.79°] from the literature to [81.31°] for the newly formed complex. The crystallographic data, together with selected bond lengths and bond angles, are given in *Tables 1* and *2*, respectively.

***Table 2.1**: Crystal and structure refinement data for [Pd(phen)(L-κO,S)]NO₃*

	[Pd(phen)(L-*κO,S*)]NO_3
Empirical formula	$C_{25}H_{24}N_5O_4PdS$
Formula weight	703.30
Crystal size (mm^{-3})	0.319x 0.074x 0.072
Temp (K)	173.15
Radiation (Å)	MoKα(λ=0.71073)
Crystal system	monoclinic
Space group	$P2_{1/c}$
a (Å); α (°)	8.6033(6); 90
b (Å); β (°)	21.9983(13); 104.329(5)
c (Å); γ (°)	14.8746(13); 90
Volume ($Å^3$)	2727.6(3)
Z	4
Density (calc) (kg/m^3)	1.713
Abs. coeff. (mm^{-1})	1.094
Index ranges	-9≤h≤10, -26≤k≤26, -17≤l≤17
Reflections collected	14637
Independent reflections	4726[R_{int} = 0.0958]
Goodness-of-fit on F^2	0.847
R_1 [$I > 2\sigma(I)$]	0.0462
R_1 (all data)	0.1033
wR_2 [$I > 2\sigma(I)$]	0.0738
wR_2 [all data]	0.0854

Large diff. peak hole (e.Å^{-3})	1.14 and -0.64

***Table 2.2**: Selected bond lengths [Å] and bond angles [°] for [Pd(phen)(L-κO,S)]NO$_3$*

Bond lengths (Å)			
N1-Pd1	2.058(4)	C20-S1	1.733(5)
N2-Pd1	2.023(4)	C20-N3	1.347(6)
O1-Pd1	1.981(3)	C13-O1	1.291(6)
Pd1-S1	2.2420(15)	C13-N3	1.294(6)
Bond angles (°)			
N2-Pd1-N1	81.31(18)	C13-O1-Pd1	129.8(4)
N2-Pd1-S1	93.46(15)	N1-Pd1-S1	174.30(12)
O1-Pd1-N2	172.02(18)	C20-S1-Pd1	107.8(2)
O1-Pd1-S1	94.33(11)		

The crystal packing shows a network of weak intermolecular hydrogen bond interactions between the aromatic C-H and the nitrate counter-ion as well as aromatic/alkyl C-H and chloroform solvent (*Figure 2.12*). Further stabilization of the crystal packing is achieved through intermolecular π-π interactions between the phenanthroline rings and the phenyl ring of the acylthiourea ligand. There is also evidence of cation----π interactions between the palladium(II) centre and the phenanthroline rings.

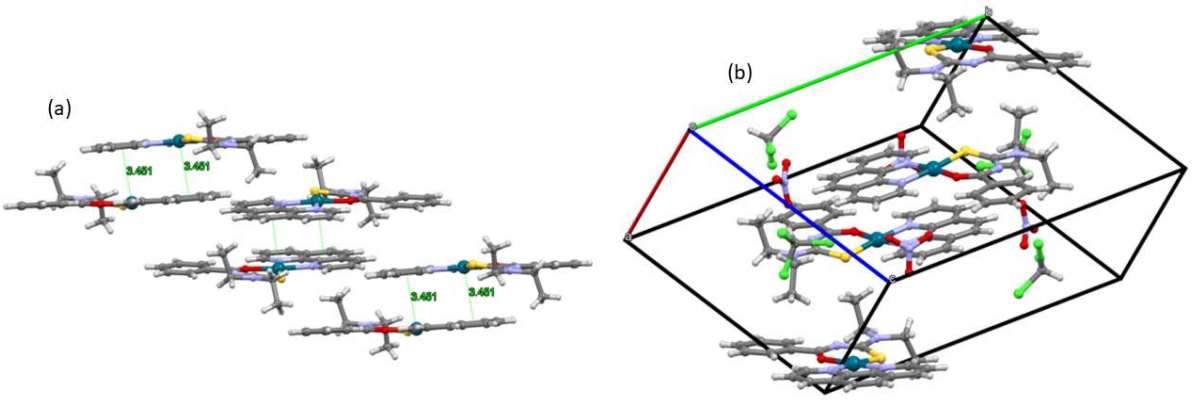

***Figure 2.12**: Crystal structure of [Pd(phen)(L-κO,S)]NO$_3$, (a) displaying packing without solvent and counterion and (b) displaying packing with counterion and solvent.*

2.2.4 Synthesis and characterization of [Pt(diimine)(L-*κO,S*)]Cl and its precursors

The first attempt for this complex was done following the one reported from literature where acetonitrile was used as a solvent to initially dissolve the [$PtCl_2$(diimine)] precursor and the base followed by refluxing the reaction mixture for 45 minutes. After this point, the ligand solution in acetonitrile was added dropwise and further reflux overnight. However, this method was not successful as the ^{1}H NMR spectrum obtained show a mixture of complexes. The method was optimized using two solvents (water and acetonitrile 70:30 % v/v). A mixture of *N,N*-di(ethyl)-*N*'-benzoylthiourea and sodium acetate dissolved in acetonitrile was added drop-wise to a suspension of [$PtCl_2$(diimine)] in water, and the reaction was heated at 70 °C and allowed to react for 24 hours. The solvents were removed under a vacuum. The solid residue was redissolved in dichloromethane and filtered to remove sodium chloride and unreacted sodium acetate. The complex was then selectively precipitated using hexane, and the precipitate was washed with diethyl ether. The reaction procedure is showed in (*Scheme 2.7*).

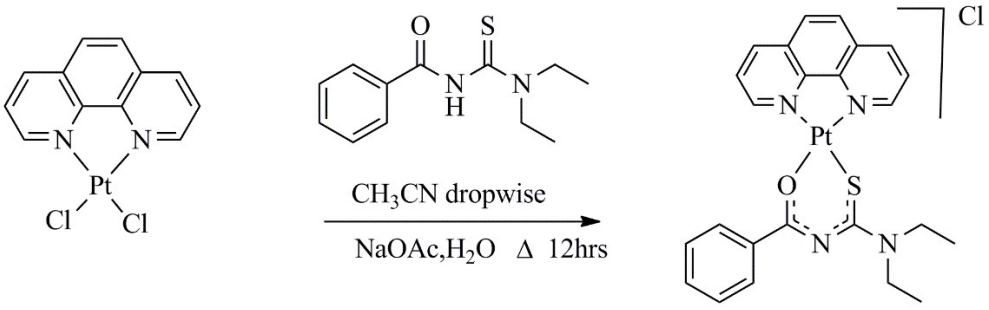

Scheme 2.7*: The general synthesis for [Pt(phen)(L-κO,S)]Cl complex.*

The isolated complex was characterized using ^{1}H and ^{13}C NMR spectroscopy, FT-IR spectroscopy, mass spectrometry and elemental analysis. The ^{1}H NMR spectrum (*Figure 2.13*) of the product now showed an increased number of proton signals which suggested a non-symmetrical [Pt(phen)(L-κ*O,S*)]Cl complex.

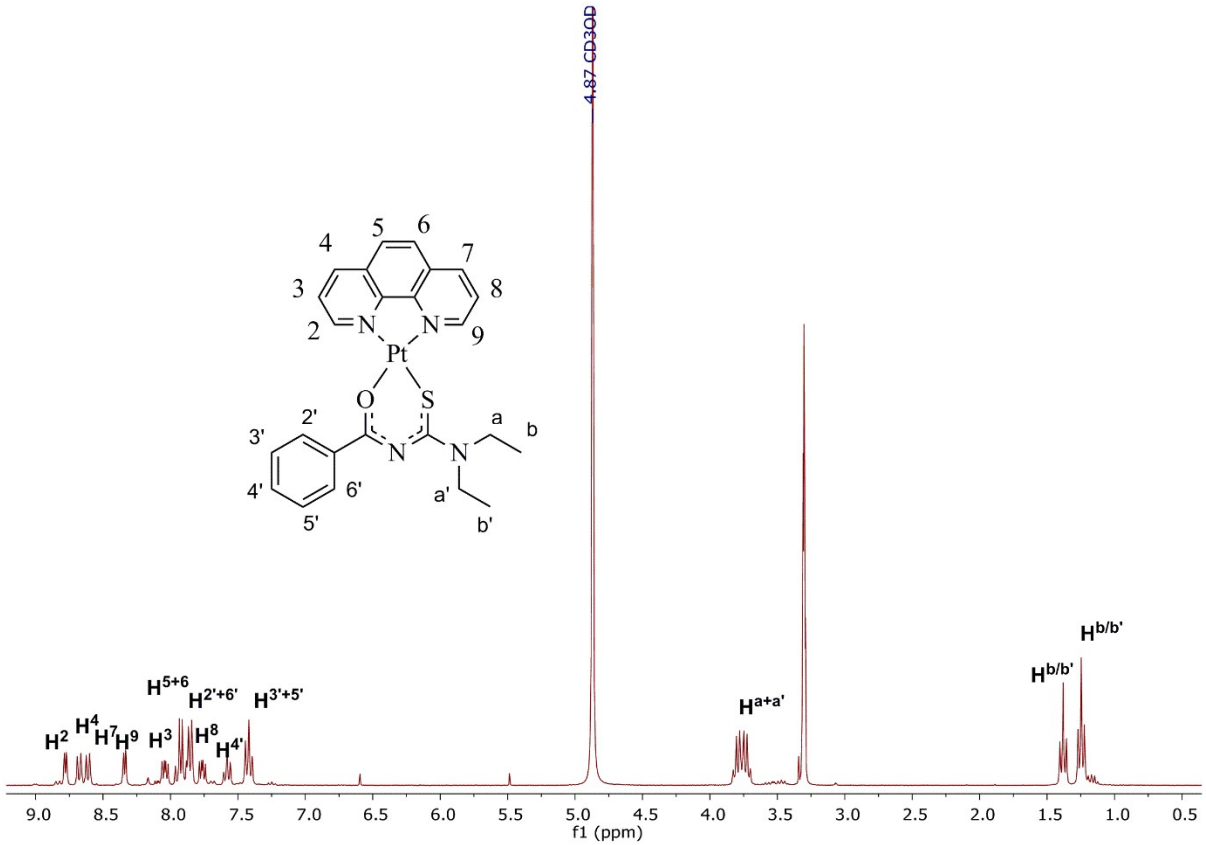

***Figure 2.13**: [1]H NMR spectrum for the [Pt(phen)(L-κO,S)]Cl complex in methanol-d_4 at 300K.*

The chemical shifts for the complexes [Pt(phen)(L-*κO,S*)]Cl and [Pd(phen)(L-*κO,S*)]Cl are very similar and discussed under the NMR section for the [Pd(phen)(L-*κO,S*)]Cl and the assignments will not be discussed in details.

2.2.5 Synthesis and characterization of [Zn(diimine)(L-κ*O,S*)]Cl and its precursors

The synthesis of the precursor was obtained by following a method described by Gouvea.[22] An appropriate ethanolic solution of the 1.10-phenanthroline (phen) or 5,6-dimethyl-1.10-phenanthroline (dmp) was added to the ethanolic solution of [$ZnCl_2$] (Scheme 2.8). Immediately after the addition of the phen or dmp ethanolic solution, a precipitate was formed. The reaction mixture was stirred at a constant rate at room temperature for 3 hours. The precipitate was isolated and washed with diethyl ether and dried.

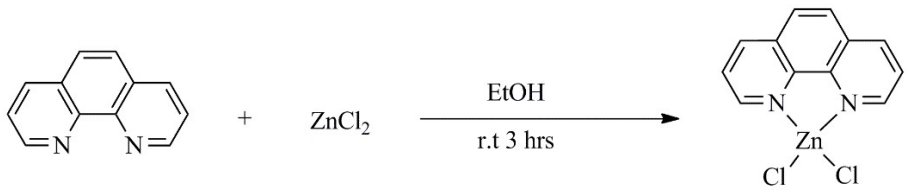

***Scheme 2.8**: General synthesis for the precursor [$ZnCl_2$(phen)].*

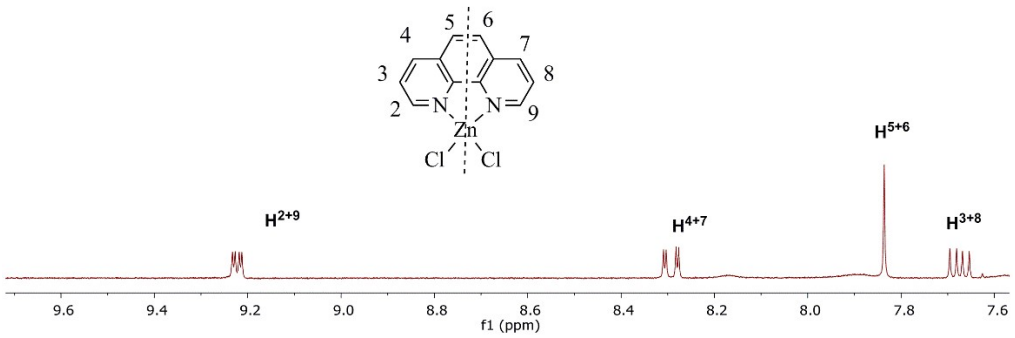

***Figure 2.14**: [1]H NMR spectra for the [ZnCl$_2$(phen)] in CDCl$_3$ at 300K.*

The complex [Zn(phen)(L-*κO,S*)]Cl was prepared following a similar method described earlier for the other metals. A solution of *N,N*-di(ethyl)-*N*'-benzoylthiourea with sodium acetate in methanol was added drop-wise into a stirred hot methanol solution [ZnCl$_2$(phen)] (*Scheme 2.9*). The colourless solution was stirred and refluxed for 12 hours. After the reaction was completed, the methanol was removed under vacuum. The solid residue was redissolved in dichloromethane and filtered to remove sodium acetate and sodium chloride. The complex was precipitated using hexane and the precipitate isolated by filtration then left to dry. After the solvent evaporated, the complex was washed with diethyl ether and dried. The complex was characterized using FT-IR spectroscopy, NMR spectroscopy, mass spectrometry and elemental analysis.

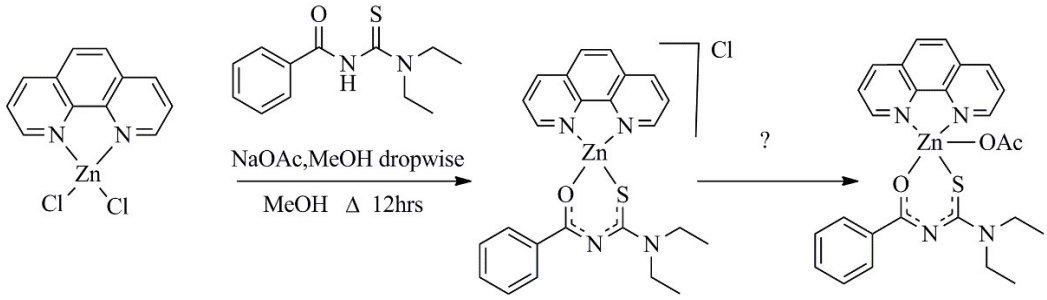

***Scheme 2.9**: General synthesis for the [Zn(phen)(L-κO,S)]Cl complex in methanol and sodium acetate to deprotonate the ligand.*

The complex was analysed using ^{1}H NMR spectroscopy, a peak observed at 2.10 ppm, indicated the presence of an acetate or acetone impurity. It was unclear if the acetate acted as a counter ion or was coordinated to the zinc metal or was just a residual acetate/acetone impurity. Therefore, the method was further modified by changing the base to sodium hydride. The advantage of using sodium hydride is that when it deprotonates the ligand, the conjugate base (the hydride ion) combines with the proton from the ligand and escape as hydrogen gas.

The ^{1}H NMR spectrum showed symmetry in the phen ligand (*Figure 2.15*) which was similarly observed with the ^{1}H NMR of the precursor [$ZnCl_2$(phen)].

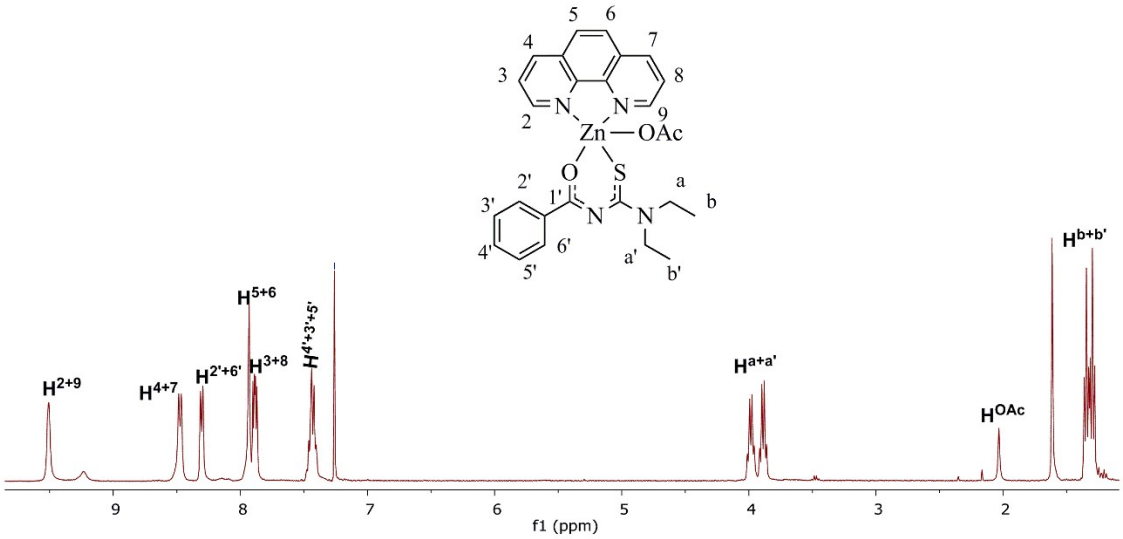

***Figure 2.15**: ^{1}H NMR characterization of the [Zn(phen)(L-κO,S)(OAc)] in $CDCl_3$ at 300K*

The similarities between the ^{1}H spectrum of the [Zn(phen)(L-κ*O*,*S*)(OAc)] complex to the ^{1}H spectrum of the [$ZnCl_2$(phen)] based on the number of the aromatic proton signals due to the phen moiety suggest that the symmetry in the [Zn(phen)(L-κ*O*,*S*)(OAc)] complex was not broken. The singlet observed at 2.01 ppm was assigned $H^{OAc,}$ which integrated for 3 protons, and it does not couple with any proton. The triplet at 7.3 ppm was assigned to $H^{3'+4'+5'}$ due to overlap of these protons and coupling to $H^{2'+6'}$. The signal at 8.5 ppm was assigned to H^{4+7}. The most deshielded signal at 9.5 ppm was assigned to H^{2+9}. The signal at 7.9 ppm was assigned to H^{5+6} which slightly overlapped with H^{3+8}.

The complex isolated from the reaction of *N,N*-di(ethyl)-*N*'-benzoylthiourea with [$ZnCl_2$(phen)] using sodium hydride was also characterized using ^{1}H and ^{13}C NMR spectroscopy, FT-IR spectroscopy, mass spectrometry, single-crystal X-ray diffraction. *Figure 2.16* show the ^{1}H NMR spectrum of the complex stacked with the ^{1}H NMR spectrum of [Zn(phen)(L-κ*O,S*)(OAc)]. The chemical shifts observed for [Zn(phen)(L-*κO,S*)Cl] were similar to those observed for the [Zn(phen)(L-*κO,S*)(OAc)] complex, which was already discussed in (*Figure 2.14*) and the assignments were similar, only the acetate and chloride substituents made the difference.

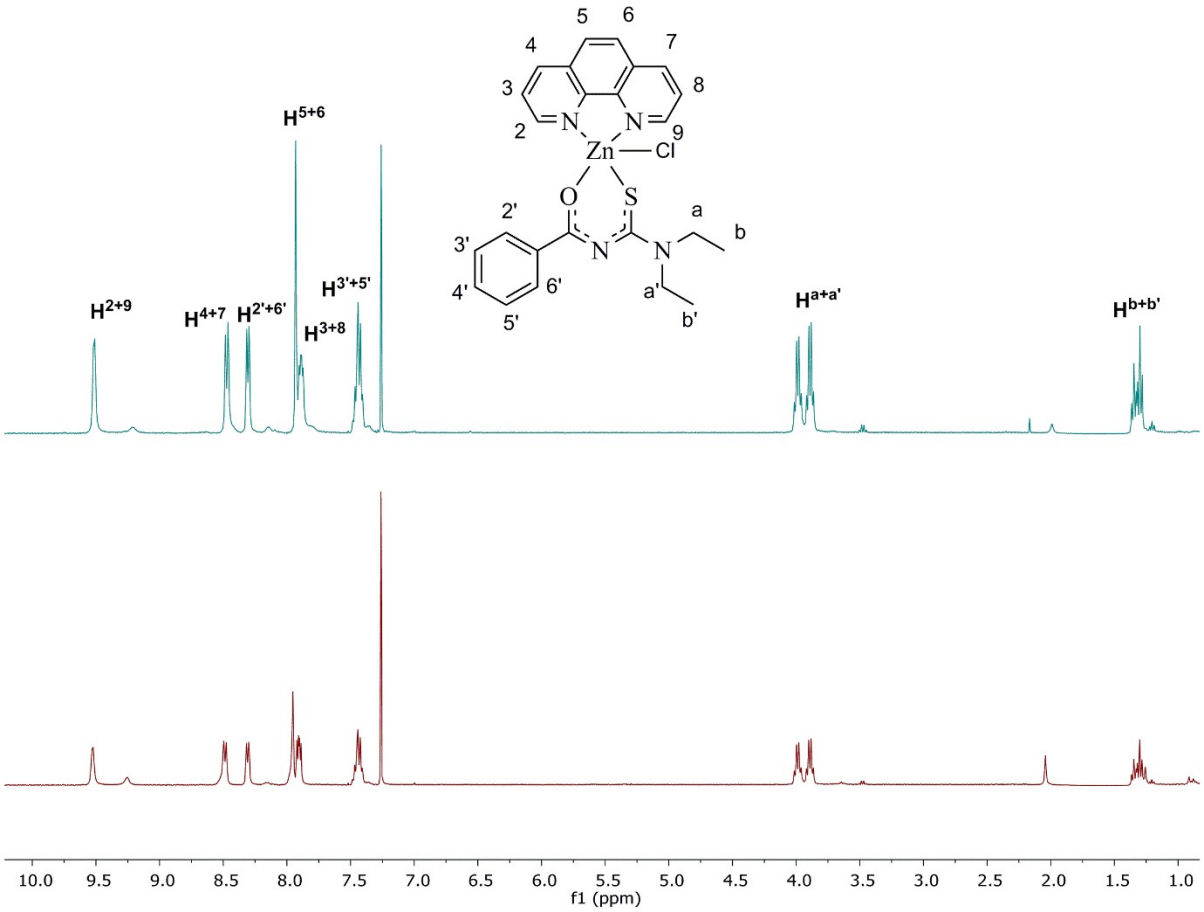

***Figure 2.16**: [1]H NMR spectrum for the [Zn(phen)(L-κO,S)Cl]on top stacked with [Zn(phen)(L-κO,S)(OAc)] at the bottom in $CDCl_3$ at 300K, observing the whole spectrum .*

Single crystals of [Zn(phen)(L-*κO,S*)(OAc)] suitable for single-crystal XRD analysis were grown using the vapour diffusion method. In this method, the complex [Zn(phen)(L-*κO,S*)(OAc)] was dissolved in dichloromethane in vial and placed in a larger vial containing diethyl ether and sealed tight. This set-up was placed in a fridge, and diethyl ether slowly diffused into the dichloromethane solution and crystals formed. The complex [Zn(phen)(L-*κO,S*)(OAc)] crystallized in the centrosymmetric triclinic space group P-1,and the crystal were colourless in circle shape (*Figure 2.17*).

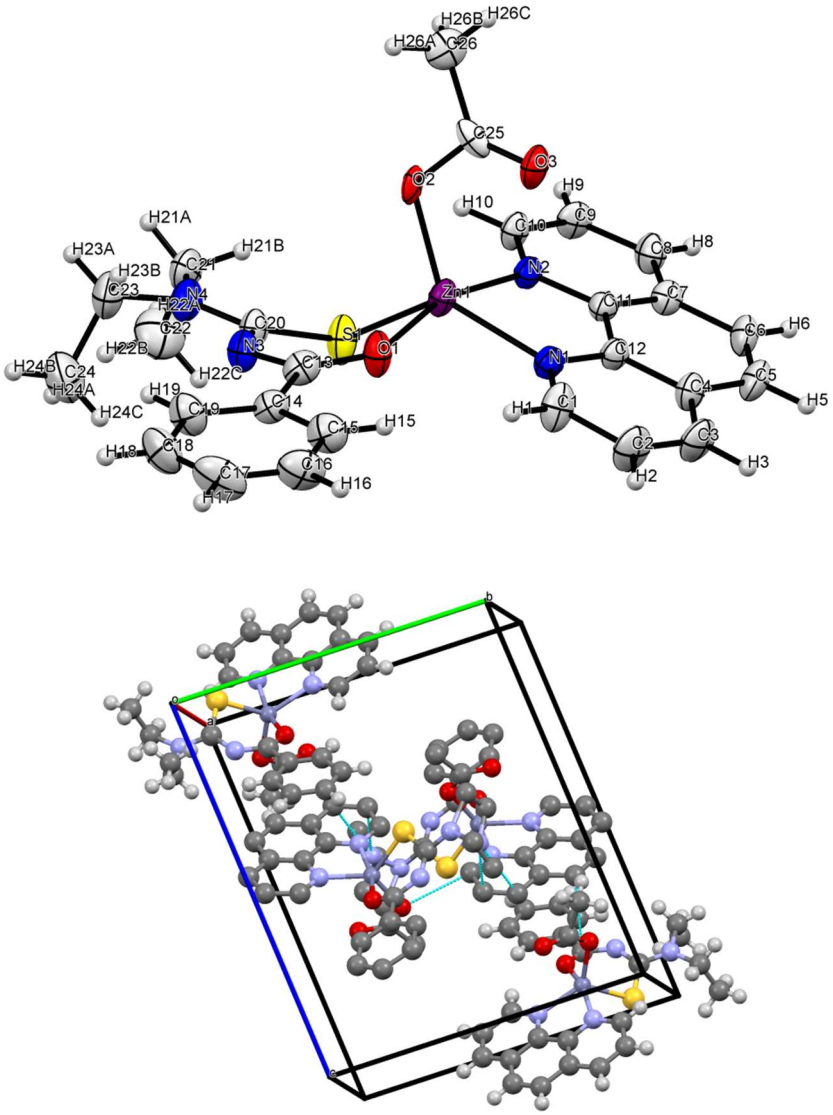

***Figure 2.17**: Single crystal structure for [Zn(phen)(L-κO,S)(OAc)] displaying the fifth coordination by acetate and crystal packing, displaying hydrogen bonding and π-----π interations.*

Zn^{2+} can have (4, 5, or 6) donor atoms biding to the central metal.[21] The [Zn(phen)(L-κO,S)(OAc)] complex exhibit a distorted square pyramidal geometry as reported from the literature for five-coordination zinc complexes.[23] Acylthioureato ligand was ligated to the zinc metal through oxygen and sulfur donor atoms. The selected bond lengths and bond angles are given in *Table 3*.

***Table 2.3**: Selected bond lengths [Å] and bond angles [°] for [Zn(phen)(L-κO,S)(OAc)]*

Bond lengths [Å]			
N1-Zn1	2.127(4)	S1-Zn1	2.3539(14)

N2-Zn1	2.171(4)	C20-S1	1.728(4)
O1-Zn1	2.050(3)	C13-N3	1.336(6)
O2-Zn1	1.967(4)	C20-N3	1.347(5)
C13-O1	1.254(5)	C20-N4	1.346(5)
Bond angles [°]			
O1-Zn1-S1	89.48(9)	C20-S1-Zn1	100.67(17)
N2-Zn1-S1	90.92(10)	C13-O1-Zn1	129.0(3)
N1-Zn1-N2	77.23(14)	O2-Zn1-O1	95.95(15)
O1-Zn1-N1	89.49(13)		

Single crystals of [Zn(phen)(L-*κO,S*)Cl] were grown from acetonitrile in the freezer by slowly evaporating the solvent (*Figure 2.18*). Colourless cubic crystals were obtained from the acetonitrile solution, which turned from red to colourless with time.

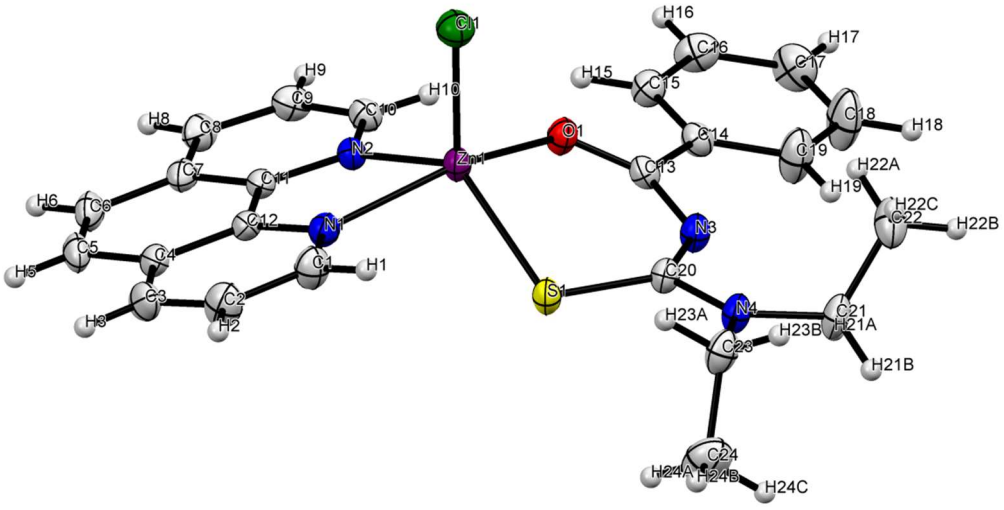

Figure 2.18*: Single crystal structure for the [Zn(phen)(L-κO,S)Cl] displaying ORTEP diagram.*

[Zn(phen)(L-*κO,S)Cl*] crystallized in the P-1 space group of a triclinic crystal system, where the phenanthroline and acylthiourea ligands coordinated in a bidentate fashion. Interestingly, the chloride was coordinated as the fifth ligand instead of being a counter-ion. The bond angle N1-Zn1-N2 (77.23°) slightly narrowed to 75.97° when chloride occupied the 5th coordination site. The C=O and C=S bond lengths of (1.2188Å) and (1.6767Å) in the ligand elongated to 1.2615Å and 1.7430Å, respectively in the complex. The O1-Zn1-S1 bond angle was observed to be significantly narrower in [Zn(phen)(L-*κO,S*)(OAc)] (89.48°) and wider in [Zn(phen)(L-*κO,S*)Cl] at about 117.32°. Selected bond lengths and bond angles are given in *Table 2.4*.

***Table 2.4**: Selected bond lengths [Å] and bond angles [°] for [ZnCl(phen)(L-κO,S)]*

Bond length (Å)			
N1-Zn1	2.2475(12) (σ)	C20-N3	1.3395(19)
N2-Zn1	2.1238(12) (σ)	C20-N4	1.3411(18)
O1-Zn1	2.0711(10)	C20-S1	1.7430(14)
S1-Zn1	2.3413(4)	C13-O1	1.2615(17)
Bond angles (°)			
N1-Zn1-C11	95.39(3)	N1-Zn1-S1	89.02(3)
N2-Zn1-C11	110.21(3)	O1-Zn1-N2	88.45(43)
O1-Zn1-C11	104.10(3)	N2-Zn1-N1	75.97(5)
O1-Zn1-S1	117.327(16)	O1-Zn1-S1	90.21(3)
Torsion angles (°)			
N3-C13-O1-Zn1	-9.4(2)		
N3-C20-S1-Zn1	-34.07(15)		

Crystal and structure refinement data for both [Zn(phen)(L-*κO,S*)(OAc)] and [Zn(phen)(L-*κO,S*)Cl] is summarized in Table 5 below.

***Table 2.5**: Crystal and structure refinement data for [Zn(phen)(L-κO,S)(OAc)] and [ZnCl(phen)(L-κO,S)]*

	[ZnCl(phen)(L-*κO,S*)]	**[Zn(phen)(L-*κO,S*)(OAc)]**
Empirical formula	$C_{24}H_{23}ClN_4OSZn$	$C_{26}H_{26}O_3N_4SZn$
Formula weight	516.34	540.80
Crystal size (mm^{-3})	0.334x0.308x0.106	0.294x 0.144x 0.046
Temp (K)	173.15	173.15
Radiation (Å)	MoKα(λ=0.71073)	MoKα(λ=0.71073)
Crystal system	Triclinic	Triclinic
Space group	P-*1*	P-*1*
a (Å); α (°)	8.6584(4); 68.421(2)	12.9846(5); 84.910(2)
b (Å); β (°)	11.7436(5); 77.269(2)	13.1593(6); 71.038(2)
c (Å); γ (°)	12.4594(5); 82.646(2)	16.5356(8); 83.793(2)
Volume ($Å^3$)	1147.59(9)	2652.1(2)
Z	2	2
Density (calc) (kg/m^3)	1.494	1.354
Abs. coeff. (mm^{-1})	1.302	1.355
Index ranges	$-11 \leq h \leq 11$	$-15 \leq h \leq 14$
	$-15 \leq k \leq 15$	$-15 \leq k \leq 13$
	$-16 \leq l \leq 16$	$-20 \leq l \leq 20$
Reflections collected	21856	21600
Independent reflections	5778[R_{int} = 0.0248]	9850[R_{int} = 0.0734]
Goodness-of-fit on F^2	1.063	0.801
R_1 [$I > 2\sigma(I)$]	0.0253	0.0491
R_1 (all data)	0.0310	0.1205
wR_2 [$I > 2\sigma(I)$]	0.0623	0.0896
wR_2 [all data]	0.0647	0.1054
Large diff. peak hole ($e.Å^{-3}$)	0.35 and -0.26	0.78nd -0.45

2.2.6 Synthesis and characterization of [Cu(phen)(L-κ*O*,*S*)]Cl and its precursor

Precursors of Cu(II) diimine precursors containing phen and dmp ligands were synthesized according to the method described by Gouvea.[22] An ethanolic solution of phen or dmp was added drop-wise to a well-stirred solution of the anhydrous copper chloride [$CuCl_2$] in ethanol at room temperature (*Scheme 2.10*). After 1 hour, a green precipitate formed. The precipitate was filtered and washed with cold ethanol and dried. The complex was obtained in good yield (87%) for phen and (76%) for dmp. The green complex was characterized using FT-IR spectroscopy with typical vibrational frequencies of; C-H stretching frequency at 3010 cm^{-1}, C=C stretching frequency at 1500 cm^{-1}, and C=N stretching frequency at 1606cm^{-1} which are a typical stretching frequencies when the complex is formed (*Appendix C; Figure 2*).

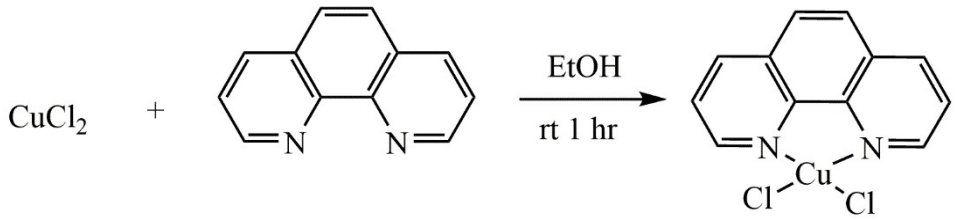

***Scheme 2.10**: General synthesis of the precursor [$CuCl_2$(phen)].*[116]

[Cu(diimine)(L-κ*O,S*)]Cl complex was synthesized according a similar methods described for the other metals. A mixture of *N,N*-di(ethyl)-*N*'-benzoylthiourea and sodium acetate in methanol was added drop-wise to a warm stirred methanolic solution of [$CuCl_2$(phen)] (*Scheme 2.11*). A green solution formed, which was allowed to react for 6 hours. The methanol was removed under vacuum. The solid residue obtained was redissolved in DCM and filtered to remove sodium chloride and sodium acetate. Hexane was used to precipitate the green complex; however, the yield was very low. The obtained green complex was washed several times with diethyl ether.

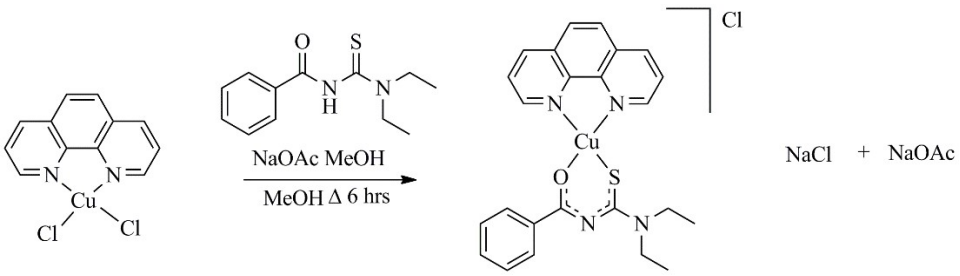

***Scheme 2.11**: Proposed reaction scheme for the synthesis of [Cu(phen)(L-κO,S)]Cl from [$CuCl_2$(phen)] and appropriate N,N-di(ethyl)-N'-benzoylthiourea in methanol.*

Characterization of the complex was performed using FT-IR spectroscopy, mass spectrometry, and elemental analysis. From the FT-IR spectrum obtained for [Cu(phen)(L-κ*O,S*)]Cl, the absence of an N-H stretch in the region 3400 to 3500 cm^{-1} indicated a deprotonated ligand in the complex (*Figure 2.19*). A significant shift to lower wavenumbers was observed for the C=O stretching frequency (1499 cm^{-1}) which indicates the bond restriction between carbonyl and thiocarbonyl. The C=N stretching frequency (1419 cm^{-1}) upon coordination. However, the weak aromatic C-H bands changed slightly.

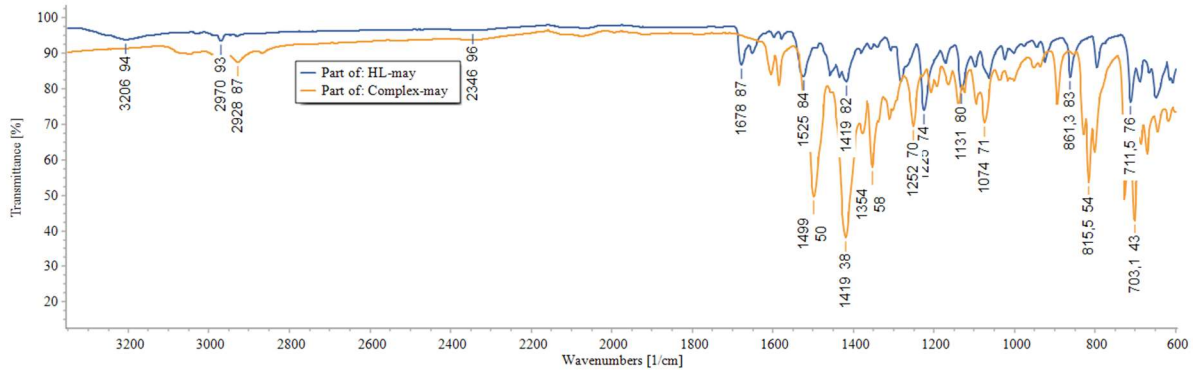

***Figure 2.19**: FT-IR spectrum for the [Cu(phen)(L-κO,S)]Cl complex.*

The mass spectrum found for [Cu(phen)(L-κ*O,S*)] (*Figure 2.20*) showed a [M+H] molecular ion peak at m/z = 479.13 with a matching isotopologue pattern compared to the predicted pattern. However, the other peaks could not be assigned and are yet to be investigated.

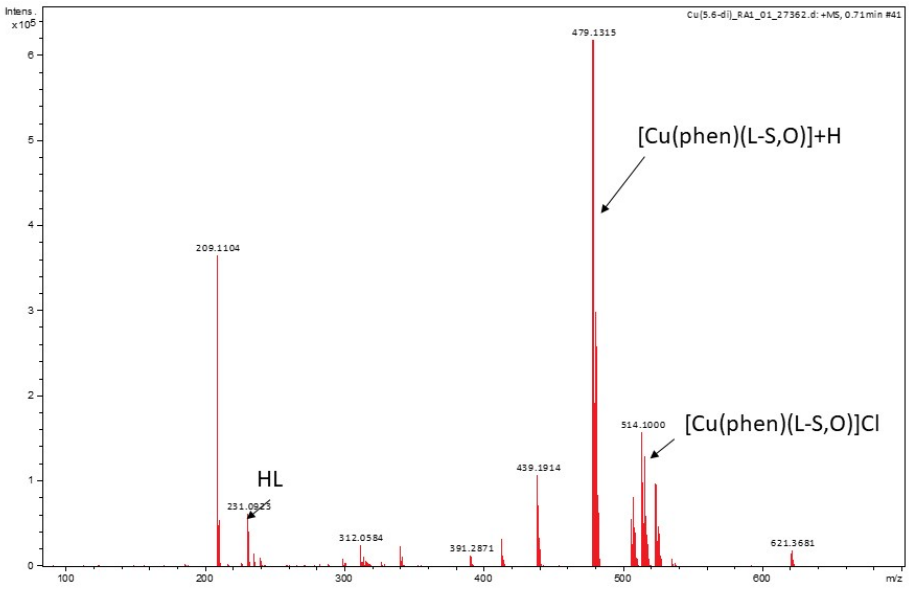

***Figure 2.20**: Mass spectrum for the [Cu(phen)(L-κO,S)]Cl complex*

2.3 Conclusion

Mixed ligand complexes bearing *N,N*-di(ethyl)-*N'*-benzoylthiourea and diimine as a co-ligand were synthesized from four different metals, Pd(II), Pt(II), Cu(II), and Zn(II). These complexes were characterized by NMR spectroscopy (where possible), FT-IR spectroscopy, mass spectrometry and elemental analysis. Single-crystal X-ray diffraction was also used for structural confirmation of [Pd(phen)(L-κ*O,S*)]NO_3, [Zn(phen)(κ*O,S*)(OAc)], and [Zn(phen)(L-κ*O,S*)Cl]. The crystal structure of the [Pd(phen)(L-κ*O,S*)]NO_3 complex showed the counter-ion exchange where a nitrate replaced chloride. The origins of the nitrate could only be speculated to be solvent contamination; however, the source is still under investigation. The Zn(II) complexes were formed, where a fifth ligand (acetate or chloride) coordinated to give pentacoordinate complexes.

2.4 Experimental Instruments and Reagents

NMR experiments were performed with a Bruker Avance 300MHz, Bruker Avance 400MHz and Bruker Avance 500MHz. Mass spectrometry was done using the Advion Expression L Compact, while FT-IR experiments were performed using Bruker Tesor 27 ATR FT-IR spectrometer.

Single x-ray crystals for complexes were collected on a Bruker Apex-II CCD diffractometer with the use of Mo Ka radiation in (Å) at a temperature of 173 (2) K. SAINT [25] was used to integrate intensity. At the same time, absorption correction based on equivalent reflections were carried out by using SADABS.6. WinGx v2014,[25] was used to solve the structures and refined them using ShelXL[26] and OLEX2. All non-hydrogen atoms were refined anisotropically, and all hydrogen atoms were geometrically allocated, thus refined using a riding model. MERCURY [27] and PLATON [28] were used to generate diagrams and publication materials.

The reagents were commercially available and used without purification. Anhydrous acetone, dried according to literature,[29] was used as a solvent in the synthesis of *N,N*-di(ethyl)-*N*-benzoylthiourea. K_2PdCl_4, K_2PtCl_4, $CuCl_2$, $ZnCl_2$ and the 1.10-phenanthroline as well as 5,6-dimethyl-1.10-phenanthroline were obtained from Sigma-Aldrich.

2.4.1 Synthesis of the *N,N*-di(ethyl)-*N'*-benzoylthiourea Ligand

The method described by Douglas and Dains,[1] was used to synthesized *N,N*-di(ethyl)-*N'*-benzoylthiourea. Dried KCSN (29.8 mmol) was dissolved in anhydrous acetone in a round-bottomed flask under an inert atmosphere. Benzoyl chloride (30 mmol) in anhydrous acetone

was then added and refluxed for 45 minutes. The reaction was cooled to room temperature, after which diethylamine (30 mmol) in anhydrous acetone was added dropwise, and the reaction further refluxed for an hour. After cooling, the reaction mixture was poured in 100 ml distilled water. The mixture was left in a fume hood to evaporate acetone and grow crystals slowly. Colourless needle-like crystals formed with a yield of 88%.

m.p (97-100 ºC); ^{1}H NMR (300MHz,CDCl3-d) δ 8.23(s, 1H), 7.91-7.84(m, 2H), 7.66-758(m, 1H), 7.56-7.47(m, 2H), 4.08(dd, *J*=7.3Hz, 2H), 3.89-3.56(m, 2H), 1.36(dd, *J*=23.9, 14.7Hz, 6H). ^{13}C NMR (500MHz, $CDCl_3$) δ 11.32, 13.14, 47.54, 50.58, 129.25, 131.68, 134.11, 137.89, 164.23, 179.97.

2.4.2 Pd(diimine)Cl_2, Pt(diimine)Cl_2 Synthetic Method

Both palladium and platinum precursors were synthesized following the procedure described by Morgan and Bustell.[112] In this instance, [$PdCl_2$(phen)] will be used as an example. A round bottom flask was charged with K_2PdCl_4 (0.4596mmol) dissolved in 45 ml distilled water (acidified with a few drops of hydrochloric acid). An equimolar amount of 1.10-phenanthroline was then added. The reaction mixture was refluxed for approximately 3 hours. A yellow precipitate formed, which was washed 3-4 times with aliquots of water and acetone.

[$PdCl_2$(phen)]: Yield 87%; ^{1}H NMR(300 MHz, DMSO-d_6) δ 9.38(dd, *J*= 1.3Hz,2H), 9.36(dd, *J* = 1.4Hz, 2H),8.31 (s, 6H), 8.17 (dd, *J* =5.4,2.5Hz, 2H): FT-IR(ATR): v=3050 (w, ar- C-H), 15547(m, C=N), 1498 (m), 1218 (m), 789 (s).

[$PdCl_2$(dmp)]: Yield 78%; Yellow powder; ^{1}H NMR (400MHz, DMSO-d_6) (ppm) δ 9.13(dd,*J*=3.68Hz,2H,H^{2+9}),8.71(dd,*J*=1.85Hz,2H,H^{4+7}),7.89(dd,*J*=6.33,2.18Hz,2H,H^{3+8}), 2.80 (s,6H,H^{5+6}), FT-IR (ATR) ν(cm^{-1}): 3035,109 (w, ar- C-H), 1440 (Ar-C-C), 1610(Ar-C=N).

[$PtCl_2$(phen)]: Yellow powder, yield 88%, ^{1}H NMR (500MHz, DMSO-d_6 at 25ºC) (ppm)δ 9.70 (dd, *J*= 1.3Hz,2H), 9.10(dd, *J* = 1.4Hz, 2H),8.17(s, 6H), 8.12 (dd,*J* =5.4,2.21Hz, 2H):FT-IR(ATR); ν(cm^{-1}): 3045(ar--CH), 1410(Ar-C-C), 1629,3(C=N). ESI, Mass spec (MeOH M/z) 485.1

[$PtCl_2$(dmp)]: Yellow powder, yield 87%, ^{1}H NMR (500MHz, DMSO-d_6) (ppm)δ, 9.11(dd,*J*=1.4Hz,2H,H^{2+9}),8.68(dd,*J*=1.6Hz,2H,H^{4+7}),7.75(dd,*J*=7.3,2.9Hz,2H,H^{3+8}), 2.72(s,6H,H^{5+6}), FT-IR (ATR); ν(cm^{-1}) 3063.97(Ar-CH),1233(Ar-C-C), 1624(Ar-C=N).

2.4.3 General Method for the Synthesis of [Cu(diimine)] and [Zn(diimine)]

These metal precursors were synthesized according to the method described by Gouvea,[114] and the procedure was slightly modified. [$CuCl_2$(phen)] will be used as an example to describe the method. One molar equivalent of 1.10-phenanthroline was added to a solution of $CuCl_2$ (1,11mmol) dissolved in 20 ml absolute ethanol, and the reaction mixture was refluxed for 2hours. As a result, a green precipitate formed, and the reaction mixture was cooled to room temperature. The green solid was isolated and subsequently washed with ethanol and THF to remove the unreacted starting material completely. For the zinc precursors, the white precipitate formed, and the solid white powder was washed several times with cold ethanol and left to dry under fume hood.

[$CuCl_2$(phen)]; Green powder, yield 86%, FT-IR (ATR); ν(cm^{-1}), 2980(Ar-C-H), 1512(C=C), 280(Cu-Cl), 230(Cu-N), 1582(C=N). ESI(+)Mass spec (MeOH M/z) 244.6

[$CuCl_2$(dmp)]; Green powder, yield 87.4%, FT-IR(ATR); ν(cm^{-1}), 2890.9(Ar-C-H), 1610(C=C),285(Cu-Cl), 240(Cu-N),1590(C=N). ESI (+), Mass spec (MeOH M/z) 272.71.

[$ZnCl_2$(phen)]; White powder, yield 90%, ^{1}H NMR (400MHz, $CDCl_3$-d_3) δ 9.69 (dd,*J*=4.3Hz,2H,H^{2+9}),9.03(dd,*J*=5.2Hz,2H,H^{4+7}),8.3(s,2H,H^{5+6}),8.18(dd,*J*=7.71,3.8Hz,2H,H^{3+8}):FT-IR(ATR); ν(cm^{-1}), 3091 (Ar-C-H), 1603 (C=C), 1210 (C-C), 1480 (C=N). ESI (+) Mass spec (MeOH, M/z) 246.286.

[$ZnCl_2$(dmp)]; White powder, yield 87%,^{1}H NMR (400MHz, $CDCl_3$-d_3) δ 9.13(dd,*J*=4.3,1.6Hz,1H),8.44(dd,*J*=8.4,1.6Hz,1H),7.64(dd,*J*=8.4,4.3Hz,1H),2.72(s,6H):

FT-IR (ATR); ν(cm^{-1}), 3101 (Ar-C-H), 1660 (C=C), 1220(C-C), 1550 (C=N). ESI (+) Mass spec (MeOH, M/z) 274.546.

2.4.4 General Procedure for the Synthesis of Pd(II) complexexs

To a suspension of [Pd(phen)Cl_2] (0.2799mmol) in 40 ml deionized water, a solution of *N,N*-di(ethyl)-*N*'-acylthiourea in DCM 10 ml with (0.2805mmol, 23mg) sodium acetate was added drop-wise, and the reaction was done in an ice bath to slow the rate of reaction. The reaction was carried out for 6 hours where two layers formed, the top layer being yellow and the bottom layer clear. Next, the reaction mixture was passed through cotton wool to remove unreacted species. The complex was then obtained by liquid-liquid extraction, and the solvent was removed under vacuum. The residue was then washed with cold methanol and filtered through cotton wool to remove the salt. Finally, the solvent was removed once again under vacuum, and the product washed several times with diethyl ether.

[Pd(phen)(L-*κO,S*)]Cl: Yellow powder,53% yield; mp (184-187 ºC); ^{1}H NMR (400MHz, Methanol-d_4), δ 8.78 (dd, *J*= 5.12 Hz, H,H^{2}), 8.68 (dd, *J*= 8.23 Hz, H,H^{4}), 8.61 (dd, *J*= 8.30, H,H^{9}), 8.34 (dd, *J*= 5.31, H,H^{7}), 8.04 (dd, *J*= 8.24, H,H^{3}), 7.94 (m, 2H,H^{5+6}), 7.86 (m, 2H,$H^{2'+6'}$), 7.76 (dd, *J*= 8.18, H,H^{8}), 3.76 (m, 4H, $H^{a+a'}$), 1.38 (t, *J*=7.13, 3H,$H^{b/b'}$), 1.25 (t, *J*=7.13, 3H,$H^{b/b'}$); ^{13}C 181.9 (C=S), 179.5(C=O), FT-IR (ATR), ν(cm^{-1}) 1480s (C=N). 1550m (C=O), 2000w (C-H, aromatic overtone), ESI (+), Mass spec (MeOH, M/z) 521.0639 for [Pd(phen)(L-κ*O,S*)]$^{+}$... elemental analysis. Calc. (%) C, 53.75, H, 4.51, N, 9.64; found. (%). C,54.56, H, 4.16, N, 9.19.

[Pd(dmp)(L-*κO,S*)]Cl: Yellow powder,60%, mp (186-189 ºC); ^{1}H NMR (400MHz, MeOD-d_4),δ δ 8.78(d,*J* =8.3Hz,1H),8.70(d,*J* =8.4Hz,1H),8.37(d,*J*=4.7Hz,1H)8.23(d,*J*=5.1Hz,1H), 8.02(dd,*J*=8.5,4.9Hz,1H),7.74(dd,*J*=8.4,5.2Hz,1H),7.68(d,*J*=7.7Hz,2H),7.62(t,*J*=7.3Hz,1H),7 .44(t,*J*=7.5Hz,2H),3.76(dq,*J*=30.0,7.1Hz,4H),2.48(d,*J*=10.7Hz,6H)1.42(t,*J*=7.1Hz,3H),1.25(t ,*J*=7.1Hz,3H)

FT-IR (ATR); ν(cm^{-1}), 1490s (C=N), 1580m (C=O). ESI (+), Mass spec, (MeOH, M/z) 549.095 for [Pd(dmp)(L-κ*O,S*)]$^{+}$.. Elemental analysis. Calc.(%). C, 55.22, H, 4.96, N, 9.20; found; (%) C, 55.17, H, 4.60, N, 9.32.

2.4.5 General Procedure for Synthesis of Pt(II) complex

A solution of *N,N*-di(ethyl)-*N'*-benzoylthiourea and excess sodium acetate in 30 ml acetonitrile was added slowly to a warm stirred of suspension of [$PtCl_2$(diimine)] (70 mmol) in water 70 ml and heated overnight. The reaction mixture was filtered to remove any unreacted sodium acetate, and the solvent was removed under vacuum. The product was redissolved in dichloromethane and filtered to remove sodium chloride and any other undissolved species. The complex was precipitated with hexane and washed with diethyl ether.

[Pt(phen)(L-*κO,S*)]Cl: Yellow powder, 51% yield, mp (226-228 ºC); ^{1}H NMR (400MHz, MeOD-d_4), δ: 8.94(d,*J* =5.0Hz, 1H), 8.76(dd,*J* =25.2, 8.2H,2H), 8.50(d, *J* =5.3Hz, 1H), 8.14(dd, *J* =8.2, 5.1Hz,2H), 8.11-7.94(m,4H), 7.87(dd, *J* = 8.2, 5.3Hz, 1H), 7.62(t,*J* =7.3Hz,1H), 7.48(t,*J* =7.6Hz,2H),3.86(dq,*J*=21.6,7.1Hz,4H),3.64-3.48(m,1H), 1.92(s,1H)1.44(t,*J*=7.1Hz,3H),1.31(t,*J* =7.1Hz,4H):FT-IR(ATR); ν(cm^{-1}),3011(aliphatic C-H), 1224(C=S), 1248(C=O). ESI (+) Mass spec (MeOH, M/z) 610.1252 for [Pt(phen)(L-κ*O,S*)]$^{+}$..

[Pt(dmp)(L-*κO,S*)]Cl: Yellow powder, 48% yield, mp (228-231 ºC); ^{1}H NMR (400MHz, MeODd$_4$),δ8.78(d,*J*=8.3Hz,1H),8.70(d,*J*=8.4Hz,1H),8.37(d,*J*=4.7Hz,1H)8.23(d,*J*=5.1Hz,1H)
,
8.02(dd,*J*=8.5,4.9Hz,1H),7.74(dd,*J*=8.4,5.2Hz,1H),7.68(d,*J*=7.7Hz,2H),7.62(t,*J*=7.3Hz,1H),7.44(t,*J*=7.5Hz,2H),3.76(dq,*J*=30.0,7.1Hz,4H),2.48(d,*J*=10.7Hz,6H)1.42(t,*J*=7.1Hz,3H),1.25(t,*J*=7.1Hz,3H)
FT-IR (ATR); ν(cm^{-1}), 1217(C=S), 1213,5(C=O). ESI (+), Mass spec (MeOH, M/z) 638, 1576 for [Pt(dmp)(L-κ*O,S*)]$^{+}$. Elem anal; calc. (%). C, 48.20, H, 4.33, N, 8.03; found. (%). C, 47.93, H, 3.95, N, 8.04.

2.4.6 Synthesis of the Cu(II) complexes

A solution of *N,N*-di(ethyl)-*N'*-benzoylthiourea (0.2226 mmoles) and excess sodium acetate in 30 ml methanol was added slowly to a warm stirred of suspension of [CuCl$_2$(phen)] (70 mmol) in 70 ml methanol and heated for 6 hours. The product was filtered to remove any unreacted sodium acetate, and the solvent was removed under vacuum. The product was redissolved in dichloromethane and filtered to remove sodium chloride and any other undissolved species. The concentrated solution was precipitated with hexane and washed with diethyl ether.

[Cu(phen)(L-*κO,S*)]Cl: Green powder: yield 45%; mp (178-181 ºC); FT-IR (ATR); ν(cm^{-1}) 1100 (w,C=S), 1560 (s,C=O), 1430 (s,C=N), 1580 (s,C=C), 3010 (w,C-H). ESI (+) Mass spec (Meot HPLC grade, M/z) 478. Elem anal; calc. (%). C, 55.80, H, 4.88, N, 11.23; found (%). C, 55.87, H, 4.16, N, 10.71.

2.4.7 General Procedure for the Synthesis of Zn(II) complexes

A solution of *N,N*-di(ethyl)-*N'*-benzoylthiourea (0.2210 mmoles) and excess sodium acetate in 30 ml methanol was added slowly to a warm stirred of suspension of [ZnCl$_2$(diimine)] (70 mmol) in 70 ml methanol and heated for 6 hours. The product was filtered to remove any unreacted sodium acetate, and the solvent was removed in the vacuum. The product was redissolved in dichloromethane and filtered to remove sodium chloride and any other undissolved species. The solution was precipitated with hexane and washed with diethyl ether. The obtained product was characterized using NMR spectroscopy, FT-IR spectroscopy, mass spectrometry and X-ray crystallography.

[Zn(phen)(L-*κO,S*)(OAc)]: White powder; 67% yield; mp (174-180 ºC); ^{1}H NMR (400MHz, CDCN-d_3),δ 9.39(d,*J*=69.6Hz,2H,H^{2+9}),8.46(d,*J*=8.2Hz,2H,H^{4+7}),8.30(d,*J*=7.3Hz,2H,$H^{2'+6'}$), 7.90(d,*J*=23.2Hz,4H,$H^{5+6,3+8}$),7.43(dt,*J*=14.7,7.0Hz,3H,$H^{3'+5'+4'}$),4.10-3.76(m,4H,$H^{a+a'}$),1.7(s,3H,H^{OAc}),1.47-1.11(m,6H,$H^{b+b'}$): FT-IR (ATR); ν(cm^{-1}), 3014 (w,Ar-C-H), 1480 (s,C-N), 1575 (s,C=O), 1205 (w,C-C). ESI (+)Mass spec (MeOH, M/z), 479 for [Zn(phen)(L-κ*O,S*)]$^{+}$.. fragment and 535 fragment respectively.

[Zn(phen)(L-*κO,S*)Cl]: White powder ;54% yield; mp (172-176 ºC); ^{1}H NMR (400MHz, CDCN-d_3),δ 9.39(d,*J*=89.7Hz,2H,H^{2+9}),8.47(d,*J*=8.1Hz,2H,H^{4+7}),8.30(d,*J*=7.3Hz2H,$H^{2'+6'}$), 7.91 (d,*J*=30.3Hz,4H,$H^{5+6+3+8}$), 7.49(dd,*J*=15.3,7.3Hz,3H,$H^{3'+5'+4'}$), 4.09-3.80(m,4H,$H^{a'+a}$), 1.47-1.14(m,6H,$H^{b+b'}$).

FT-IR (ATR); ν(cm^{-1}), 3014 (w,Ar-C-H), 1480 (s,C-N), 1575 (s,C=O), 1205 (w,C-C). ESI (+)Mass spec (MeOH, M/z), 479 for the [Zn(phen)(L-*κO,S*)]$^{+}$ fragment and 535 fragment respectively

[Zn(dmp)(L-*κO,S*)]Cl: White powder: yield 48%; mp (177-183 ºC); ^{1}H NMR (500MHz, CDCN-d_3),δ9.38 (d,*J*=10.4Hz,2H,H^{2+9}),8.62(d,*J*=8.4H,2H,H^{4+7}),8.29(d,*J*=7.2Hz,2H,$H^{2'+6'}$), 7.87(s,2H,H^{5+6}),7.42(dd,*J*=11.1,7.4Hz,2H,H^{3+8}),4-3.89(m,4H,$H^{a+a'}$),3-2.9(s,6H,H^{5+6}),1.94 (s,3H,H^{AOc}), 1.27 (s,6H,$H^{b+b'}$): FT-IR (ATR); ν(cm^{-1}), 3011(w, Ar-C-H), 1490 (s, C-N), 1580 (s, C=O), 1210 (w, C-C). ESI (+), Mass spec (MeOH, M/z) 507 for the [Zn(dmp)(L-*κO,S*)]:.

2.5 References

[1] A. Lapasam, M. R. Kollipara, *Phosphorus, Sulfur Silicon Relat. Elem.* **2020**, *195*, 779–804.

[2] A. Saeed, M. N. Mustafa, M. Zain-ul-Abideen, G. Shabir, M. F. Erben, U. Flörke, *J. Sulfur Chem.* **2019**, *40*, 312–350.

[3] K. Ghazal, S. Shoaib, M. Khan, S. Khan, M. K. Rauf, N. Khan, A. Badshah, M. N. Tahir, I. Ali, A. ur Rehman, *J. Mol. Struct.* **2019**, *1177*, 124–130.

[4] W. Hermindez, E. Spodine ', L. Beyer, U. Schrtider, R. Richter, J. Ferreira, M. Pavani, *Bioinorg. Chem. Appl.* **2005**, *3*, 299–317.

[5] A. M. Plutín, A. Alvarez, R. Mocelo, R. Ramos, E. E. Castellano, M. M. Da Silva, L. Colina-Vegas, F. R. Pavan, A. A. Batista, *Inorg. Chem. Commun.* **2016**, *63*, 74–80.

[6] C. I. Sacht, M. S. Datt, S. Otto, A. Roodt, *J. Chem. Soc. Dalt. Trans.* **2000**, 727–733.

[7] K. M. Engle, J. Q. Yu, *J. Org. Chem.* **2013**, *78*, 8927–8955.

[8] K. R. Koch, *Coord. Chem. Rev.* **2001**, *216–217*, 473–488.

[9] A. Saeed, U. Flörke, M. F. Erben, *J. Sulfur Chem.* **2014**, *35*, 318–355.

[10] M. C. Risi, Copyright Statement : An Investigation of the Coordination Chemistry of N , N ` -Disubstituted Sulfonylthiourea Ligands with d 6 and d 8 Transition Metal Centres.Book ., **1994**.

[11] L. Ciszewski, D. Xu, O. Repič, T. J. Blacklock, *Tetrahedron Lett.* **2004**, *45*, 8091–8093.

[12] R. N. Magwaza, S. Africa, R. N. Magwaza, Exploring the Use of Sulphobutyl-Ether- β -Cyclodextrin and Surfactant Micelles as a Drug Delivery System, **n.d.2017**

[13] A. R. Katritzky, X. Cai, B. V. Rogovoy, *J. Comb. Chem.* **2003**, *5*, 392–399.

[14] I. Yavari, N. Iravani, S. Z. Sayyed-Alangi, R. Hajinasiri, *Monatshefte fur Chemie* **2009**, *140*, 1199–1204.

[15] K. G. Bedane, G. S. Singh, *Arkivoc* **2015**, *2015*, 206–245.

[16] Y. Lin, W. J. Hirschi, A. Kunadia, A. Paul, I. Ghiviriga, K. A. Abboud, R. W. Karugu, M. J. Vetticatt, J. S. Hirschi, D. Seidel, *J. Am. Chem. Soc.* **2020**, *142*, 5627–5635.

[17] I. B. Douglass, F. B. Dains, *J. Am. Chem. Soc.* **1934**, *56*, 1408–1409.

[18] R. Koch, C. Wentrup, *J. Org. Chem.* **2013**, *78*, 1802–1810.

[19] E. F. Kangara, Exploring Rare Monodentate Coordination of Disubstituted

Acylthioureato Ligands, **2019**.

[20] G.T. Morgan and F.H.Burstall.*J.Chem.Soc* **1933**, 965–971.

[21] I. A. Kotzé, W. J. Gerber, J. M. Mckenzie, K. R. Koch, A High-Resolution 1H and DOSY NMR Study, **2009**.

[22] L. R. Gouvea, D. A. Martins, G. Jean, M. De Nazare, **2013**, 813–825.

[23] D. Lu, G. A. Voth, *Proteins Struct. Funct. Genet.* **1998**, *33*, 119–134.

[24] D. J. Awad, F. Conrad, A. Koch, U. Schilde, A. Pöppl, P. Strauch, *Inorg Chim. Act.***2010**, *363*, 1488–1494.

[25] T. Salzillo, M. Masino, G. Kociok-Köhn, D. Di Nuzzo, E. Venuti, R. G. Della Valle, D. Vanossi, C. Fontanesi, A. Girlando, A. Brillante, E. Da Como, *Cryst. Growth Des. Inorg. Chem.Act*. **2016**, *16*, 3028–3036.

[26] G. M. Sheldrick, *Acta Crystallogr. Sect. A Found. Crystallogr.* **2008**, *64*, 112–122.

[27] C. F. Macrae, I. J. Bruno, J. A. Chisholm, P. R. Edgington, P. McCabe, E. Pidcock, L. Rodriguez-Monge, R. Taylor, J. Van De Streek, P. A. Wood, *J. Appl. Crystallogr.* **2008**, *41*, 466–470.

[28] A. L. Spek, *Acta Crystallogr. Sect. D Biol. Crystallogr.* **2009**, *65*, 148–155.

[29] D. B. G. Williams, M. Lawton, *J. Org. Chem.* **2010**, *75*, 8351–8354.

[30] A. Bahuguna, I. Khan, V. K. Bajpai, S. C. Kang, *Bangladesh J. Pharmacol.* **2017**, *12*, 115–118.

[31] M. Galanski, V. Arion, M. Jakupec, B. Keppler, *Curr. Pharm. Des.* **2005**, *9*, 2078–2089.

[32] I. Ott, R. Gust, *Arch. Pharm. (Weinheim).* **2007**, *340*, 117–126.

[33] A. Alama, B. Tasso, F. Novelli, F. Sparatore, *Drug Discov. Today* **2009**, *14*, 500–508.

CHAPTER 3

Cytotoxicity screening of [M^{II}(diimine)(L-κ*O*,*S*)]X complexes

3.1 Introduction

The search for novel non-platinum DNA, and protein-targeting metal-based cancer agents with potential in *vitro* toxicity have acquired significance interest in recent years.[1] These anticancer complexes could be a substitute for platinum-based drugs because of their potentially improved characteristics and less negative side effect.[2] Such unresolved limitations stimulated research on novel non-platinum metal-containing anti-cancer therapeutics.[3] Even though there is currently no non-platinum metal anti-tumor drug on the market, considerable progress has been made in the advancement of such an agent, like for instance the copper based drugs called Casiopeina IIIia and NAMI-A have gone to the first phase clinical trial .[4-5] Some different transitional metal ions such as Zn, Cu and Fe are important cellular components involved in many biochemical processes. [6] The choice of ligands that will interact with free protein-bound metal ions is also a recent focus of medicinal inorganic chemistry studies. For instance, chelating ligands for copper and zinc complexes are being investigated as a potential treatment for Alzheimer's disease.[7]. A copper (II) complex bearing a phen ligand was investigated and it was found to show great intercalation with DNA nucleobases because of the planar aromatic presence in phen.[8] Therefore, the design of a newly synthesized potentially anti-cancer agent bearing 1.10-phenanthroline ligands and transitional metals Pd, Pt, Cu and Zn in this study requires a dose-dependent cell viability screening on cancer cells.

Several ways are deployed to test the synthesized complexes against the targeted cells. However, for the purposed of this study, an MTT cytotoxic assay was used to investigate the effect of the synthesized complexes on a lung cancer cell line (A549) and on a human embryotic cancer cell line (HEK-293). The development of the colorimetric is based on the principle that the mitochondrial enzyme, succinate dehydrogenase in healthy viable cells will leave the tetrazolium salt and converting into a water insoluble purple formazan crystal.[9] This method has simplified a large scale screening of drugs against targeted cells.[10] The MTT infiltrates the cell and permits through mitochondria where it is lowered to an insoluble dark purple formazan product.[11] An organic solvent is used to solubilized-formazan and the solubilized formazan reagent is measured spectrophotometrically. To evaluate the different effects on cell proliferation and viability, two assays were performed, trypan blue to measure cell number and the MTT assay for viability.[12]

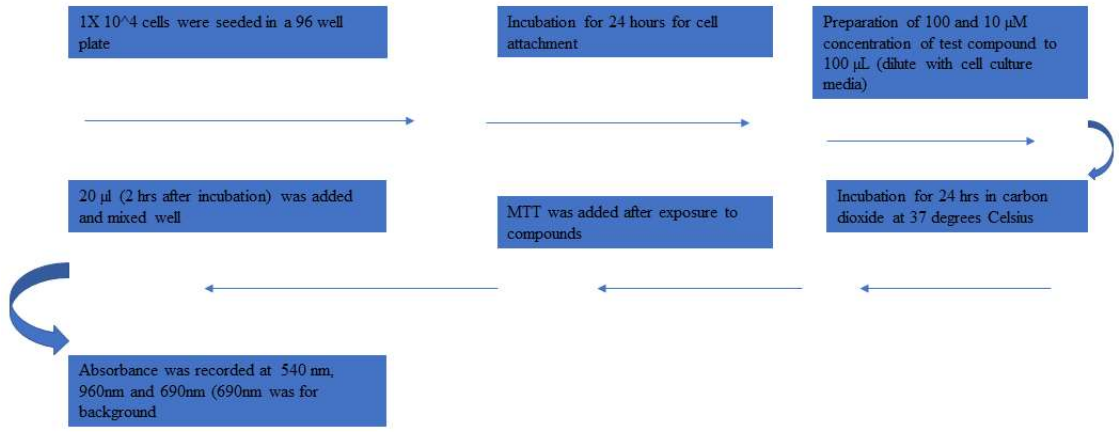

***Scheme 3.1**: Schematic representation of MTT assay procedure to probe cytotoxicity.*

Complexes that were screened against the two cancer cell lines at different concentration are shown in (*Figure 3.1*). These complexes were grouped together according to their molecular structures. This was done to distinguish between the different complexes and compare them to each other.

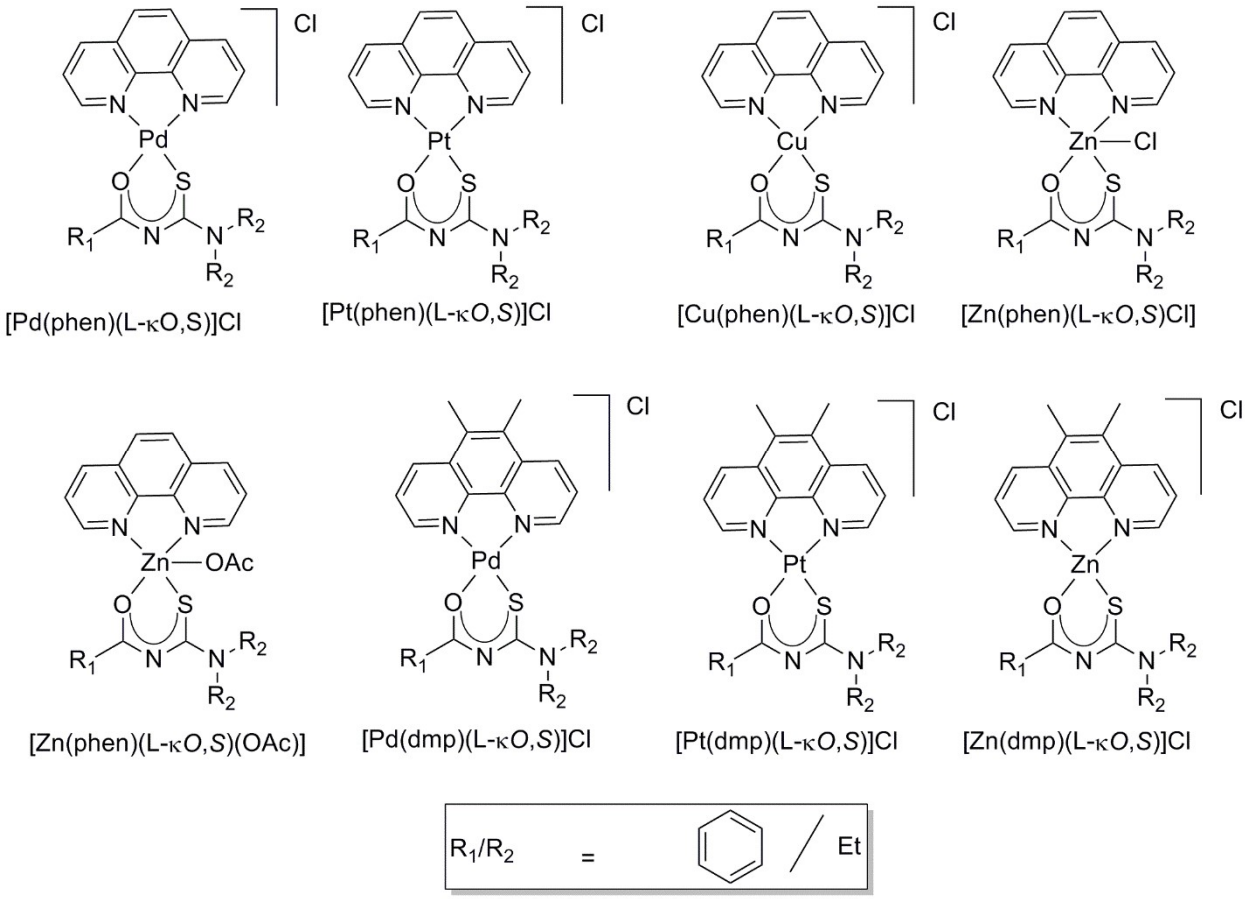

***Figure 3.1**: The [M(diimine)(L-κO,S)]$^+$ complexes that were screened against A549 lung and HEK-293 cancer cell lines using the MTT assay*

3.2 Results and discussion

A series [M(diimine)(L-κ*O,S*)]$^{+}$ of complexes as shown in (*Figure 3.1*) were tested against A549 lung carcinoma cancer and HEK 293 human embryonic kidney cancer cell lines. The results are presented graphically where cells were exposed using two different concentrations of each complex 100 μM (figure 3.1a) and 10 μM (figure 3.1b). The experiment was conducted in triplicate for each compound.

[Cu(phen)(L-κ*O,S*)]Cl, [Pd(phen)(L-κ*O,S*)]Cl, [Pt(phen)(L-κ*O,S*)]Cl were highly active against HEK-293 cancer cell and the ([Zn(phen)(L-κ*O,S*)Cl] being the least active, but also show 23% cell viability which is good. When these complexes were screened against A549 carcinoma cancer cell at 100 μM, [Cu(phen)(L-κ*O,S*)]Cl was the most highly active amongst the four complexes and followed by the square-panar complexes Pd(II) and Pt(II) which both showed less than 20% cell viability. The ([Zn(phen)(L-κ*O,S*)Cl] being the least active with indication of 40% of cell viability.

When the concentration of the complexes was reduced to 10 μM (*Figure 3.1b*), the [Cu(phen)(L-κ*O,S*)]Cl complex was once again the most active complex amongst the phen complexes evaluated with 0% cell viability against the HEK-293 cancer cell line, followed by the Pt(II) complexes with a 5% cell viability. At this concentration, the Pd(II) complex was the least active towards the HEK-293 cancer cells followed by the Zn(II) complex. Looking at the A549 lung carcinoma cancer cells, the Zn(II) complex was the least active complex followed by the Pd(II) complex. The Cu(II) complex remains the most active complex showing 20% cell viability followed by the Pt(II) complex with 55% cell viability.

(a)

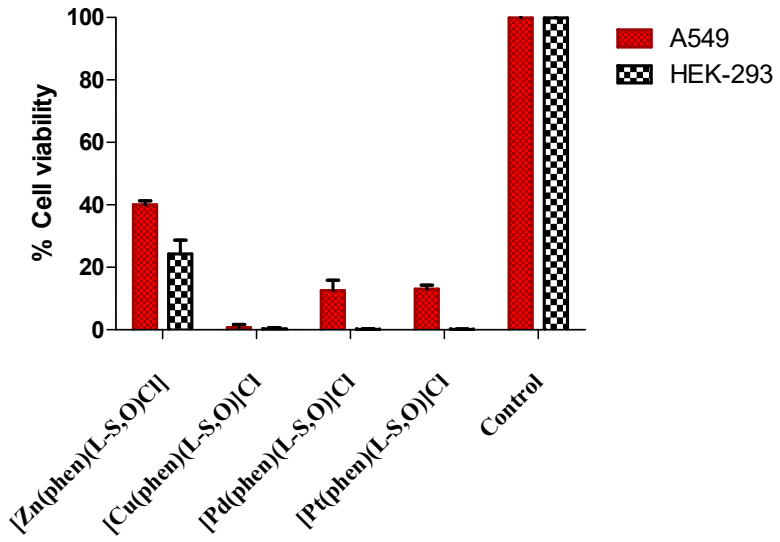

(b)

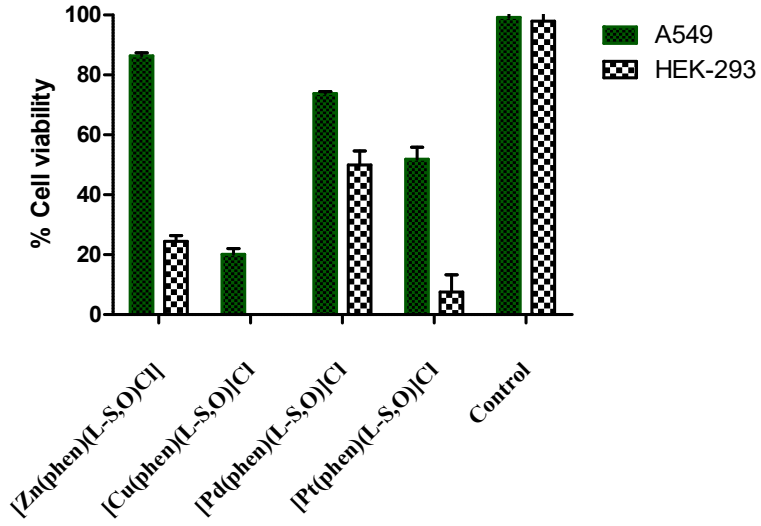

Figure 3.*2: % Cell survival of the two cell lines following increase in concentration of complexes to 100 µM (a) and reduce concentration to 10 µM (b).*

Square-planar complexes were grouped together as shown in figure 3.2 which were tested in A549 lung carcinoma and HEk-293 embryotic kidney. This was done to assess which metal complexes had a greater activity. These complexes were evaluated by using a high

concentration 100 µM (figure 3.2a) and a lower concentration 10 µM (figure 3.2b). All these complexes showed high activity against HEK-293 cancer cells with 0% cell viability. However, evaluating the complexes against A549 lung carcinoma cancer cells, there was no significant difference for phen complex, slight difference for dmp complexes between the Pd(II) and Pt(II) complexes at high concentration (*Figure 3.2a*). A significant difference was observed when the lower concentration was used to evaluate these complexes against the same cancer cell lines. It can be seen that the Pt(II) complexes showed high activity in both cancer cell lines and especially the HEK-293 cancer cells with 5% cell viability for the phen containing complex. The dmp complexes showed a great activity compared to the phen in both metals (Pd and Pt).

(a)

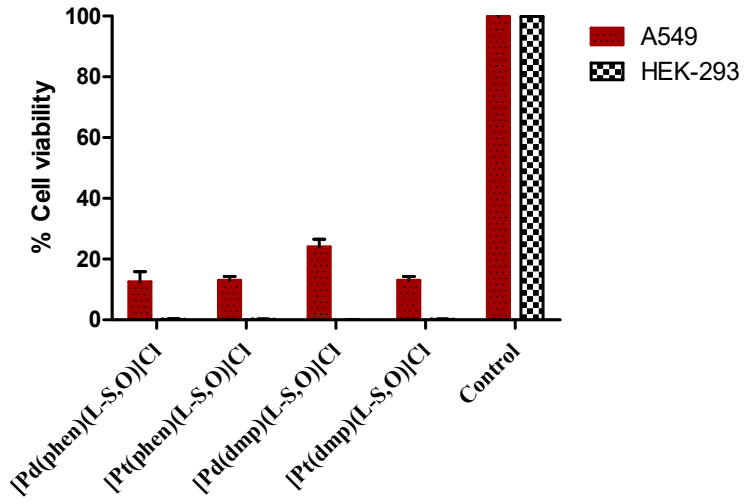

(b)

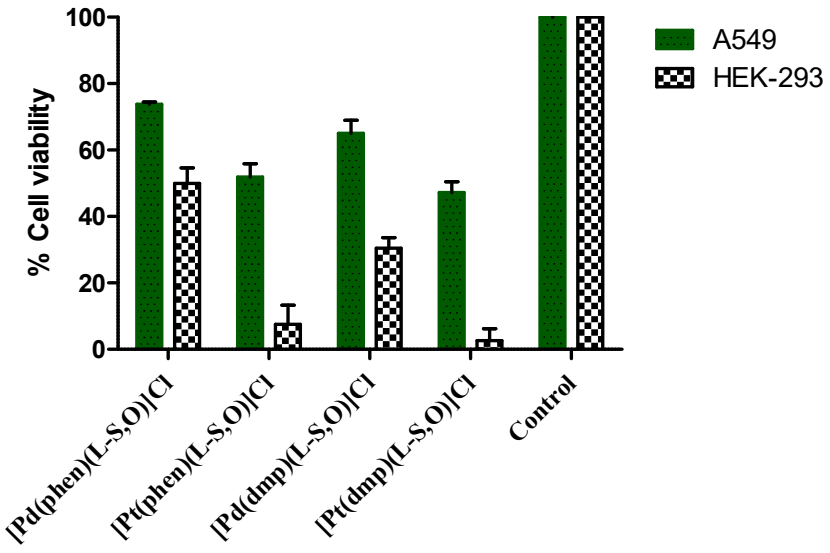

***Figure 3.2**: % Cell survival of the two different cell lines against square-planar complexes at increase in concentration of complexes to 100 µM (a) and low concentration to 10 µM (b).*

In (*Figure 3.3*) metal complexes containing a substituted phen with methyl group in 5 and 6 positions were plotted together to show the effect of varying the metal center. These complexes contains three different metals (Pd, Pt and Zn), Cu(II) was not teste as the full characterization of the [Cu(dmp)(L-κO,S)]Cl variation was not obtained. At 100 µM, we note that [Zn(dmp)(L-κ*O,S*)]Cl complex was highly active against the A549 lung cancer cell line with 15% cell viability followed by [Pt(dmp)(L-κ*O,S*)]Cl with 17% cell viability and [Pd(dmp)(L-κ*O,S*)]Cl being the least active complex with 23% cell viability. All the complexes were sensitive against HEK-293 cancer cell at high concentration (100 µM) showing 0% cell viability. We observed that [Pt(dmp)(L-κ*O,S*)]Cl was the most active compound especially against HEK-293 cancer cell with less than 5% cell viability followed by [Zn(dmp)(L-κ*O,S*)]Cl with less than 30% cell viability, while [Pd(dmp)(L-κ*O,S*)]Cl being the least active with 30% cell viability at lower concentration (10 µM) (Figure 3.3b). Only a minor difference in activity was observed when comparing Pt and Zn complexes of the same type against the A549 lung carcinoma cancer cells in both high a low concentration. There was not much of a difference between these complexes (Pt and Zn), they again showed high activity with below 45% cell viability. On the other hand

[Pd(dmp)(L-κ*O,S*)]Cl was the least active against the A549 lung carcinoma cancer cells with 61% cell viability at lower concentration.

(a)

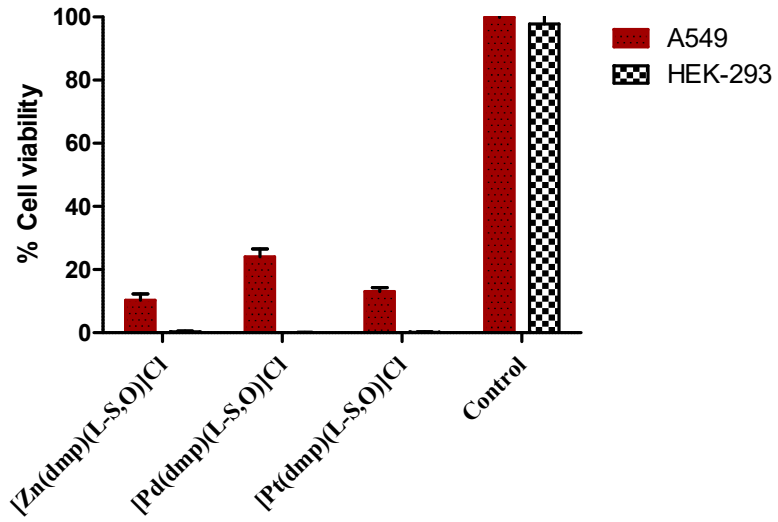

(b)

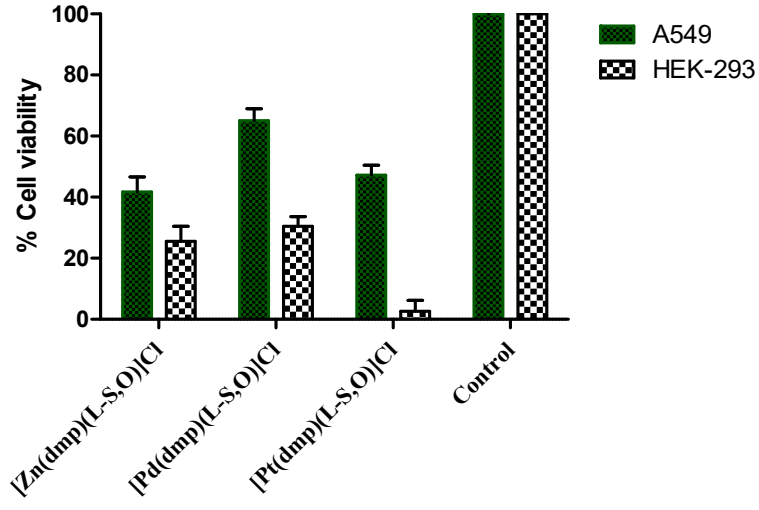

***Figure 3.3**: % Cell viability of the two different cancer cell lines screened against dmp containing complexes at 100 µM (a) and low concentration 10 µM (b).*

The data for the variation of Zn(II) complexes evaluated is plotted in (*Figure 3.4).* Three of the Zn complexes were presented in (*Figure 3.4*) and they showed a significant difference in each cancer cell line. The Zn complex bearing dmp was the one showing high activity in both cancer cell lines, with 15% cell viability at high concentration against A549 lung carcinoma and 0% cell viability against HEK-293 embryotic cancer cell lines. This complex showed 40% cell viability against A549 lung carcinoma and less than 30% cell viability against HEK-293 human embryotic cancer cell lines at lower concentration (10 µM). The acetate containing complex in the fifth position also showed good anticancer activity with 38% of the cell viability for the A549 cells and no cell survival for the HEK-293 cancer cells (*Figure 3.4b*). The complex containing the chloride as the least active for both cancer cell lines. The dmp containing complex again showed high activity compared to the complexes containing the phen ligand.

(a)

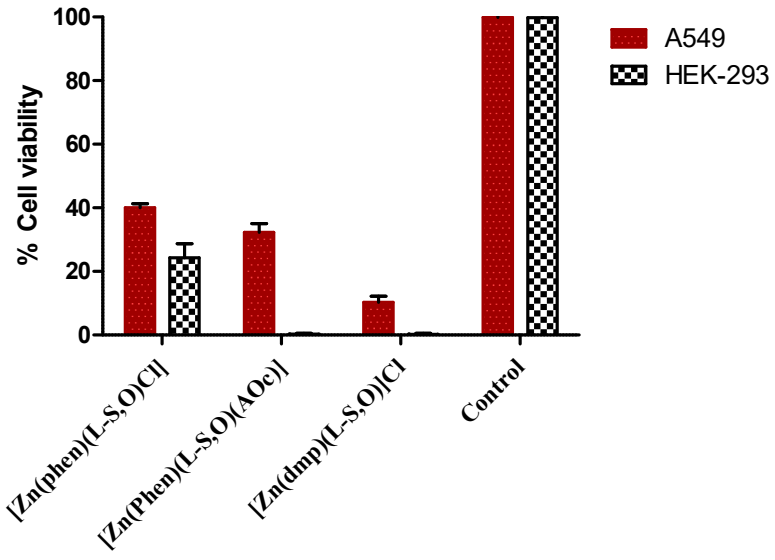

(b)

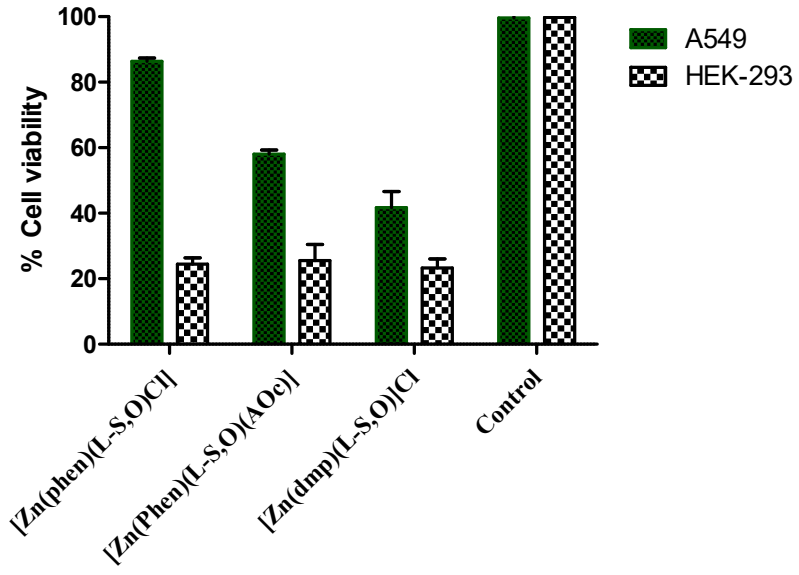

***Figure 3.4**: Three of variation of Zn(II) complexes plotted together to compared their cytotoxicity effect in two different cancer cell lines at 100 µM (a) and 10 µM (b).*

3.3 Conclusion

The results obtained, showed that all the [M(diimine)(L-κ*O,S*)]Cl complexes containing dmp ligand were highly active against the HEK-293 embryotic kidney cancer cell line showing almost 0% of cell viability at 100 µM. At lower concentration (10 µM), these complexes still showed activity with a cell survival below 50%. The [Cu(phen)(L-κ*O,S*)]Cl was the most active complex showing 0% of cell viability against HEK-293 at 100 µM and 23% cell viability against A549 lung cancer cells at 10 µM. The [Pd(phen)(L-κ*O,S*)]Cl was the least active complex at 100 µM killing only 50% of cells. The [Cu(phen)(L-κ*O,S*)]Cl complex showed activity against the A549 lung carcinoma cancer cells. There was a significant difference in biological activity between complexes containing dmp and phen, with dmp bearing complexes being the most active. The higher activity towards these cancer cells can be attributed by the influence of the dmp ligand. We also found that the Zn(II) complex bearing phen ligand, and the one coordinated with the acetate had a higher activity than the chloride variation.

Experimental section

The A549 lung carcinoma cancer cell line was chosen for this study to show the percentage cell viability for the triplicate trial in 100 μM and 10 μM. This information was showed in table form for both cancer cell lines.

Table 1. Cell viability of the complexes screened against A549 lung carcinoma cancer cell line using MTT assay at 100 μM for 24 hours.

Compound	**Trial 1**	**Trial 2**	**Trial 3**
[Zn(phen)(L-κ*O,S*)Cl]	41.30	40.03	38.67
[Zn(dmp)(L-κ*O,S*)]Cl	12.01	8.32	10.65
[Zn(phen)(L-κ*O,S*)(OAc)]	29.64	35.08	32.16
[Cu(phen)(L-κ*O,S*)]Cl	0.00	1.10	2.03
[Pd(phen)(L-κ*O,S*)]Cl	15.45	8.87	13.20
[Pd(dmp)(L-κ*O,S*)]Cl	25.03	21.14	25.90
[Pt(phen)(L-κ*O,S*)]Cl	12.79	11.86	14.38
[Pt(phen)(L-κ*O,S*)]Cl	11.63	6.89	12.15

Table 2. Cell viability of the complexes screened against A549 lung carcinoma cancer cell line using MTT assay at 10 μM for 24 hours.

Compound	**Trial 1**	**Trial 2**	**Trial 3**
[Zn(phen)(L-κ*O,S*)Cl]	85.71	87.11	86.95
[Zn(dmp)(L-κ*O,S*)]Cl	45.78	36.32	43.08
[Zn(phen)(L-κ*O,S*)(OAc)]	56.59	59.02	58.41
[Cu(phen)(L-κ*O,S*)]Cl	21.05	17.96	21.44
[Pd(phen)(L-κ*O,S*)]Cl	74.24	73.33	74.09
[Pd(dmp)(L-κ*O,S*)]Cl	62.23	67.83	65.47

[Pt(phen)(L-κ*O,S*)]Cl	56.05	48.14	51.38
[Pt(phen)(L-κ*O,S*)]Cl	44.38	46.42	50.81

Table 3. Cell viability of the complexes screened against HEK-293 embryotic kidney cancer cell line using MTT assay at 100 μM for 24 hours.

Compound	**Trial 1**	**Trial 2**	**Trial 3**
[Zn(phen)(L-κ*O,S*)Cl]	21.84	25.95	19.74
[Zn(dmp)(L-κ*O,S*)]Cl	0.00	0.45	0.58
[Zn(phen)(L-κ*O,S*)(OAc)]	0.00	0.76	0.19
[Cu(phen)(L-κ*O,S*)]Cl	0.00	0.78	0.00
[Pd(phen)(L-κ*O,S*)]Cl	0.12	0.37	0.16
[Pd(dmp)(L-κ*O,S*)]Cl	0.00	0.03	0.00
[Pt(phen)(L-κ*O,S*)]Cl	0.00	0.96	0.00
[Pt(phen)(L-κ*O,S*)]Cl	0.00	0.42	0.00

Table 4. Cell viability of the complexes screened for HEK-293 embryotic kidney cancer cell line using MTT assay at 10 μM.

Compound	**Trial 1**	**Trial 2**	**Trial 3**
[Zn(phen)(L-κ*O,S*)Cl]	22.15	25.50	25.60
[Zn(dmp)(L-κ*O,S*)]Cl	21.32	25.20	23.26
[Zn(phen)(L-κ*O,S*)(OAc)]	20.39	26.18	25.55
[Cu(phen)(L-κ*O,S*)]Cl	0.00	0.31	0.00
[Pd(phen)(L-κ*O,S*)]Cl	49.81	44.29	49.87
[Pd(dmp)(L-κ*O,S*)]Cl	27.62	29.96	30.48

[Pt(phen)(L-κ*O,S*)]Cl	8.45	9.54	12.20
[Pt(phen)(L-κ*O,S*)]Cl	2.94	7.59	0.00

3.4 References

[1] D. B. G. Williams, M. Lawton, *J. Org. Chem.* **2010**, *75*, 8351–8354.

[2] A. Bahuguna, I. Khan, V. K. Bajpai, S. C. Kang, *Bangladesh J. Pharmacol.* **2017**, *12*, 115–118.

[3] M. Galanski, V. Arion, M. Jakupec, B. Keppler, *Curr. Pharm. Des.* **2005**, *9*, 2078–2089.

[4] I. Ott, R. Gust, *Arch. Pharm. (Weinheim).* **2007**, *340*, 117–126.

[5] A. Alama, B. Tasso, F. Novelli, F. Sparatore, *Drug Discov. Today* **2009**, *14*, 500–508.

[6] R. Tabti, N. Tounsi, C. Gaiddon, E. Bentouhami, L. Desaubry, *Med. Chem. (Los. Angeles).* **2017**, *07*, 875–879.

[7] P. Jia, R. Ouyang, P. Cao, X. Tong, X. Zhou, T. Lei, Y. Zhao, N. Guo, H. Chang, Y. Miao, S. Zhou, *J. Coord. Chem.* **2017**, *70*, 2175–2201.

[8] H. Kozlowski, M. Luczkowski, M. Remelli, D. Valensin, *Coord. Chem. Rev.* **2012**, *256*, 2129–2141.

[9] A. M. Pizarro, P. J. Sadler, *Biochimie* **2009**, *91*, 1198–1211.

[10] I. Mitra, S. Mukherjee, P. B. Reddy Venkata, S. Dasgupta, C. K. Jagadeesh Bose, S. Mukherjee, W. Linert, S. C. Moi, *RSC Adv.* **2016**, *6*, 76600–76613.

[11] M. V. Berridge, P. M. Herst, A. S. Tan, *Biotechnol. Annu. Rev.* **2005**, *11*, 127–152.

[12] G. Banfalvi, *Apoptosis* **2017**, *22*, 306–323.

CHAPTER 4

SUMMARY AND CONCLUSION

4.1 Synthesis and characterization of N,N-di(ethyl)-N'-benzoylthiourea and [M(diimine)(L-κO,S)]Cl complexes

This thesis reports the synthesis, spectral characterization, and some of the structures of metal complexes; Pd(II), Pt(II), Cu(II), and Zn(II) bearing *N,N*-di(ethyl)-*N*'-benzoylthiourea ancillary ligand (**HL**) and two diimine ligands. The characterization techniques which were used are: FT-IR spectroscopy, NMR spectroscopy, Mass spectrometry, Single-crystal X-ray diffraction and elemental analysis. The first step was to synthesize *N,N*-di(ethyl)-*N*'-benzoylthiourea and metal precursors [MCl_2(diimine)], which were synthesized successfully in good yields. The *N,N*-di(ethyl)-*N*'-benzoylthiourea was the ligand of choice for the synthesis of the various metal complexes [M(phen)(L-*κO,S*)]Cl as the project mainly focused on the interchange of metals.

The preparation of the complexes involved *in-situ* deprotonation of *N,N*-di(ethyl)-*N'*-benzoylthiourea with sodium acetate or sodium hydride. The deprotonated **HL** ligand then reacted with the metal precursor [MCl_2(diimine)] in the ratio 1:1 , resulting in the formation of the complex. Different solvents were used in the preparation of these complexes to suit the chemical properties of each metal. Different methods, as discussed in chapter 2 were necessary to obtain the desired complexes. 2D-NMR spectroscopy was used where applicable to assign ^{1}H and ^{13}C-NMR signals unambiguously of the complexes.

Crystals of some of the complexes were grownded and used to confirm the structures of the obtained complexes. For the [Pd(phen)(L-*κO,S*)]NO_3 complex instead of the expected chloride counter ion, the crystal structure had the nitrate counter ion. Two Zn(II) crystal structures were obtained, one with penta-coordinated with acetate and the other penta-coordinated with chloride. Both these complexes have a distorted square pyramidal geometry. The purity of the complexes was true for only some of the complexes with the use of the elemental analysis and melting point measurements.

4.2 Biological application

The original goal for this project was accomplished, various complexes of the metals Cu(II), Pd(II), Zn(II), and Pt(II) bearing *N,N*-di(ethyl)-*N*-benzoylthiourea and diimine ligand were screened against the two different cancer cell lines. The results showed that the [Cu(phen)(L-κ*O,S*)]Cl complex had a better cytotoxicity effect against the two cancer cell lines. Even though Cu(II) complex showed the great activity, almost all the complexes were highly active towards HEK-293 embryotic kidney cancer cells with a cell. The [Cu(phen)(L-κ*O,S*)]Cl complex showed 0% of the cells viability while 95% cells death for the [Pt(phen)(L-*κO,S*)]Cl complexes. The [Pd(phen)(L-*κO,S*)]Cl and [Zn(phen)(L-*κO,S*)Cl] complexes were the least active with 65% and 25% of the cells viability. The dmp bearing ligand complexes showed higher activity at concentration lower of 10 μM compared to the complexes bearing phen ligand. The influence of the dmp ligand was significantly noticeable with complexes bearing dmp showing higher activity, killing 49 % of most cancer cells.

The [Zn(phen)(L-*κO,S*)Cl] and [Pd(phen)(L-*κO,S*)]Cl were least active complexes showed a higher number of cells survival with the cell death of 15% and 37% of the A549 cancer cells. Comparing the PGMs group metals (Pd and Pt), which possess similarities; The Pt(II) complexes have better cytotoxic activity than the Pd(II) complexes. The three Zn(II) complexes were grouped and compared for activity against A549 lung carcinoma and HEK-293 embryotic kidney cancer cell lines. Like in the other complexes, dmp ligand bearing complexes showed the best activity for both cancer cell lines with cell death of 60% for the A549 cancer cells and of 73% cell death of the HEK-293 cancer cells.

4.3 Future work

Given the information obtained from the MTT assay, which indicated the best activity against the A549 lung carcinoma cancer cells for the Cu(II) complex. The future work will focus on

IC_{50} assays which can be carried out to evaluate the potential anticancer properties of this complex.

As mentioned in Chapter 2, [Cu(phen)(L-*κO,S*)]Cl did not form crystals suitable for single X-ray crystal studies. It would be great to crystallize this complex for future work to have a better understanding of their geometry. It would also be great to synthesize the dmp bearing Cu(II) complex and screen. In future, variations of acylthiourea ligands will be used for the Cu(II) complexes and evaluated for improve activity, by introducing more lypophilic on the acylthiourea to potentially improve cellular uptake of the drug.

Appendix

NMR data

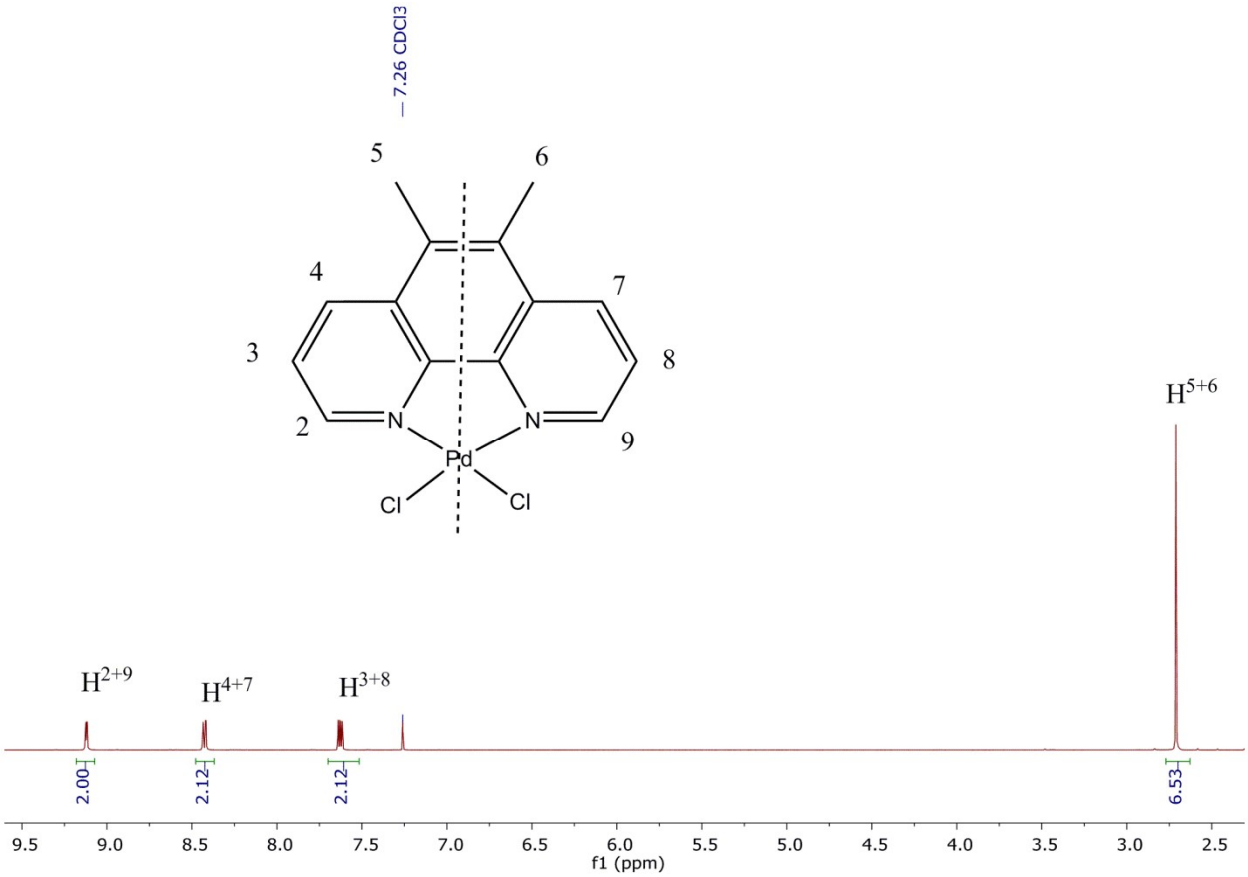

***Figure 1**: [1]H NMR of [$PdCl_2$(dmp)] in DMSO-d6 at 300K*

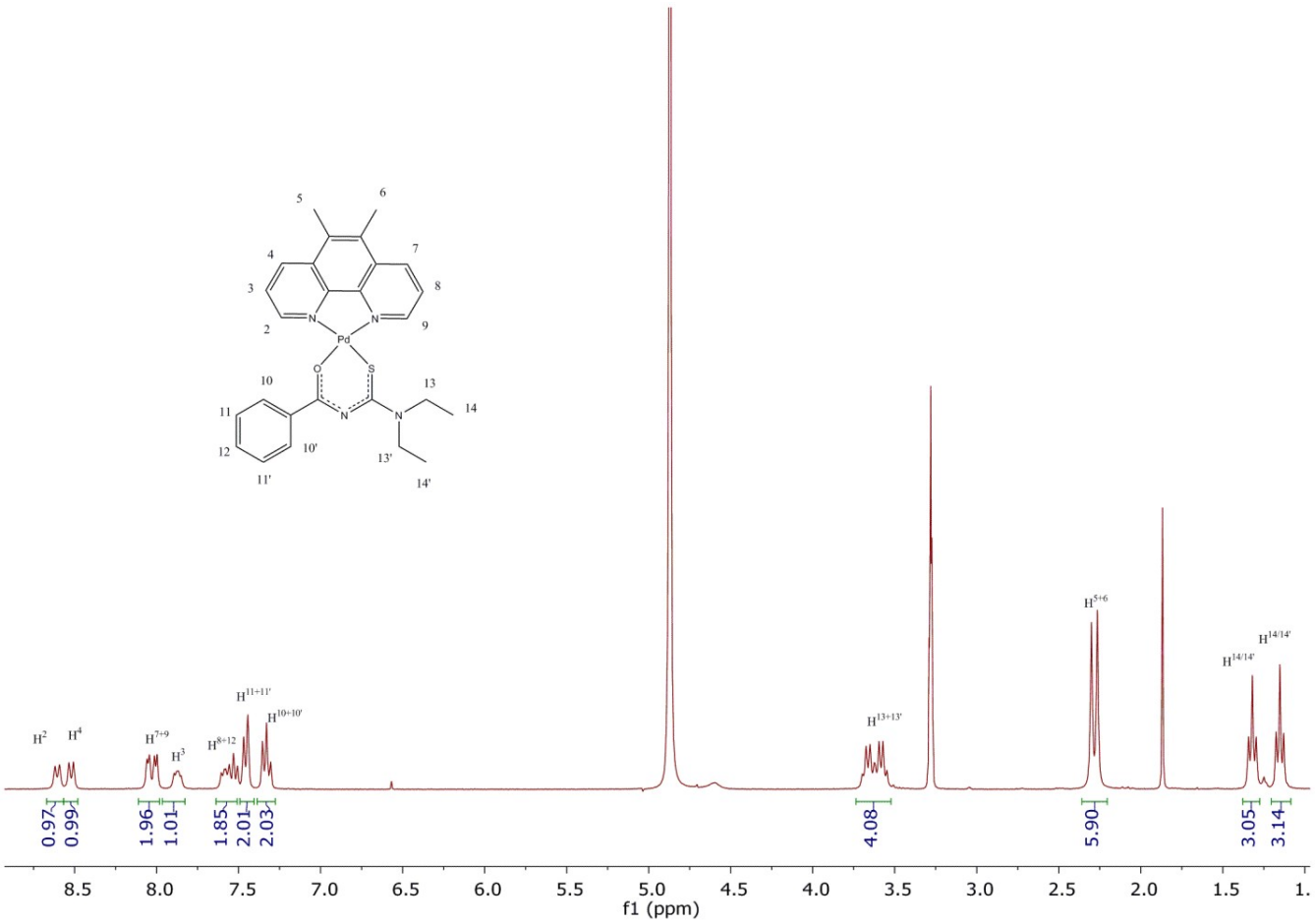

Figure 2: *^{1}H NMR of the [Pd(dmp)(L-κO,S)]Cl in methanol-d4 at 300K*

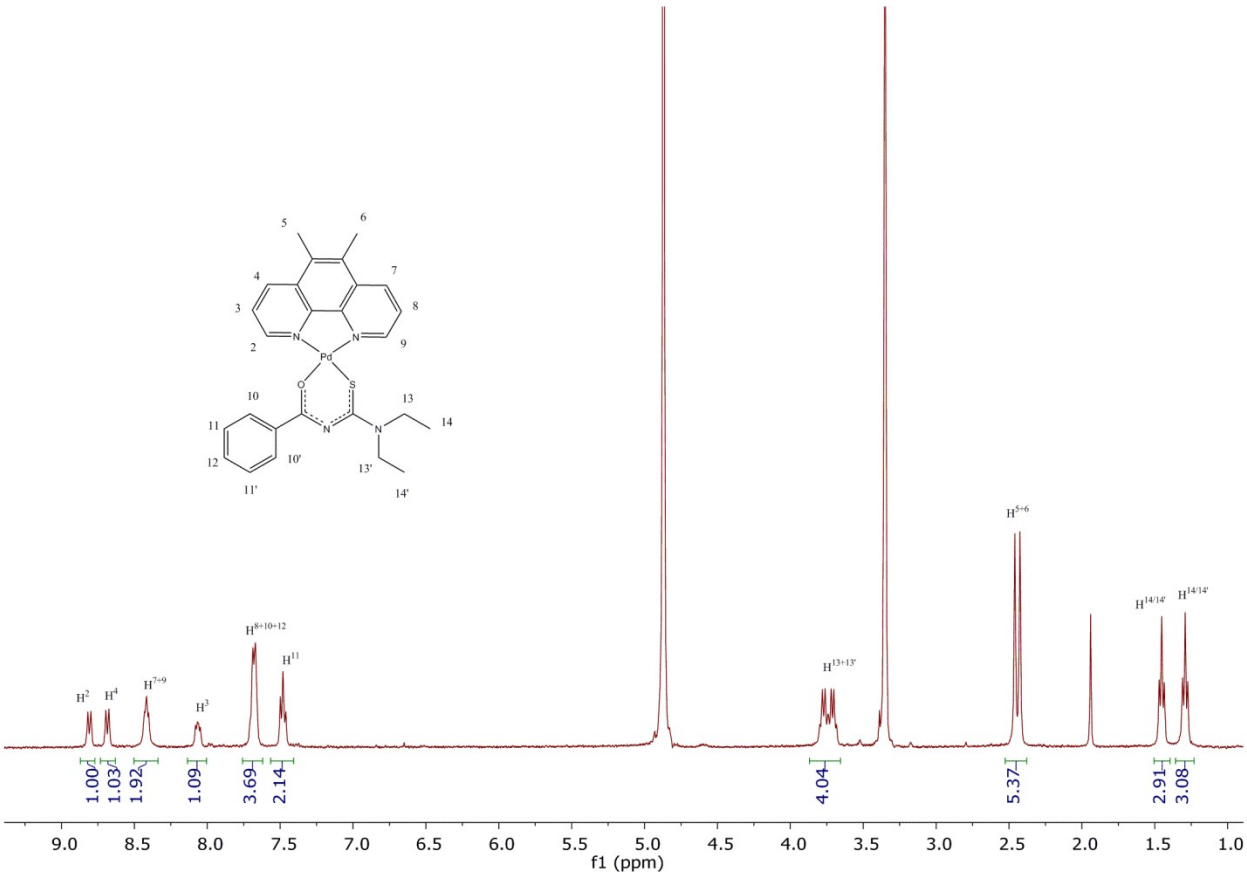

Figure 3: *^{1}H NMR of the [Pt(dmp)(L-κO,S)]Cl in methanol-d4 at 300K*

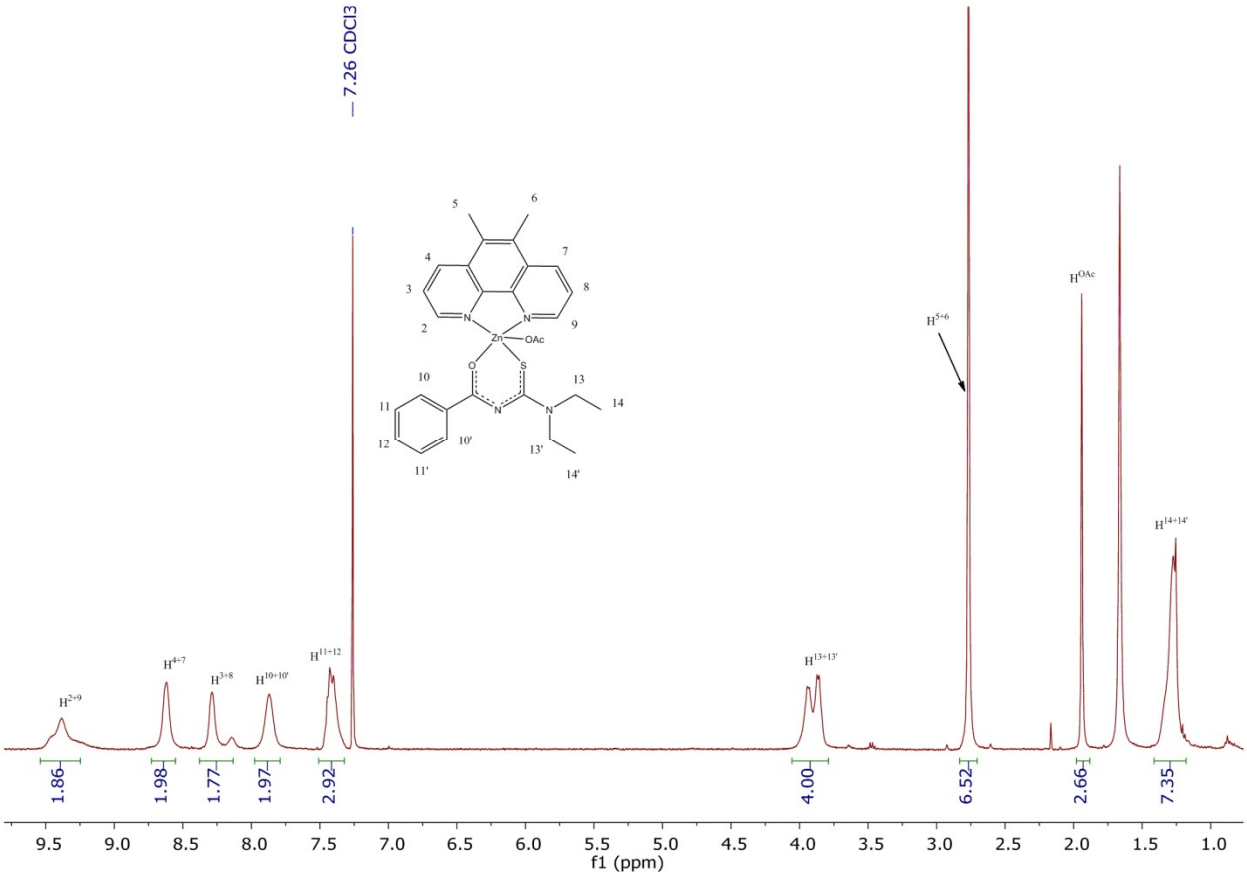

Figure 4: *[1]H NMR of the [Zn(dmp)(L-κO,S)]Cl in CDCl3 at 300K*

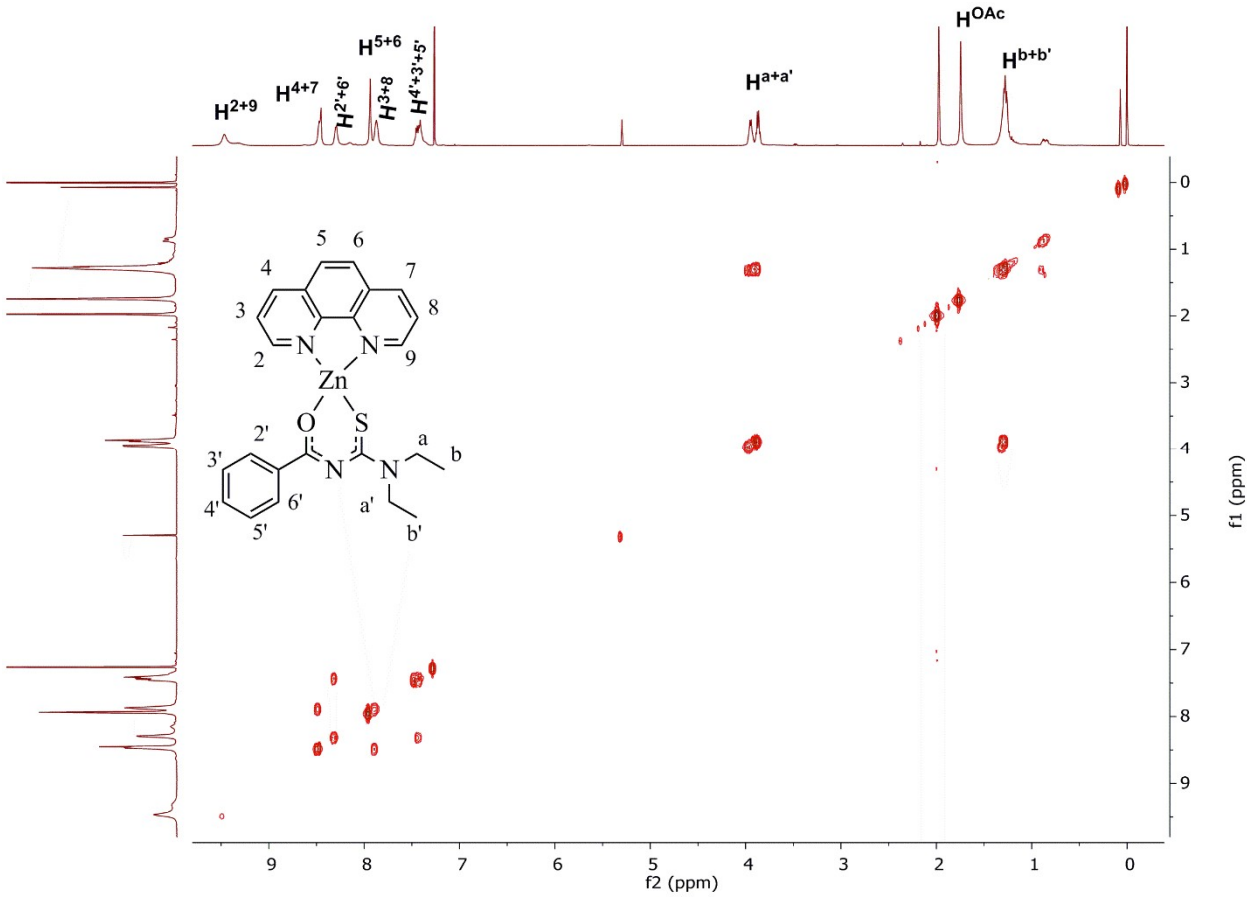

Figure 5: *COSY spectra for the [Zn(phen)(L-κO,S)Cl] in CDCl3 at 300K*

Appendix-B

Mass Spectroscopy for complexes

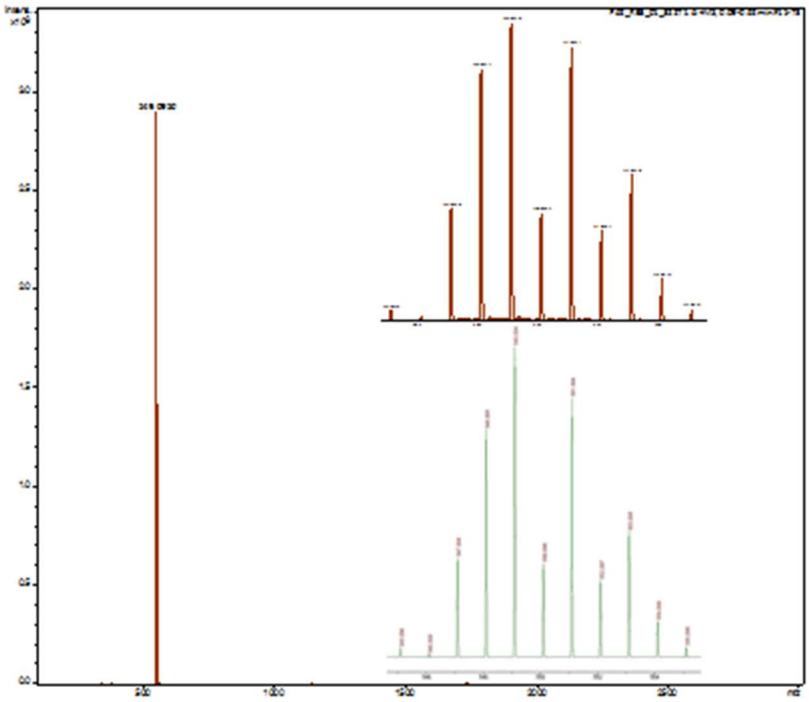

Figure1*:Mass spectrum of [Pd(dmp)(L-κO,S)]Cl*

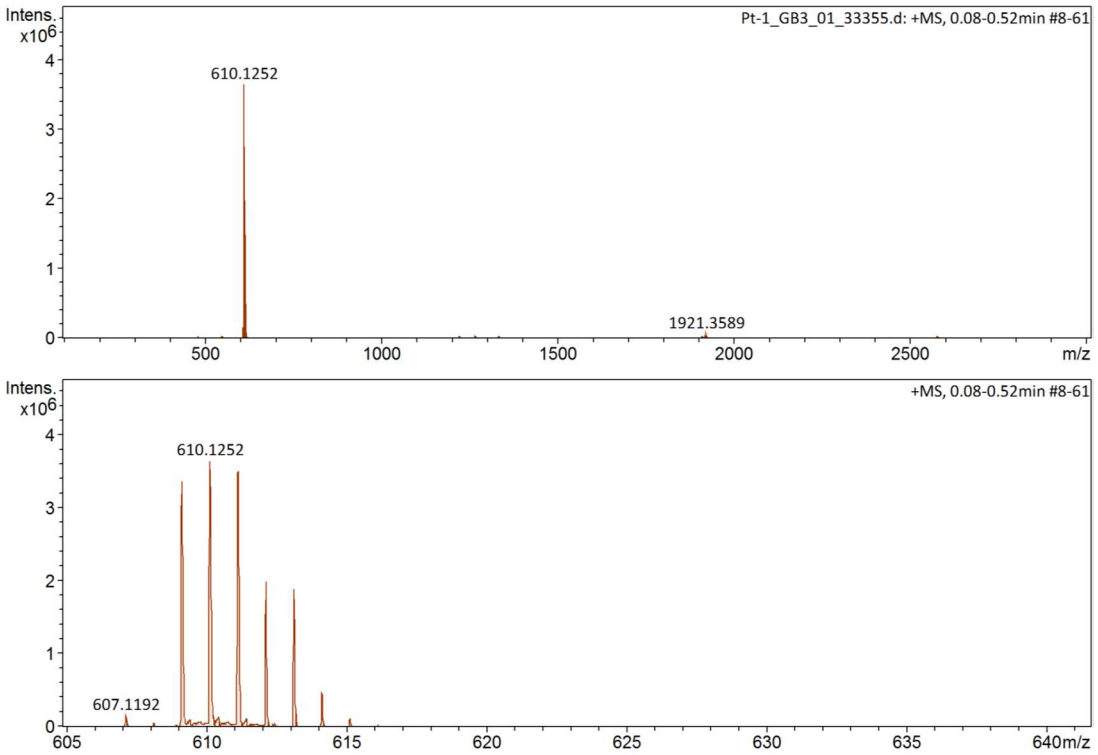

***Figure2**: Mass spectrum of [Pt(phen)(L-κO,S)]Cl*

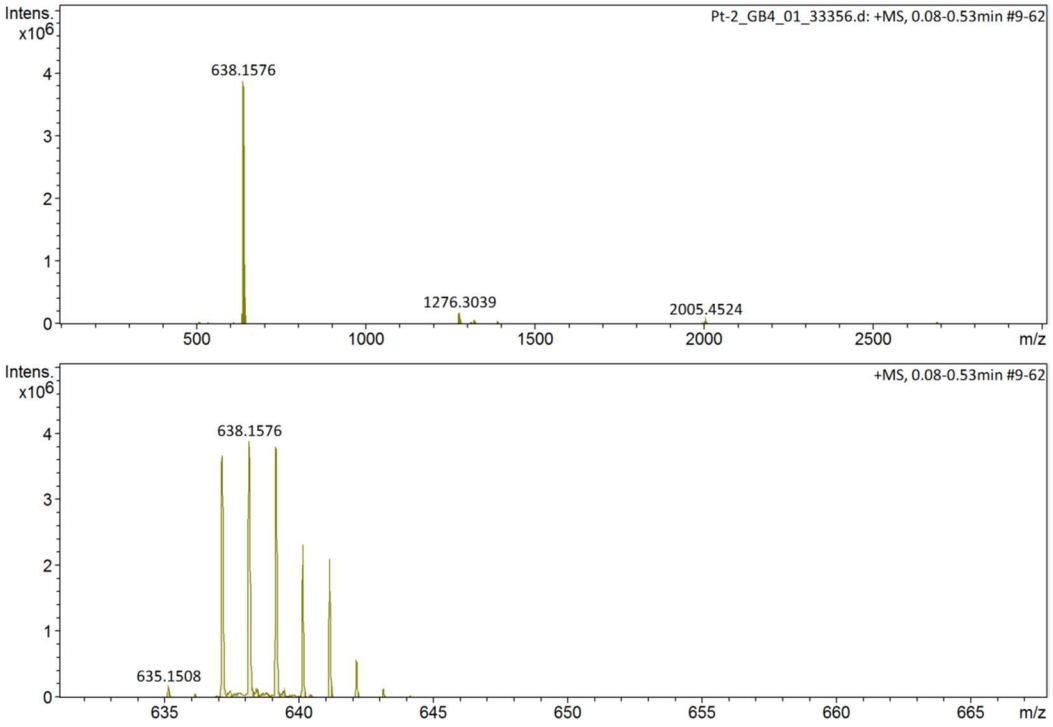

***Figure 3**:Mass spectrum of [Pt(dmp)(L-κO,S)]Cl*

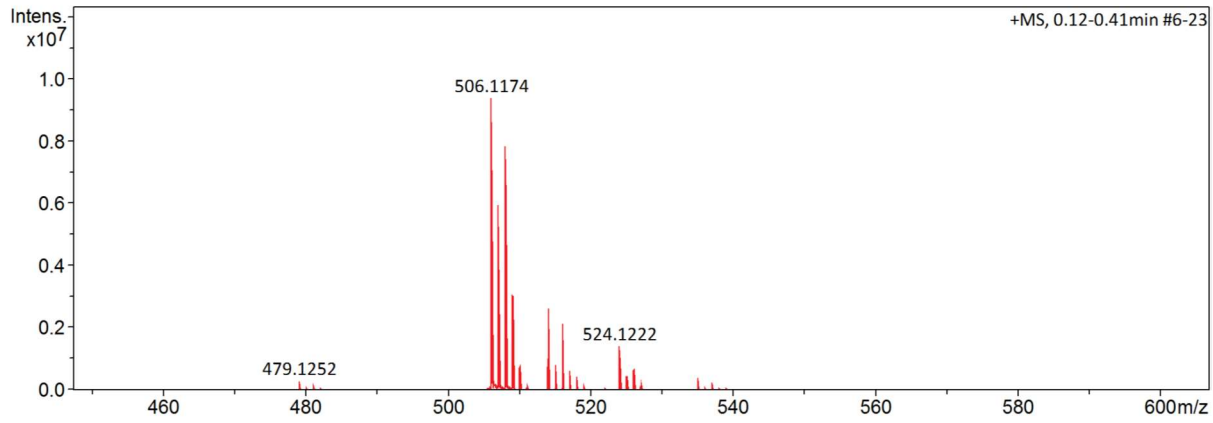

Figure4: *Mass spectrum of[Cu(dmp)(L-κO,S)]Cl*

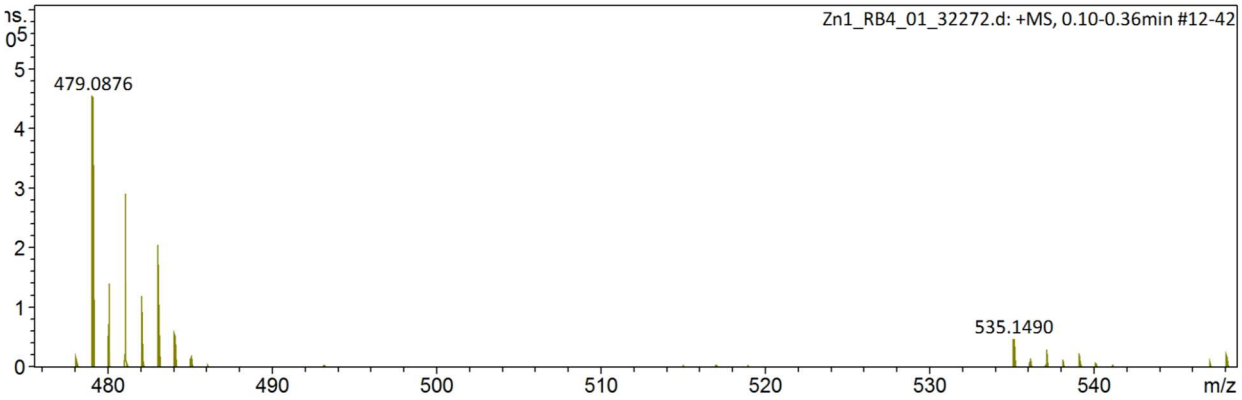

Figure 5*:Mass spectrum of [ZnCl(phen)(L-κO,S)]*

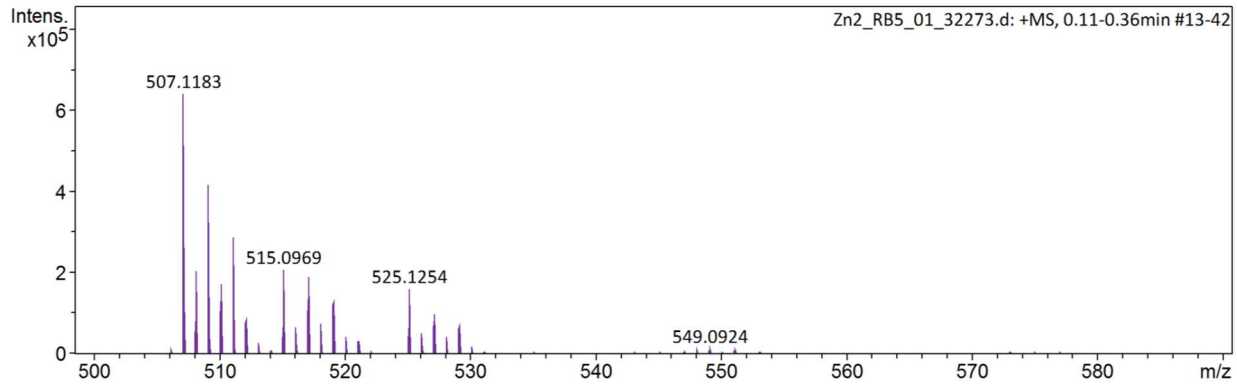

Figure 6*:Mass spectrum of [Zn(dmp)(L-κO,S)]Cl*

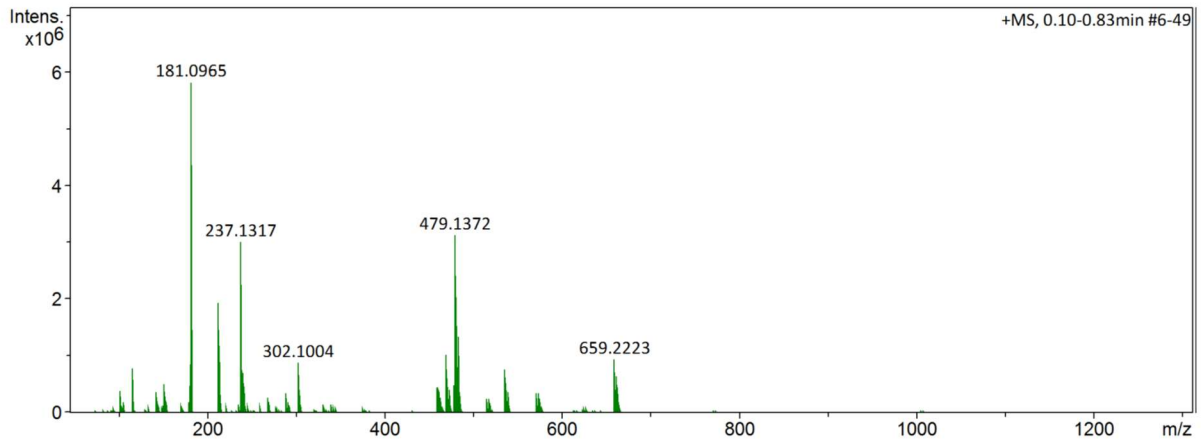

***Figure 7**:Mass spectrum of[Zn(OAc)(phen)(L-κO,S)]*

Appendix-C

FT-IR

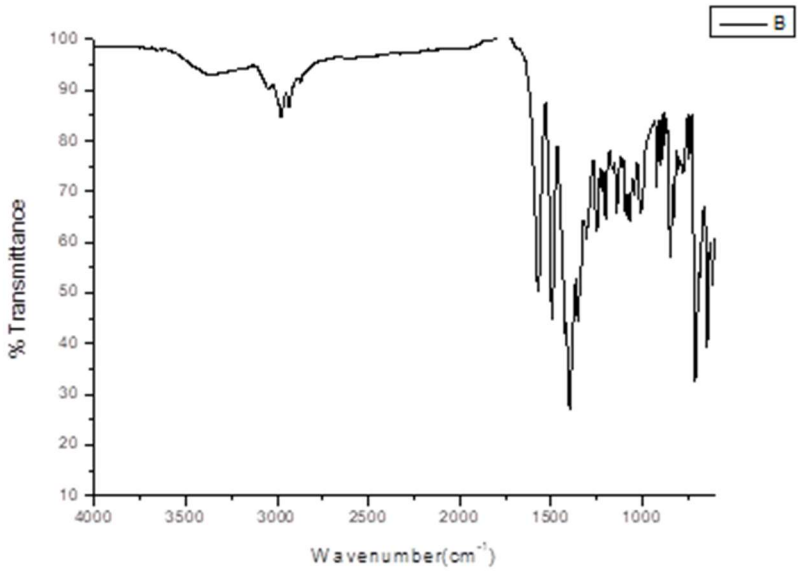

***Figure 1**:IR spectra for [$PdCl_2$(phen)*

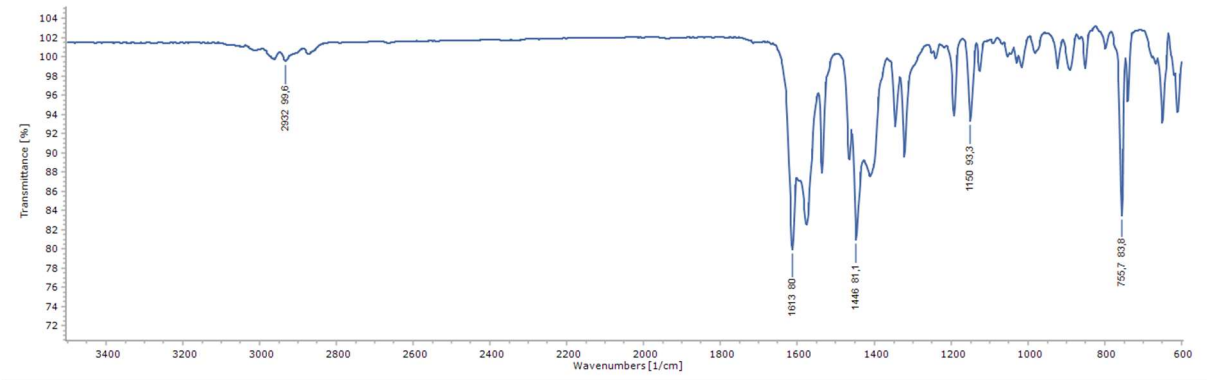

***Figure 2**:IR spectrum for the [$CuCl_2$(phen)] complex*

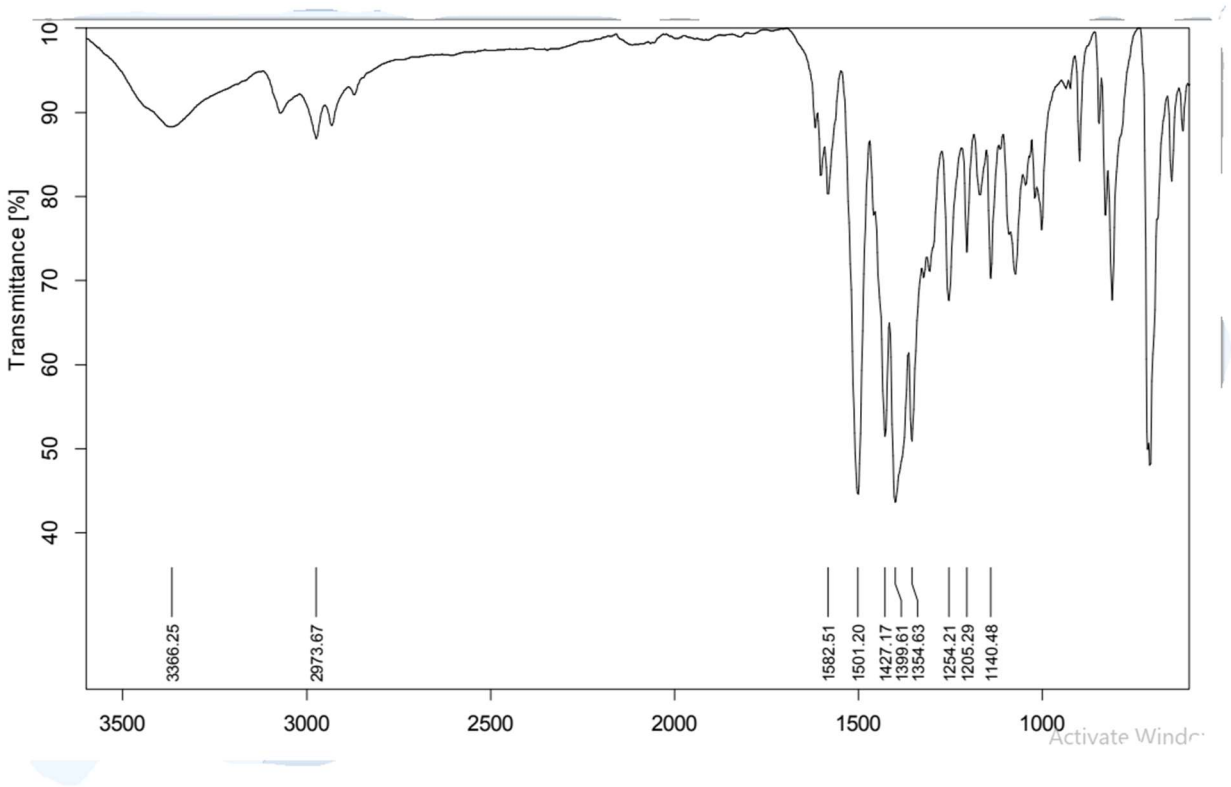

***Figure 3**; IR spectra for the [Pd(phen)(L-κO,S)]Cl*

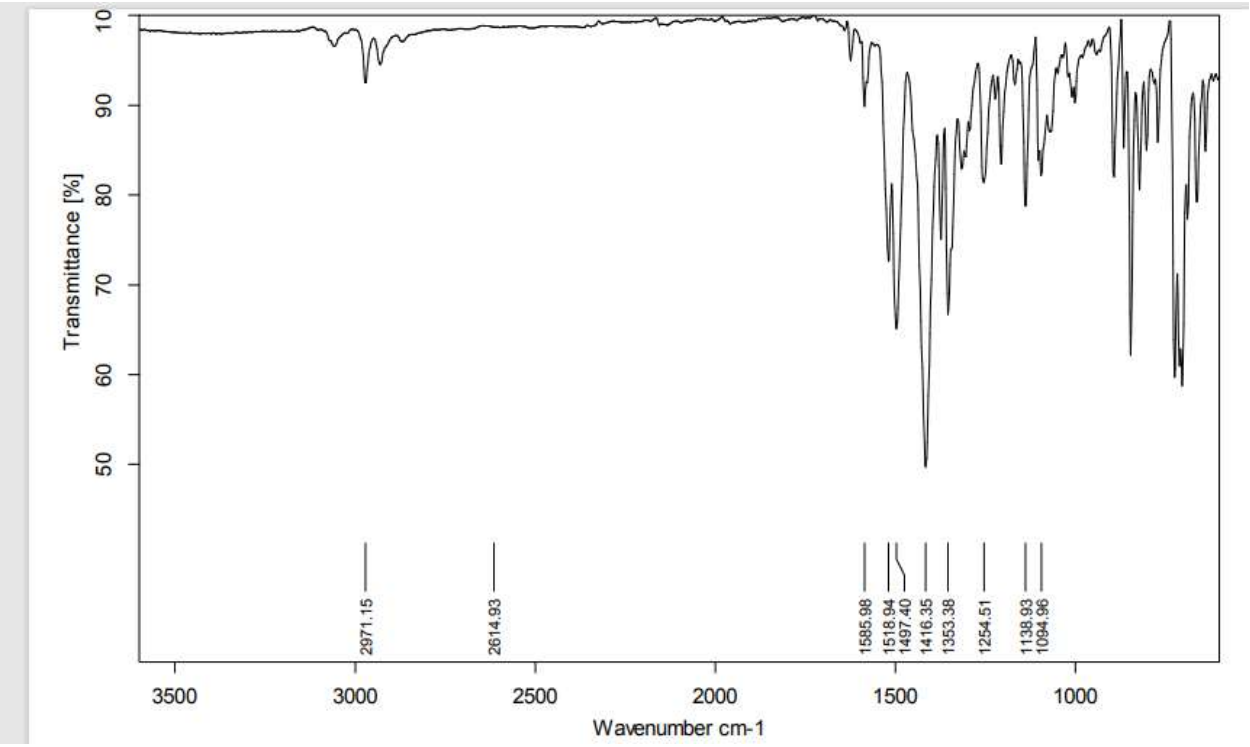

***Figure 4**:IR spectra of the [Zn(phen)(OAc)(L-κO,S)]*

Appendix-d

Crystallography

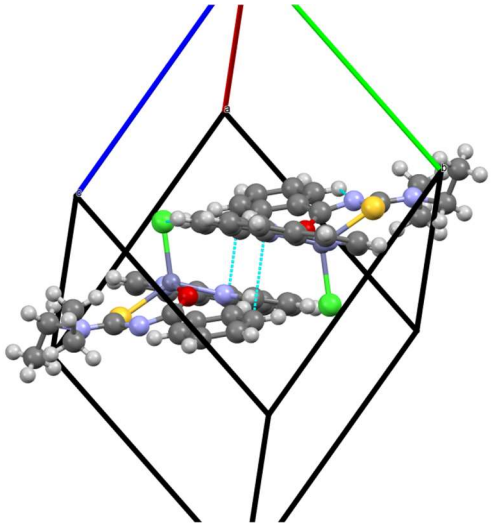

Crystal packing for the [ZnCl(phen)(L-κS,O)] complex showing π—π interaction.